



NATIONAL INSTITUTE FOR **NUCLEAR PHYSICS** AND **HIGH-ENERGY PHYSICS**

ANNUAL REPORT

2000

Kruislaan 409, 1098 SJ Amsterdam
P.O. Box 41882, 1009 DB Amsterdam

Colofon

Publication edited for NIKHEF:

Address: Postbus 41882, 1009 DB Amsterdam
Kruislaan 409, 1098 SJ Amsterdam

Phone: +31 20 592 2000

Fax: +31 20 592 5155

E-mail: directie@nikhef.nl

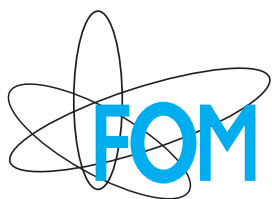
Editors: Stan Bentvelsen & Eddy Jans

Layout & art-work: Kees Huysen

Organisation: Anja van Dulmen

Cover Photograph: Higgs candidate at the L3 detector (Photo: CERN)

URL: <http://www.nikhef.nl>



The National Institute for Nuclear Physics and High-Energy Physics (NIKHEF) is a joint venture of the Stichting voor Fundamenteel Onderzoek der Materie (FOM), the Universiteit van Amsterdam (UVA), the Katholieke Universiteit Nijmegen (KUN), the Vrije Universiteit Amsterdam (VUA) and the Universiteit Utrecht (UU). The NIKHEF laboratory with its accelerator facility (AmPS) is located at the Science Research Centre Watergraafsmeer (WCW) in Amsterdam.

The activities in experimental subatomic physics are coordinated and supported by NIKHEF with locations at Amsterdam, Nijmegen and Utrecht. The scientific programme is carried out by FOM, UVA, KUN, VUA and UU staff. Experiments are done at the European accelerator centre CERN in Geneva, where NIKHEF participates in two LEP experiments (L3 and DELPHI), in a neutrino experiment (CHORUS) and in SPS heavy ion experiments (NA57 and NA49). NIKHEF participates in the Tevatron experiment D0 at Fermilab, Chicago. At DESY in Hamburg NIKHEF participates in the ZEUS, HERMES and HERA-B experiments. Research and development activities are in progress for the future experiments ATLAS, ALICE and LHCb with the Large Hadron Collider (LHC) at CERN.

NIKHEF is closely cooperating with the University of Twente. Training and education of students are vital elements in the research climate of the laboratory.

Contents

Preface	1
A Experimental Programmes	3
1 AmPS	3
1.1 Introduction	3
1.2 Experiments at EMIN	3
1.3 Experiments at ITF	4
1.4 Experiments abroad	8
2 ANTARES	11
3 ATLAS	13
3.1 Introduction	13
3.2 ATLAS experiment	13
3.3 D0 experiment	17
3.4 ATLAS detector R&D spin-off	18
4 B Physics	19
4.1 Introduction	19
4.2 HERA-B	19
4.3 The LHCb Experiment	20
4.4 Vertex detector	21
4.5 Track Reconstruction	23
4.6 Physics Performance	25
5 CHORUS	27
5.1 Introduction	27
5.2 Neutrino oscillation analysis	27

5.3	Charm production	27
6	Heavy Ion Physics	31
6.1	Introduction	31
6.2	Direct photons with WA98	31
6.3	Strangeness enhancement in NA57	32
6.4	Charm and strangeness with NA49	33
6.5	Preparations for ALICE	34
7	HERMES	37
7.1	Introduction	37
7.2	Data taking	37
7.3	Physics analysis	38
7.4	The JLab experiment	40
7.5	The Lambda Wheel project	40
7.6	Outlook	41
8	ZEUS	43
8.1	Introduction	43
8.2	Physics highlights	43
8.3	Microvertex Detector	45
B	LEP in 2000	49
1	Higgs search	49
2	DELPHI	53
2.1	Data taking and detector status	53
2.2	Selected research topics	53
2.3	Tau topological branching ratios	53
2.4	Other research topics	54
2.5	Trilinear Gauge Boson Couplings	54
3	L3	57
3.1	Introduction	57
3.2	Searches	57
3.3	W physics	57
3.4	L3+Cosmics	59

C	Theoretical Physics	61
1	Theoretical Physics Group	61
1.1	Research program Theoretical Physics	61
1.2	QCD	61
1.3	String theory	61
1.4	Supersymmetry	62
1.5	Computational Physics	62
D	Technical Departments	63
1	Computer Technology	63
1.1	Introduction	63
1.2	Upgrade network infrastructure	63
1.3	Compute farms for off-line analysis	64
2	Electronics Technology	67
2.1	Introduction	67
2.2	Projects	67
2.2.1	ZEUS	67
2.2.2	HERMES	68
2.2.3	ATLAS	68
2.2.4	B-Physics	69
2.2.5	LHCb-Vertex	69
2.2.6	ALICE	70
2.2.7	ANTARES	70
2.2.8	Several small projects	70
2.3	Department development	71
3	Mechanical Technology	73
3.1	Introduction	73
3.2	Projects in exploitation	73
3.3	Projects in development	73
3.4	Projects for third parties	75
E	Publications, Theses and Talks	77
1	Publications	77

2	PhD Theses	87
3	Invited Talks	88
4	Seminars at NIKHEF	92
5	NIKHEF Annual Scientific Meeting, December 14-15, 2000, Amsterdam	93
F	Resources and Personnel	95
1	Resources	95
2	Membership of Councils and Committees during 2000	96
3	Personnel as of December 31, 2000	97

Preface

The tragic death of Eric Wassenaar has shocked us all. Eric was responsible for the local network and its connection to Internet. As a spider in his web he controlled all incoming and outgoing traffic with great dedication.

In the year 2000 we received with joy the approval of the proposal to join the ANTARES collaboration. The Netherlands' Organization for Scientific Research (NWO) made available resources for a major capital investment in parts of the prototype neutrino detector to be launched in the Mediterranean Sea near Toulon. The design, including R&D work, of the data transmission from the detector to a shore station and the fast handling of the data –within the NIKHEF 'all data to shore' concept– has well advanced.

The three LHC experiments in which NIKHEF participates are approaching the final design specifications such that the Memorandum of Understanding for each experiment has either been signed or was ready to be signed in 2000 (LHCb). This also signals that in several cases, notably for the ATLAS detector, the R&D phase is moving into the production phase. NIKHEF is now in the position to start the fabrication of the large monitored drift tube (MDT) muon chambers, after it had shown the first real prototype chamber to meet specifications. Likewise, the production by Dutch industry of major parts for the ATLAS end cap toroidal magnets is well in progress.

Two of the experiments at the HERA collider of DESY received major upgrades in which NIKHEF had a leading role. The micro vertex detector for the ZEUS experiment was almost completed in the NIKHEF workshops by the end of 2000; the first completed half was shipped to DESY in December. Similarly, most of the wheel shaped silicon detector for the HERMES experiment –again with major NIKHEF involvement– was installed in the experiment. Both projects largely benefited from the development of a silicon lab within NIKHEF over the past three years. This lab, with state-of-the-art equipment, will also play an important role in the construction of the vertex detectors for the ATLAS, ALICE and LHCb experiments thereby ensuring even more NIKHEF's future in the physics analysis of the data from the LHC collider.

NIKHEF is also preparing its future in computing for

the LHC era. Together with four other major partners and CERN, the Institute signed an EU proposal for data grid. Together with its participation in a virtual laboratory, for which additional funds from the Dutch Government are available, NIKHEF could significantly upgrade its connection to the outside world (to the 1Gb/s level). It also successfully installed a compute farm with 50 dual processor PC's which is now running Monte Carlo simulations for the D0 experiment at Fermilab, later to be used for data reconstruction. This activity can also be seen as a precursor of NIKHEF's role in a global data grid.

The year 2000 was very important for physics results. First and for all there was the heroic attempt of the four LEP experiments to try and find the Higgs boson. The NIKHEF groups in DELPHI and L3 participated enthusiastically. The combined signal, however, only allowed a three standard deviations result for a Higgs particle with a mass of $115 \text{ GeV}/c^2$. Possibly, with five years of hard work at the Tevatron (Fermilab) and provided a similar result is obtained at the same mass, the Higgs can just be seen before the LHC is switched on. Apart from the non-significant Higgs signal, LEP has produced a wealth of impressive, very precise tests of the Standard Model of the weak interaction and also of QCD. This year also saw the announcement made at CERN of the existence of the quark-gluon plasma based on the evidence of a number of experiments with heavy ion beams at the SPS. NIKHEF played a modest role in this through its participation in the WA98 and NA57 experiments.

The NIKHEF team in the CHORUS experiment took advantage of the large sample of neutrino-induced deep inelastic reaction events by deducing the structure functions F_2 and $x\bar{F}_3$ from these data. They turned out to be of a precision comparable to that of the results of two earlier studies (CCFR and CDHSW) and helped to solve the discrepancy between them.

The ZEUS collaboration has now fully analyzed –up to a resolution of $Q^2 = 800 \text{ GeV}^2/c^2$ – the proton structure with a precision of typically 2%. Comparable precision for higher Q^2 is in part in the data taken in 2000. Good precision data for the ultimate resolution of $Q^2 > 10^4 \text{ GeV}^2/c^2$ has to wait for the luminosity

upgrade of the HERA collider. The HERMES collaboration succeeded among others in obtaining with high precision the flavor decomposition of the nucleon spin. The HERA-B collaboration at DESY, finally, was less fortunate. They were plagued by a not fully commissioned detector and a relatively short run period. After a review, the DESY directorate decided for a two-year program for the time being.

At the end of the year 2000 NIKHEF was subjected to a heavy evaluation (past performance and future prospects) by the principal funding agency NWO by an external panel set up by FOM. This evaluation, including a site visit, was well stood. The final outcome of the process may well be some room for an additional long term physics and R&D programme.

A handwritten signature in black ink, appearing to read 'Ger van Middelkoop', with a long horizontal stroke extending to the right.

Ger van Middelkoop

A Experimental Programmes

1 AmPS

1.1 Introduction

The analysis of the experiments performed with the former in-house facility MEA/AmPS reaches its final stage. One experiment is related to the work in the endstation EMIN, the remaining part is related to the work in the internal target facility ITF. One of the most challenging parts of the research program was the measurement of the charge form factor of the neutron. Although the neutron has no net electric charge, it does exhibit a charge distribution. Precise measurements in which thermal neutrons are scattered from atomic electrons, show that it has a positive core surrounded by a region of negative charge, the exact distribution being described by the charge form factor $G_E^n(Q^2)$. Since stable free neutron targets are not readily available, experimentalists mostly resorted to precise unpolarized elastic electron-deuteron scattering measurements to determine this form factor. An extensive analysis has been performed by Platchkov *et al.* However, the G_E^n results of these experiments are flawed by large model-related uncertainties; they constrain the shape of $G_E^n(Q^2)$, while the scale remains poorly known. In order to obtain model-independent results, several years ago a worldwide effort (Mainz, JLab, MIT/Bates, and NIKHEF) was started to constrain G_E^n by using polarized electrons, and where either the target is polarized, or the polarization of the knocked-out neutron is measured. At NIKHEF both polarized ^2H and ^3He targets have been used. In spite of the fact that the amount of beam time was quite limited, the experiment with polarized ^2H has resulted in a data point for the charge form factor of the neutron with unprecedented precision.

The polarized ^1H experiment yields information on the spin content of the nucleon and possible deformation of baryons. The analysis of the data on quasi-elastic scattering from polarized ^3He in the $(e, e'p)$, $(e, e'n)$ and $(e, e'd)$ channel allows a comparison to results of state-of-the-art three-body models, e.g., the non-relativistic continuum-wave Faddeev model by Golak *et al.*, where re-scattering is taken into account to all orders.

Several research subjects, initiated at the AmPS facility, will be further studied at JLab, MIT/Bates and Mainz with the help of parts of the instrumentation from EMIN and ITF.

The experiment to measure the pion form factor at the Thomas Jefferson National Accelerator Facility, JLab, has resulted in a PhD thesis. Finally, the first data have been taken for the experiment on $^3\text{He}(e, e'pn)p$ in Mainz. This is the complementary reaction to $^3\text{He}(e, e'pp)n$, one of the last experiments we have done at EMIN.

1.2 Experiments at EMIN

Depletion of the Fermi sea in ^{208}Pb

(Prop. 94-13; with *Glasgow, Saclay, INFN-Rome, INFN-Lecce*)

In the first study of the reaction $^{208}\text{Pb}(e, e'p)$ with the MEA facility it was found that the spectroscopic factors for knockout of valence protons were about 50% of the independent-particle shell-model (IPSM) prediction unity. This observation was attributed to long-range and short-range correlations not accounted for in the IPSM wave functions. In a next $^{208}\text{Pb}(e, e'p)$ experiment carried out with the AmPS facility the high-momentum components in the wave functions of these valence protons were measured up to a missing momentum (p_m) of 500 MeV/ c . The resulting momentum distribution for the summed transitions showed that the data lie well above the values calculated with IPSM wave functions for $p_m > 300$ MeV/ c . They can only be described if long-range and short-range correlations are included in the wave functions. However, a difficulty in the interpretation here is that for valence orbitals both types of correlations contribute to the quenching of the spectroscopic strength. This is in contrast to the spectroscopic strength for protons in deeply bound states, where the long-range correlations no longer play a role and only short-range correlations contribute to the depletion.

Therefore, a follow-up experiment was performed in which the reaction $^{208}\text{Pb}(e, e'p)$ was studied up to a missing energy of 100 MeV. This experiment succeeded in determining the strength of deep-lying orbits in the binding-energy range 30-60 MeV. The obtained value is $78 \pm 6\%$ of the IPSM prediction unity (see Fig. 1.1). Since *ab initio* calculations for a heavy finite nucleus are difficult to perform, the data are compared to calculations for correlated (infinite) nuclear matter (NM). Such calculations produce values between 79 and 83% for the occupation (n^{NM}) of the deepest bound states.

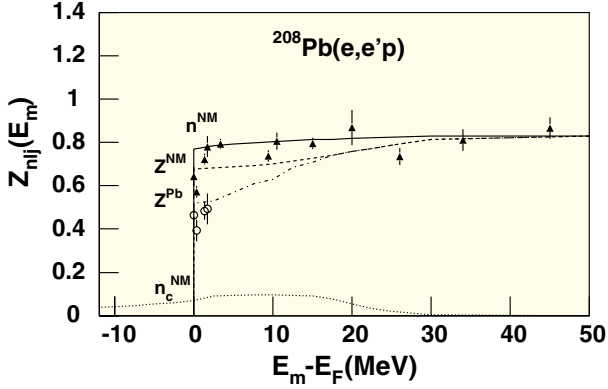


Figure 1.1: Spectroscopic strength, relative to the IPSM value, as deduced for proton orbitals in ^{208}Pb , as a function of the mean removal energy in each orbit. The triangles represent the present data for each orbital, the circles represent earlier data for the quasi-hole pole of orbits near the Fermi energy (E_F). The curves represent the calculated occupation n_c^{NM} (solid curve) and quasi-hole strength Z^{NM} (dashed curve) for correlated infinite nuclear matter and for ^{208}Pb (Z^{Pb} , dashed-dot curve). The dotted curve is the background contribution (see text).

As shown in Fig. 1.1 this is in good agreement with our data. For orbits closer to the Fermi energy the measured strength comes down to 60-70% of the IPSM value. Here, long-range correlations that invoke 2p2h excitations (as indicated by the background contribution n_c^{NM}) start to play a role. Such a further depletion is indeed predicted by the nuclear-matter calculation for the spectroscopic strength ($Z^{\text{NM}} = n^{\text{NM}} - n_c^{\text{NM}}$). Finally we observe a difference between the earlier measured spectroscopic factors (circles) and the spectroscopic strength (triangles) from the present experiment. This is due to the presence of higher lying fragments for each orbit that were included in the present data, whereas the earlier data represent only the strength for the quasi-hole pole. These higher lying fragments are due to coupling of the quasi-hole state to RPA surface vibrations, which do not exist in infinite nuclear matter. The dashed-dot curve is an approximation to describe these effects by adding RPA effects to the nuclear matter results.

The total depletion of the Fermi sea, i.e. $\sum(2j+1)Z_{nlj}$ amounts to 62 ± 4 protons. This means that about a quarter of the 82 protons in ^{208}Pb is not found in the energy-momentum region range ($E_m < 60$ MeV,

$p_m < 270$ MeV/c) of the present experiment. Advanced calculations predict that these protons should be found at much higher energies and momenta.

In conclusion, we now avail of a consistent picture that explains why the spectroscopic strength for proton knockout rises from about 50-60% at the Fermi level to about 80% for the deepest lying states. In order to describe such a behavior both long-range and short-range correlations should be included in the nuclear wave function.

1.3 Experiments at ITF

Quasi-free pion production on ^4He

(Prop. 91-08; with ODU and Virginia)

The reactions $^4\text{He}(e, e'p^3\text{H})\pi^0$ and $^4\text{He}(e, e'p^3\text{He})\pi^-$ have been studied at invariant energies ranging from the pion production threshold to the delta resonance region. Comparison of the cross sections with those of pion production on the proton will provide information on ΔN and πN dynamics inside the nucleus ^4He .

The triple coincidence measurements were carried out at the internal target facility at NIKHEF with a 670 MeV electron beam and a ^4He open-ended storage cell target. The scattered electrons were detected in the BigBite magnetic spectrometer and the knocked out protons in the HADRON4 detector. Simultaneous measurement of both reaction channels was achieved by detecting the recoiling nuclei in a recoil detector positioned opposite to the three-momentum transfer. In this way the detection of the neutral pion was avoided.

The target density of 5.3×10^{14} atoms/cm² was determined from the $^4\text{He}(e, e'^4\text{He})$ reaction, for which the cross section is accurately known, resulting in an integrated luminosity of 2.60 pb⁻¹. About 700 neutral and 1200 charged pion production events were identified in the missing mass spectrum, which was shown in the NIKHEF annual report of 1999.

Various methods were used to determine the efficiencies of the three detection systems and the trigger system. The detection efficiency of the low-pressure wire chamber of the recoil detector was determined as a function of the kinetic energy of the particle and the impact angle and varied between 20% and 100% for tritons and between 90% and 100% for ^3He particles. The dead time of the HADRON4 frontends was determined for each datafile and as a function of the beam current. GEANT Monte Carlo simulations were used to determine the proton reconstruction efficiency. The

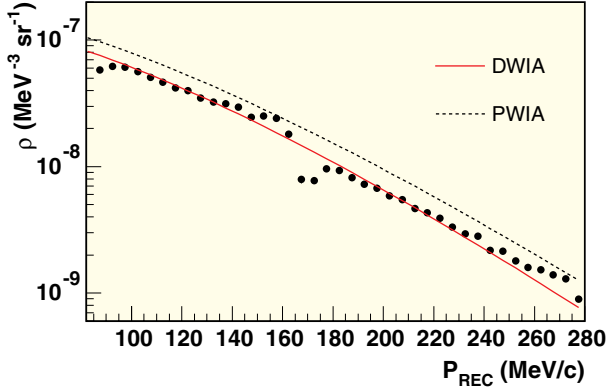


Figure 1.2: Comparison of the measured ${}^4\text{He}$ momentum density with PWIA and DWIA calculations.

detection efficiency of the Čerenkov detector of BigBite was determined from the number of photoelectrons as a function of impact position. The trigger efficiencies of the three detectors were taken into account for each datafile. The detection volume was calculated by means of a Monte Carlo simulation for the three-detector setup.

The analysis method could be verified by applying it to ${}^4\text{He}(e, e'p{}^3\text{H})$ coincidence events, for which reaction channel the cross section is well known in the kinematical regime covered by the experiment. In Fig. 1.2 the measured momentum density is compared to DWIA calculations, for which the parameters of the optical model have been adjusted to describe the data of references [1, 2]. The agreement between the DWIA calculation and the data is satisfactory, except in the middle of the spectrum, justifying the analysis method.

The determination of the cross sections, that will be presented as a function of the invariant mass of the pion-nucleon system and the pion angle with respect to the transferred three-momentum, is almost completed.

G_E^n with vector polarized deuterium

(Prop. 97-01; with ETH, Virginia, Arizona, JLab, MIT, Hampton, Novosibirsk)

The measured sideways asymmetry A_x^i (or recoil polarization) arises from an interference of the small charge form factor with the dominant magnetic form factor G_M^n . Such spin observables are predicted to be rather insensitive to details of the nuclear wave function. We show here the results of a measurement utilizing a polarized electron beam and a vector-polarized deuterium target.

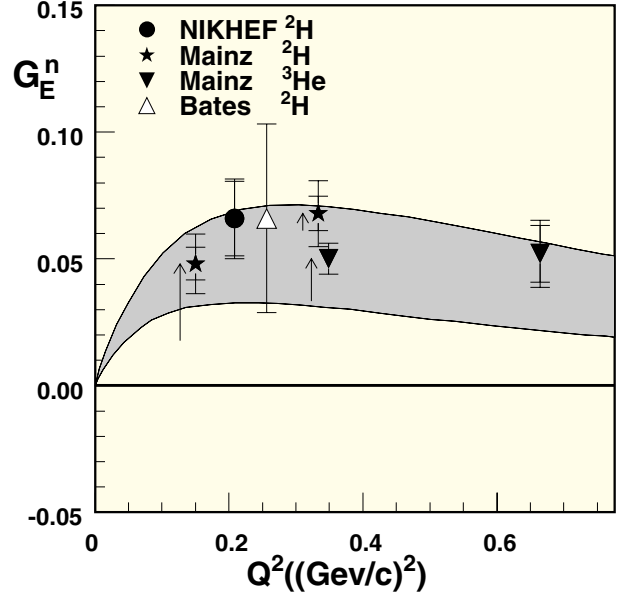


Figure 1.3: Data on G_E^n obtained in exclusive spin-dependent measurements. The deuterium data from NIKHEF and Mainz have been extracted by using full model calculations by Arenhövel. The datum from Bates has been extracted from a PWIA calculation. The lowest Q^2 point from ${}^3\text{He}$ from Mainz has been corrected for the effects from FSI, while the highest Q^2 datum from Mainz has been determined from a PWIA analysis. The arrows indicate the correction on G_E^n when FSI are taken into account. The shaded area indicates the uncertainty due to the model dependence in the analysis of unpolarized results by Platchkov *et al.*

By simultaneously detecting both protons and neutrons in the same detector, one can construct asymmetry ratios for the two reaction channels ${}^2\bar{\text{H}}(\vec{e}, e'p)n$ and ${}^2\bar{\text{H}}(\vec{e}, e'n)p$, in this way minimizing systematic uncertainties associated with the deuteron ground-state wave function, absolute beam and target polarizations, and possible dilution by cell-wall background.

We performed the measurement at a momentum transfer $Q^2 = 0.21$ (GeV/c)², i.e. at the maximum of $G_E^n(Q^2)$ determined from the analysis of Platchkov *et al.* Combination of these data with our result and the known slope of the charge form factor at $Q^2 = 0$ puts strong constraints on G_E^n up to $Q^2 = 0.6$ (GeV/c)². By a comparison of the data to the predictions of the model of Arenhövel, averaged over the detector acceptance for various values of G_E^n , we

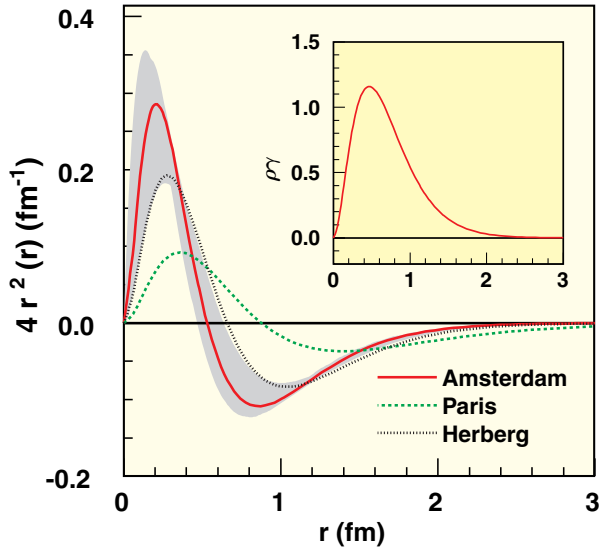


Figure 1.4: Radial charge density distribution of the neutron according to the Amsterdam parameterization (full curve), the parameterization of Platchkov et al. for the Paris potential (dashed curve) and the Mainz parameterization (dotted curve). The shaded area indicates the uncertainty in the Amsterdam parameterization. The inset shows the charge density distribution of the proton according to the dipole parameterization.

extract $G_E^n(Q^2 = 0.21 \text{ (GeV}/c^2\text{)})$ with an overall accuracy of 23%. The result is shown in Fig. 1.3, together with data from other spin-dependent measurements.

Our result for G_E^n favors the extraction from the unpolarized data using the Nijmegen nucleon-nucleon potential. By comparison to the predictions of vector-meson dominance model of Gari and Krümpelmann, with and without including the ϕ -meson, our result favors the latter. This indicates that the strangeness content of the nucleon may be small.

The results can also be transformed to r -space as shown in Fig. 1.4. The figure confirms the expectation that the neutron consists of a positive core surrounded by a region of negative charge. This can be interpreted as a bare nucleon surrounded by a meson cloud. The fact that the central charge density of the neutron is about five times smaller than in the proton (see inset) indicates that only a fraction of the physical neutron is determined by the $|p\pi^- \rangle$ state.

Spin correlation effects in the Δ region for the ${}^1,2\bar{H}(\vec{e}, e')$ reaction

(Prop. 97-01; with ETH, Virginia, Arizona, JLab, MIT, Hampton, Novosibirsk)

A topic of interest in particle physics concerns the spin content of the nucleon, in particular the contribution of orbital angular momentum, of which little is known. It has been argued that the failure of the quark model to properly describe fundamental observables such as G_A/G_V , the SU(3) decay ratio $(D + F)/(D - F)$ and the $\pi N\Delta$ coupling constant, might be removed if one allows for a substantial D-state admixture in the wave functions of the baryons. This issue can be experimentally addressed by measuring double-polarization electromagnetic observables in the Δ region which are sensitive to the quadrupole transition form factors (C2 and E2) of the $N\text{-}\Delta$ excitation, hence to a possible D-state admixture in the nucleon and Δ wave function. Considerable work has been done at a four-momentum transfer $Q^2 = 0$, using polarized real photons, constraining the E2/M1 ratio. The present experiment was performed with a 720 MeV polarized electron beam and an upgraded internal gas target (target thickness up to 1.1×10^{14} atoms/cm² and polarization up to 0.7). Scattered electrons were detected in the large acceptance magnetic spectrometer BigBite, the ejected hadrons in a single time-of-flight scintillator array. The well-known elastic form factors of the proton were used to predict the spin correlation parameters in the elastic channel and determine the product of the beam and target polarizations.

Fig. 1.5 shows preliminary results for the spin correlation parameter $A_{T'}$ from measurements in which the target polarization was parallel to the momentum transfer in the Δ region for the ${}^1\bar{H}(\vec{e}, e')$ reaction, at an average Q^2 value of $0.11 \text{ GeV}/c^2$. The $N\text{-}\Delta$ quadrupole form factor E2 enters $A_{T'}$ via an interference with the dominant magnetic (“spin-flip”) dipole form factor M1. Comparison of the data to model predictions reveals that a correct description of the data requires a non-zero amount of quadrupole strength in the nucleon and/or Delta.

Polarized electron scattering from polarized ${}^3\text{He}$

(Prop. 94-05; with ETH, Virginia, Arizona, JLab, MIT, Hampton, Novosibirsk)

Currently, continuum-wave Faddeev calculations are available that give an exact solution for both the bound state and the final state of the 3-nucleon system for a given NN -potential. Therefore, theory and experiment can be compared on a sound basis. Some micro-

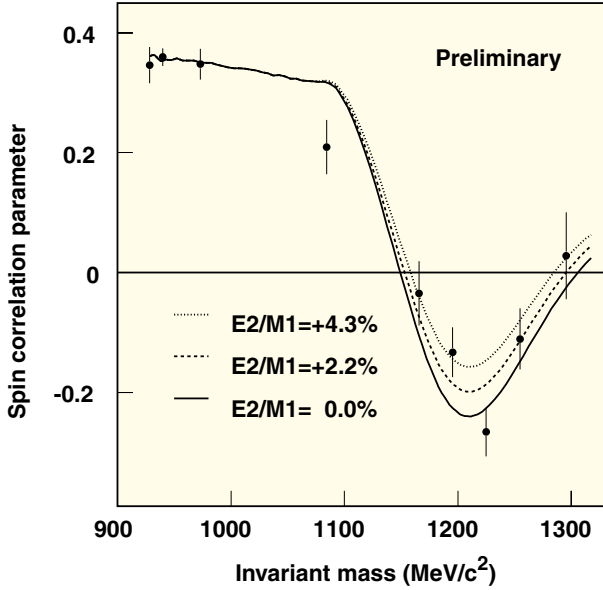


Figure 1.5: Longitudinal spin correlation parameter $A_{T'}^{\parallel}$ in the Δ region for the ${}^1\text{H}(\vec{e}, e')$ reaction. The curves represent the predictions of a Monte Carlo calculation. The solid curve shows the prediction for a pure M1 transition ($C2 = E2 = 0$). The dashed and dotted curves assume 2.2 and 4.3% E2 strength, respectively.

scopic nuclear-structure issues cannot be addressed in deuterium but are optimally accessible in ${}^3\text{He}$ (most notably the possible existence of 3-body forces and the presence of the mixed-symmetry S' -configuration). Furthermore, polarized ${}^3\text{He}$ can be considered as an effective polarized neutron target, since the spins of the two protons pair off to a large extent.

The ITF facility provided the means for executing a program with spin dependent electron scattering from polarized ${}^3\text{He}$. In order to be able to study all aspects of the ${}^3\text{He}$ nuclear structure (and to use ${}^3\text{He}$ as an effective neutron target), a setup has been developed in which large acceptance detectors were employed, enabling the simultaneous study of various reaction channels - (e, e') , $(e, e'p)$, $(e, e'd)$, $(e, e'n)$, and channels with pions in the final state - in a broad kinematic range.

Spin-exchange optical pumping was employed to obtain polarized ${}^3\text{He}$ gas, which was fed via a capillary from a glass pumping cell to the storage cell, consisting of an open-ended cylindrical tube co-axial to the polarized electron beam. The storage cell was cooled to typically 20 K in order to further enhance the tar-

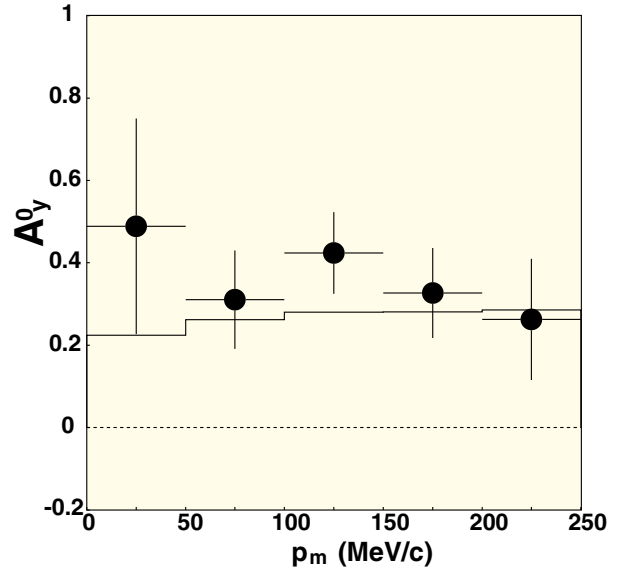


Figure 1.6: Induced asymmetry A_y^0 for the reaction ${}^3\text{He}(e, e'n)$ as a function of missing momentum at four-momentum transfer squared $Q^2 = 0.16$ (GeV/c^2). The solid (dashed) curve represents the full Faddeev result (the PWIA result) by Golak *et al.*

get density. Three sets of orthogonal Helmholtz coils around the target were employed so that the target polarization axis could be selected in any given direction. Neutrons and charged hadrons were measured using a time-of-flight detector consisting of two walls of scintillator bars. Protons and deuterons were in addition detected by a range telescope, preceded by wire chambers to obtain sufficient angular resolution. Recoiling low-momentum particles were detected by a silicon detector located in the vacuum of the target area.

Although the focus of the experiment was on G_E^p , we simultaneously accumulated large amounts of data in the Δ resonance region (both inclusive and exclusive channels).

As an example we show in Fig. 1.6 the induced asymmetry A_y^0 as a function of missing momentum p_m for the reaction ${}^3\text{He}(e, e'n)$. This asymmetry is particularly sensitive to reaction-mechanism effects, since it arises from the interference of Feynman diagrams. Due to the Fermi-Watson theorem it is strictly zero in PWIA, where only a single diagram contributes to the cross section. It is compared to the continuum Faddeev calculations by Golak *et al.* The asymmetries are sizeable, and the calculations describe the data well.

1.4 Experiments abroad

Study of the Charged Pion Form Factor

(with the TJNAF E93-021/E96-007 collaboration)

The charge form factor of the pion was studied at JLab by scattering electrons from a virtual pion in the proton. Using the High Momentum Spectrometer and the Short Orbit Spectrometer of Hall C and electron energies between 2.4 and 4.0 GeV, data for the reaction ${}^1\text{H}(e, e'\pi^+)n$ were taken for central values of Q^2 of 0.6, 0.75, 1.0 and 1.6 $(\text{GeV}/c)^2$, at a central value of the invariant mass W of 1.95 GeV. Several calibrations were performed with the over-determined ${}^1\text{H}(e, e'p)$ reaction.

Cross sections were obtained from the measured yields using a Monte Carlo simulation of the experiment. Because of correlations between the relevant variables W , Q^2 , t and θ within the experimental acceptance, a detailed cross section model was used in the Monte Carlo simulation.

The cross section for pion electroproduction can be written as

$$\frac{d^3\sigma}{dE'd\Omega_{e'}d\Omega_{\pi}} = \Gamma_V(\epsilon\sigma_L + \sigma_T + \sqrt{2\epsilon(\epsilon+1)}\sigma_{LT}\cos\phi + \epsilon\sigma_{TT}\cos 2\phi), \quad (1.1)$$

where Γ_V is the virtual photon flux factor, ϵ is the virtual-photon polarization parameter, and ϕ the azimuthal angle of the outgoing pion with respect to the electron scattering plane. The cross sections σ_X depend on W , Q^2 and the Mandelstam variable t .

The ϕ acceptance of the experiment allowed the interference terms σ_{LT} and σ_{TT} to be determined. A representative example of the cross section as function of ϕ is given in Fig. 1.7. Since data were taken at two energies at every Q^2 , σ_L could be separated from σ_T by means of a Rosenbluth separation. The longitudinal cross section σ_L is dominated by the t -pole term, which contains F_{π} . The results for the pion form factor are shown in the form of $Q^2 F_{\pi}$ in Fig. 1.8 in comparison to the results of various theoretical calculations [3]. The data globally follow a monopole form obeying the pion charge radius, and are well above values predicted by pQCD calculations. In the extraction of F_{π} from σ_L use was made of a Regge model by Vanderhaeghen, Guidal and Laget. The model uncertainty is displayed as the grey band.

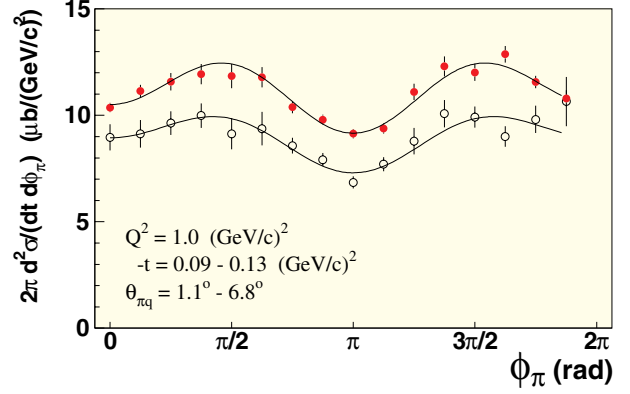


Figure 1.7: ϕ dependence of the cross section at $Q^2=1.0 (\text{GeV}/c)^2$ for high and low ϵ (filled and empty circles, respectively). The curves represent the results of the fits.

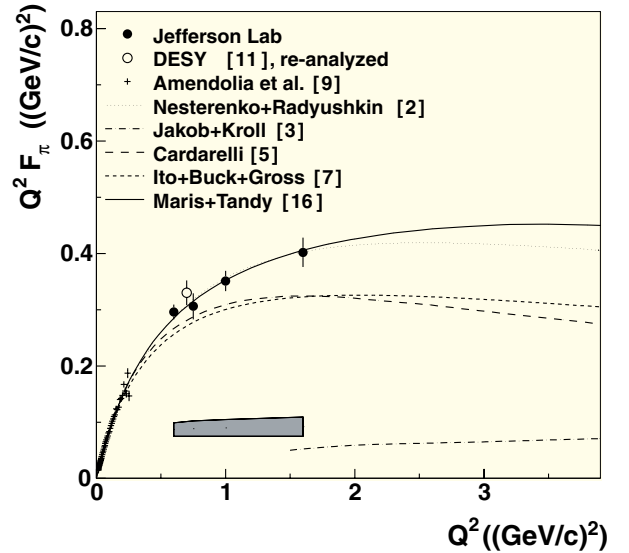


Figure 1.8: Values for F_{π} in comparison to the results of several calculations.

Study of the ${}^3\text{He}(e, e'pn)$ Reaction

(Prop. A1/4-98; with *the Universities of Mainz, Tübingen and Glasgow*)

Nucleon-nucleon correlations in the three-nucleon system are under investigation by means of a ${}^3\text{He}(e, e'pn)$ experiment. This system has been chosen because Faddeev calculations with realistic NN interactions are presently available. The interpretation of these data will be done in combination with the existing data of the complementary ${}^3\text{He}(e, e'pp)$ reaction, obtained at AmPS. This will permit to investigate the relative importance of pp and pn correlations, as well as the contribution of isobar and meson exchange currents in the three-nucleon system.

The first beam time period of the ${}^3\text{He}(e, e'pn)$ experiment took place in the A1 hall at MAMI, in Mainz, during April 2000. The scattered electrons were detected by the magnetic Spectrometer B. Proton detection was performed with the highly segmented scintillator array HADRON3, while the neutrons were detected by a time of flight unit placed opposite to HADRON3.

In the preparation phase of the experiment the HADRON3 detector was made fully operational and capable of rotating independently with respect to the beam line in the A1 hall. Its data format was modified and its data-stream incorporated in the data-acquisition system of A1. In the backward direction, three TOF stands were positioned, each consisting of 8 veto counters followed by three layers of E-counters. The total wall surface of this detector is 16.56 m^2 and its thickness amounts to 16 cm. The double-sided readout of the scintillator bars is performed by means of 192 photomultipliers.

The presence of an electron trigger signal provided by Spectrometer B was required in HADRON3 to enable the sending of a proton trigger to the coincidence electronics. However, TOF was always read out under the condition of a HADRON3 and Spectrometer B coincidence signal.

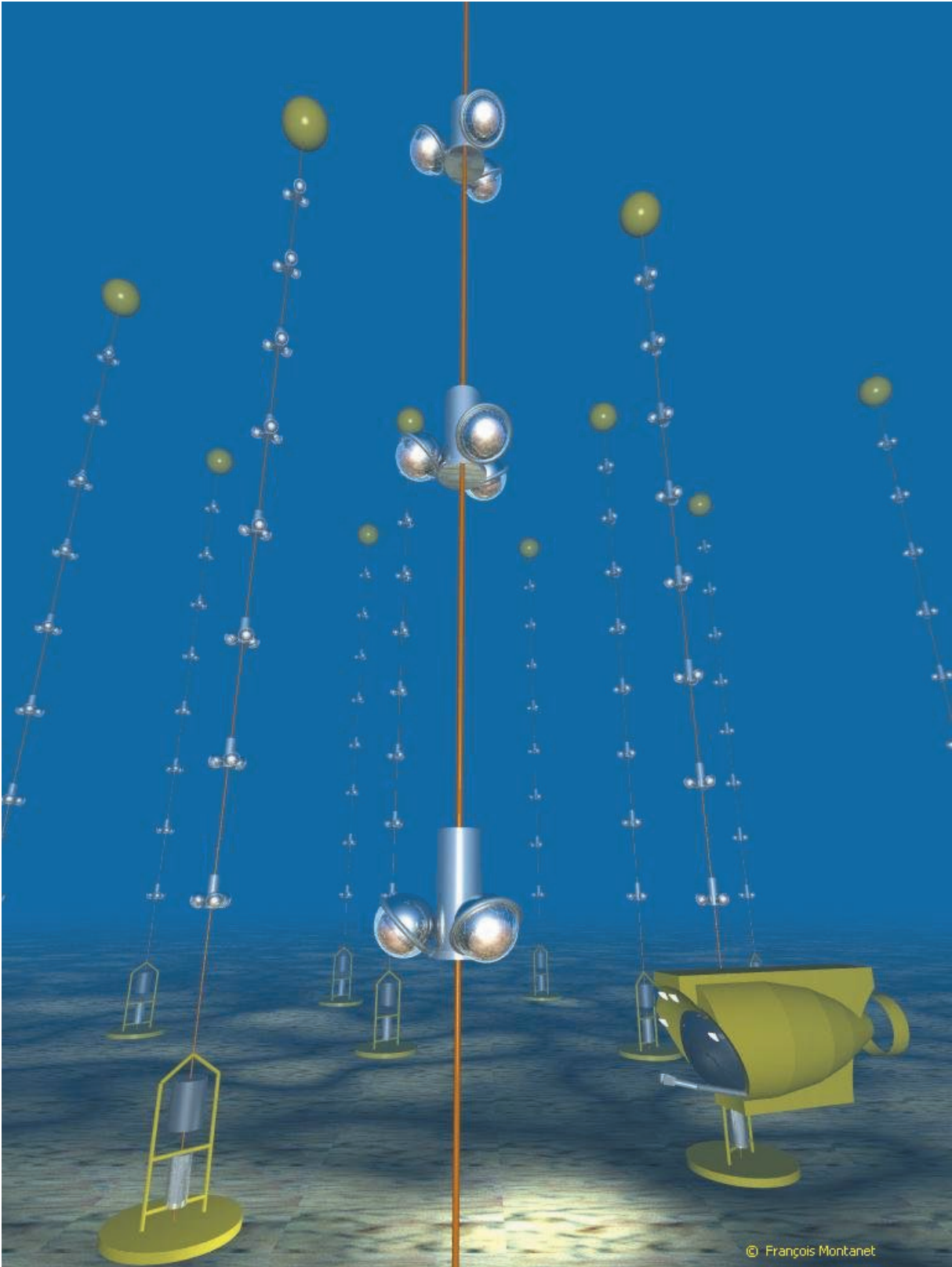
A set of ${}^3\text{He}(e, e'pn)$ data were taken at a momentum transfer $q = 375\text{ MeV}/c$ and an energy transfer $\omega = 220\text{ MeV}$ at an incident electron of energy $E_e = 855\text{ MeV}$. These data are collected at beam currents of $2\text{ }\mu\text{A}$ and $4\text{ }\mu\text{A}$.

A second but small set of ${}^3\text{He}(e, e'pn)$ data was also taken at $q = 375\text{ MeV}/c$ and $\omega = 310\text{ MeV}$. These data will be used to optimize the next beam time period of this experiment.

The single arm calibrations of the HADRON3 detector, like gain fitting, determination of attenuation factors and particle identification windows, have been accomplished via its single event data. The development of the codes for the TOF and HADRON3 detectors for the analysis of double and triple coincidence events is in progress.

References

- [1] J.F.J. van den Brand *et al.*, Nucl. Phys. **A534** (1991) 637.
- [2] J.J. van Leeuwe *et al.*, Phys. Rev. Lett. **80**, 2543 (1998).
- [3] J. Volmer *et al.*, Phys. Rev. Lett., **86**, 1713 (2001).



© François Montanet

An artist's view of the ANTARES detector. (Artwork by F. Montanet CPPM/IN2P3/CNRS - Univ. Mediterranee)

2 ANTARES

The Antares collaboration will deploy a detector consisting of 1000 photomultipliers in the deep sea (2.5 km) off the Mediterranean coast near Toulon. The Čerenkov light associated with muons originating from charged current neutrino scattering in or near the active volume of the detector ($0.1 \text{ km}^2 \times 0.3 \text{ km}$) will be measured (arrival time and amplitude). Reconstruction of the muon track will yield an estimate of the muon's - and therefore of the parent neutrino's - energy and a measurement of its direction.

The cosmic neutrino spectrum is unknown. Antares will measure it from a few times 10 GeV up to the highest energies occurring in nature (in excess of 10^{21} eV) consistent with a detectable flux. The angular resolution of the track reconstruction will allow the identification of point sources, if they exist. The exploratory research programme of Antares holds the promise of contributing new and unique knowledge for astrophysics, cosmology and high energy physics.

In 2000 the collaboration completed a Conceptual Design Report, stipulating the choices for the technical realization of the project (Optical Modules, front end electronics, timing and position calibration and monitoring, electrical power generation and distribution, lay out, deployment procedures, etc.). The photomultipliers will be organized in triplets, 12 meters apart in the vertical direction, along 13 'strings' with an instrumented length of 300 meters. The strings will be, typically, 60 meters apart.

In view of the exploratory nature of the research programme a data sample as unbiased as possible is desirable. The NIKHEF group therefore developed the 'All Data to Shore' concept: timing, amplitude and in some cases waveform information will be sent to the data acquisition station on shore (40 km away from the detector) for *all* photomultiplier hits. This will allow maximum flexibility in devising optimal algorithms for data filtering in view of new insights or external information (e.g. a Gamma Ray Burst warning).

The counting rate of the 10" photomultipliers is entirely dominated by beta-decay of ^{40}K in the sea water and by, intermittent, bioluminescence. The (in situ) measured counting rate per photomultiplier is about 100 KHz, leading to a total data rate of about 1 GByte/sec. The technology of choice for transporting the data is DWDM: dense wavelength division multiplexing. The NIKHEF group is designing a read-out system based on this modern technology. The design will allow to trans-

fer all data from the detector to the shore station. A proof of concept of the readout-system has been established and the production is expected to start in summer 2001. The group is also designing the on-shore data processing system which will consist of a large PC farm. A fast algorithm has been developed which can filter the physics signals from the background at the foreseen maximum data rate. The involvement of the group in the off-line reconstruction software developments has lead to a significant improvement of the muon reconstruction efficiency.

During the year 2001 the definitive Technical Design Report will be completed and construction of the first string will start. Deployment of one sector, a modular unit corresponding to 1/6 of a string, is foreseen for 2002. After successful deployment and recovery of this first sector, 'routine' production of subsequent strings should lead to a detector producing first physics data in 2003 and to a full detector in 2004.

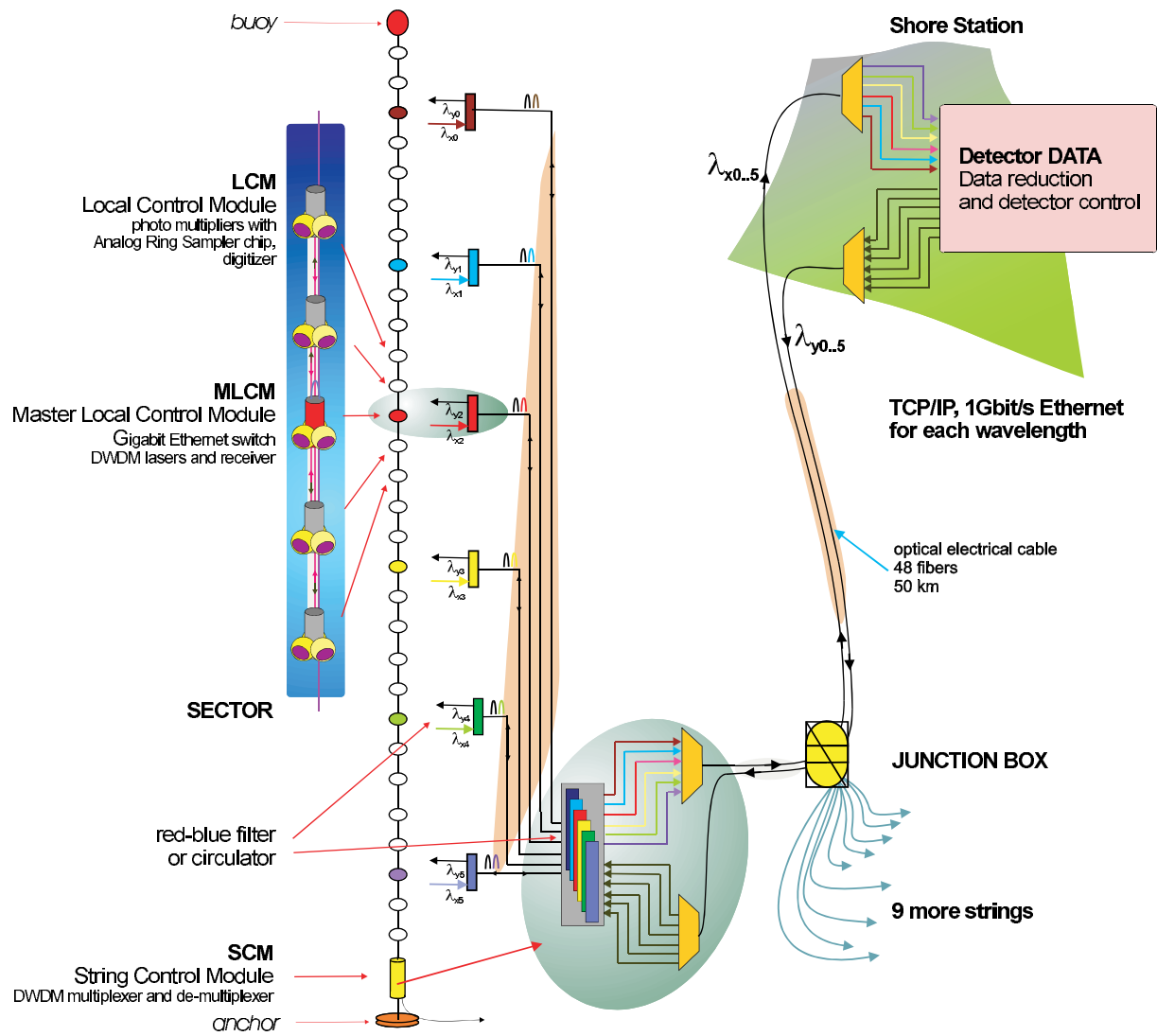


Figure 2.1: Principle of dense wavelength division multiplexing (DWDM) read out illustrated for one string.

3 ATLAS

3.1 Introduction

In the year 2000 the ATLAS/D0 group extended its interest towards massive computing using the GRID concept in view of the challenging data handling requirements of the LHC. Our expertise with the RASNIK alignment system led one of us to explore the possibility to improve the determination of the gravitational constant G_N using coupled pendulae monitored by RASNIK systems.

Regarding the detector construction efforts for the ATLAS experiment at CERN, major milestones were passed with the successful completion of the module-0 MDT chamber and with the assembly of the first silicon detector module. Concerning the D0 experiment at FermiLab, the detector hardware components constructed in the Netherlands were commissioned and we are now eagerly awaiting the first $p\bar{p}$ collisions¹ in the spring of 2001 to confront our reconstruction and analysis code with real data as opposed to Monte Carlo simulation!

3.2 ATLAS experiment

Muon Spectrometer

MDT chamber construction

Early 2000 the semi-automated MDT wiring line ("robot") developed jointly by CERN, NIKHEF and Frascati was installed in the large clean-room. The robot successfully wired about 700 tubes. These tubes were all individually tested for mechanical wire tension, wire location, gas leak rate and high voltage behaviour. Few tubes were found to be defective. In parallel with this work the spacer structure with the important RASNIK alignment components was assembled using the precision jig mounted on the large granite table. As a final step six (2×3) layers of each 72 tubes were glued onto the spacer structure using again the precision jig. Fig. 3.1 shows the module-0 MDT chamber during one of the gluing steps.

After completion, the gas manifold has been connected and tested. Subsequently the chamber was sent to CERN to undergo an X-tomography scan to determine the position of each of the $6 \times 72 = 432$ wires. The analysis software, written by us, gave an overall r.m.s. on the location of the wires of $16 \mu\text{m}$, well below the specified $20 \mu\text{m}$. With this the MDT assembly line in

¹First $p\bar{p}$ interaction were registered by the D0 experiment on April 3, 2001.



Figure 3.1: Photograph of the module-0 MDT chamber during the final assembly step.

Amsterdam has been certified for the subsequent production of the 96 MDT chambers.

Despite the excellent mechanical quality of the module-0 MDT chamber, it was decided to adapt some specific parts of notably the quality control equipment (e.g. the single tube gas leak rate and the high voltage test setups). This in view of a reduction of the required manpower during the four years of MDT chamber production. These changes will delay the start of production to the summer of 2001. By the end of 2001 we expect to have completed ten MDT chambers.

RASNIK alignment system

In 2000 the design of the RASNIK CCD camera, light source and data-acquisition electronics has been largely completed. Thousands of CCD cameras and light sources have been delivered to and are presently employed at many institutes world-wide. Even though the industrial supplier of the lenses had serious difficulties to meet the agreed upon characteristics, the lenses required for the RASNIK in-plane systems are available in large quantities. With this a major commitment of the NIKHEF ATLAS group has been completed successfully although not entirely within the foreseen budget.

Apart from ATLAS other parties have shown interest in the RASNIK as well. E.g. tests are ongoing to use RASNIK systems for the alignment of the magnets for the LHC machine, for the CLIC project (one of the candidate technologies for a multi-TeV e^+e^- collider), for



Figure 3.2: *Half Vacuum Vessel Shell ready for final Machining at Machine Fabriek Amersfoort (IJsselstein). Photo: courtesy Charles de Graaff, Schelde Exotech*



Figure 3.3: *Final machining at Machinefabriek Amersfoort (IJsselstein) of a half Vacuum Vessel Endplate. Photo: courtesy Charles de Graaff, Schelde Exotech*

the monitoring of elements of the optical delay lines of the Very Large Telescope at the European Southern Observatory and for the quality control of the dimensions of metal sheets produced by the CORUS (former Hoogovens) group.

End Cap toroids

The ATLAS End Cap Toroids (ECTs) are an in kind contribution of NIKHEF to the ATLAS collaboration. Their basic design was made by the Rutherford Appleton Laboratory (RAL). Dutch Industry is responsible for the manufacturing. Contracts for the manufacturing were signed in February 1999. NIKHEF's supply for the ECTs consists of three major parts:

1. a 1:5 scale model of the vacuum vessels, completed and tested in 1998.
2. two aluminium vacuum vessels of 10.7 m diameter and 5 m axial length and a weight of 80 ton each. Each vessel houses a cold mass.
3. two cold masses each consisting of eight superconducting coils of $4 \times 4.5 \text{ m}^2$ and eight keystone boxes. The keystone boxes are used as reinforcement of the whole structure and form a major part of the cold "buffer". The coils are indirectly cooled. The weight of a cold mass is 160 ton.

Vacuum vessel

The vacuum vessels are made by Schelde Exotech (EXO) in Vlissingen. Manufacturing started mid

1999 after a successful Production Release Review (PRR). Manufacturing is done in two steps. First half shells (Fig. 3.2) and end-plates (Fig. 3.3) are made to oversized dimensions by cutting, bending and welding of 40 to 75 mm thick aluminium plates. This step was mainly realized by EXO. Then the parts are machined to within the required 1 mm and even 0.1 mm tolerances. Machinefabriek Amersfoort (MFA) in IJsselstein is able to machine the halves in "one go" while machining at EXO would require four translations on the cutting machine. Therefore it was decided to subcontract this part to MFA. End of 2000 the end-plate halves were completed at MFA. The huge amount of full penetration welds required much more time than expected. This results in a six month delay in the delivery of the first vessel which now will be shipped to Geneva in June 2001. The ATLAS Magnet Project has enough float to accommodate this delay. Production of the second vessel is well underway. This vessel will be delivered on schedule, i.e. assembled and tested by March 2002.

Cold mass

HMA Power Systems in Ridderkerk manufactures the cold masses. RAL's design was completed but at the request of ATLAS it was decided to improve the reliability of the cooling by implementing dual cooling circuitry and additional heat shields. Fortunately only manufacturing drawings had to be modified "thanks" to a delay in the schedule. The commissioning and fine tuning of the winding street was performed by winding a dummy coil. This full size coil is made prior to the manufac-

turing of the 16 double pancake coils. The fabrication problems encountered by one of the two suppliers of the super-conducting conductor encounters have not been resolved yet but fortunately the second supplier can supply all required conductor if needed. The delivered conductor is cleaned by bead blasting prior to impregnation. An in-line set-up in the winding street is operational. The aluminium coil formers are made by RDM in Rotterdam. All required aluminium has been delivered. A total of 650 m of aluminium pipe for the liquid He cooling circuitry has been supplied. Its bending and welding will be sub-contracted. Vacuum impregnation of the coils is foreseen. A vacuum mould is under construction and commissioning of the resin mixing machine was ongoing end of 2000. A mixture of two resins and a hardener will be used. The recipe has been developed by RAL and should yield a more (thermal) crack resistant epoxy at 4.5 K. The procedure will be tested through the impregnation of the dummy coil. Proper cleaning of all material that has to be impregnated is essential for the bonding. Tests on the procedure for the production series are ongoing. April 2000 the UK based FKI company became the new owner of HMA. There was a change in HMA's directorate and also the cold mass project leader left the company end of 2000. Although the new owner's focus is on the production of generators the completion of the cold mass contract is not endangered. Nevertheless there is a delay of about six months in the delivery of both cold masses.

Semi-Conductor tracker

This year saw the successful production of a carbon fiber disc prototype with a new core material, Korex, which is easier to glue and reduces the cost of an individual disc significantly. This disc is undergoing vibration testing and checks are being made on how stable the structure remains when the relative humidity changes. In parallel we also started the preparations to build 100 silicon detector modules. The highly automated assembly station has been completed, with reliable pattern recognition routines to help position the silicon detectors to a precision of $5 \mu\text{m}$ before gluing. Three prototypes have been made, showing the system can reach the required accuracy. A photograph of such a module constructed at NIKHEF is shown in Fig. 3.4. We expect to finalise both the disc and module designs in 2001 such that in 2002 all discs and silicon modules can be constructed. The integration of discs and modules commences in 2002 as well.

The modules transfer their data via laser diodes and fiber optics. We have set up an optical readout system

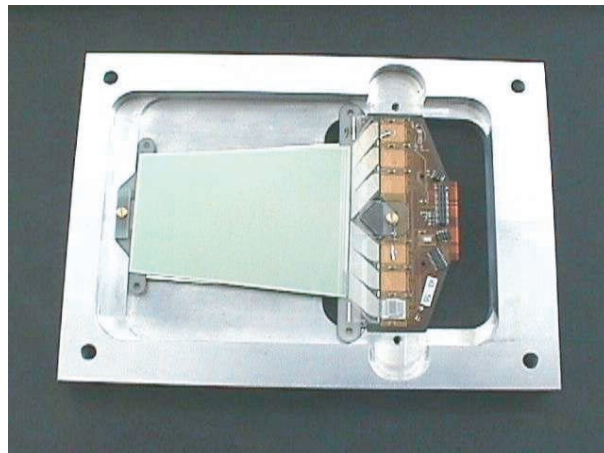


Figure 3.4: *Photograph of a silicon detector module for the ATLAS Semi-Conductor Tracker.*

in Amsterdam, using a homemade data encoder in place of the future Atlas encoder which could not be realized in time by the responsible institute. Our setup is crucial for the quality control of the components and for the testing the final modules at NIKHEF. Since there are very few test stands working within the collaboration, other institutes (like e.g. Universität Freiburg) also employ our test stand to test their modules.

Detector simulation and reconstruction software

In the last years, the ATLAS collaboration produced large samples of fully simulated data using procedure based software (written in FORTRAN). This data was successfully used to validate the physics performance of the detector. Nevertheless, it became clear that experiments like ATLAS should benefit from the use of modern object oriented software techniques (C++, JAVA, Eiffel, etc.). These techniques have been explored within the context of a CERN based R&D project managed by a Dutch ATLAS group member. As a result ATLAS has decided to opt for the object oriented C++ programming language. The current mission for the software development in ATLAS is to merge the large knowledge of the procedure approach with the best practice of object oriented design. NIKHEF continues to play a very active role in these developments.

Detector description

One of the crucial improvements of the object oriented design is its compatibility with a completely modular architecture. In particular, the description of the detector geometry is isolated from all "clients" programs,

i.e. simulation, reconstruction and visualisation packages. To describe the detector geometry, including logical structure, readout tree and a material database, a syntax in XML was developed and adopted by the ATLAS collaboration. The syntax utilises the symmetries as present in the geometry of the ATLAS detector; as an example Fig. 3.5 shows the XML generated geometry for the forward semi-conductor tracker. By using the XML industry standard many utility tools like inspection, validation and visualisation tools are facilitated.

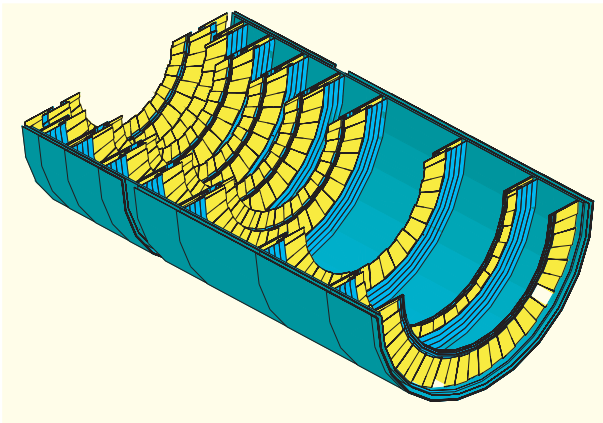


Figure 3.5: Visualisation of the lower half of the forward semi-conductor tracker, using the XML description.

Current effort is underway to obtain a complete description for each of the ATLAS sub-detectors using this XML syntax (see Fig. 3.6). This information is parsed through a 'generic model' that creates a transient representation, and can be inferred by the client software. For example, the geometry information can be translated via the generic model to GEANT4 objects and subsequently be used for simulation of the response of the geometry to traversing particles. Other packages have been developed that allow instantaneous visualisation of the geometric description of the detector as described by XML. Various reconstruction programs will interface to this 'generic model' in the near future as well.

Track reconstruction

Apart from these contributions to the central software architecture, NIKHEF plays a very active role in the development of track reconstruction programs. The AMBER and COBRA programs, developed and implemented in C++ at NIKHEF, are the first object oriented reconstruction programs that perform equally well or better than the FORTRAN equivalents. One of

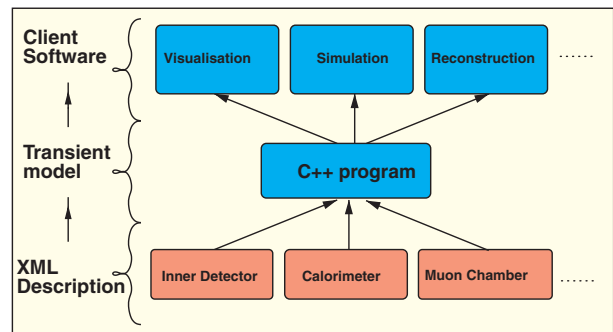


Figure 3.6: Schematic view of the interfaces between the XML descriptions, the transient model, and all application programs.

them was used to successfully reconstruct cosmic muon tracks in the DATCHA experimental set-up.

The 'COmBined Reconstruction for ATLAS' (COBRA) package, is developed to reconstruct tracks from muons by combining the results from the ATLAS sub-detectors. Relying on the pattern recognition and cluster finding algorithms of the sub-detectors, COBRA adds general tracking and fitting. Thus, COBRA allows for individual re-fits to obtain the covariance matrix for any point along the track, a global re-fit, including both trackers in ATLAS, propagation of tracks (including propagation of the covariance matrix) for track matching and statistical combination of track segments. The reconstruction method does not depend on the detector-version. As a consequence, the package can be applied to detectors other than ATLAS as well. Its physics performance both in combined and in stand-alone mode is very good.

Trigger, data-acquisition & detector control

In 2000 the ATLAS trigger, Data-Acquisition (DAQ) and Detector Control (DCS) Technical Proposal was submitted to the LHCC. Contributions to this proposal and to further work on the development of trigger, DAQ and DCS systems were made by NIKHEF in four areas:

1. Study of the Read Out Buffers (ROBs): very good results were obtained with the hardware and software developed for this purpose.
2. Paper and computer modelling results essential for the design have been obtained.
3. Work on the "On-Line Software" (responsible for control of the DAQ system); in particular on the

information exchange between the DCS and the "On-Line Software".

4. We assumed responsibility for the software for the ELMB. This is a dual processor CAN node developed jointly by CERN and NIKHEF. It will be used for control of the various ATLAS sub-detectors. General purpose application software and a framework for dedicated software were supplied.

Directly related to these contributions is the development of the MROD, a Read-Out Driver for the MDT muon chambers. This is a joint project of the Nijmegen and Amsterdam groups. The function of the MROD is to decode and multiplex the data from six MDT chambers onto a single link. In total about 200 MROD modules are needed. Each MROD is connected via one output link to a ROB. A first partial prototype of the MROD was successfully tested. This prototype made use of the hardware developed for the ROB study, the 100,000 gate FPGA was reconfigured to obtain the ROD functionality. Fault-tolerant decoding of the input data from one chamber (using simulated data based on data taken in the L3+COSMICS experiment) at full speed was demonstrated. Also the multiplexing function was studied with hardware developed for the ROB study: it was shown that full speed operation most probably can be obtained with the new prototype MROD-1 design. This design has almost been finished in 2000, production and testing will take place in 2001.

3.3 D0 experiment

NIKHEF has further developed the NIKHEF D0 Monte Carlo Production farm to a state that it can now run productions and do the reconstruction and analysis of the Monte Carlo generated data without human intervention. The production manager also takes care of the storage of the meta-data in the database ("SAM") and the transfer of the results to the tape-robot at FermiLab. At this time NIKHEF is the most productive site for Monte Carlo generated events in the D0 collaboration and has produced more events than all other institutes together.

The farm consists of 100 CPUs plus a dedicated farm server which runs the batch software and a dedicated file server where the results are stored temporarily before being declared in the database and sent to FermiLab to be stored on tape. The latest version of the production software is now continuously used to produce in the order of one event per three minutes per CPU for a typical $t\bar{t}$ event with 2.5 minimum-bias events superimposed. This means we can produce 50,000 events per

day. One event produces 2 MBytes of data. So per day the farm produces 100 GBytes of data. One such calculation of three minutes includes the generation of an event with Pythia or Isajet, the full D0 detector Monte Carlo (using GEANT3), the addition of minimum-bias events, the reconstruction using the latest version of the D0 reconstruction code and the analysis package.

Much work has been invested in trying to use the network connection between NIKHEF and FermiLab to minimise the transfer time and the failure rate. This connection is now in such a stable state that it becomes feasible to also use the NIKHEF D0 farm for on-line event reconstruction from experimental data from the detector. This mode of operation has not been tried but will be seriously considered and could give NIKHEF collaborators first hand access to the real data from the detector.

Another option which is under test is the local storage of data. The results produced by the farm using Monte Carlo generated or experimental data does not always have to be stored in the tape robot at FermiLab. The meta-data describing the data has to be stored in SAM, the D0 database of which a "local station" has been installed on the farm server. In the meta-data one has to specify where the real data is stored and this could be the FermiLab tape-robot but also the SARA tape-robot. In the event that somewhere else in the world somebody requests a file from SAM which happens to be stored at SARA, the system will take care that the data will be read back from the tape at SARA and transferred to the user and cached locally for further analysis. It is expected that this will reduce the file transfers by a considerable amount as the data is only transferred when needed. This system is operational in principal but has not been tried with real users yet.

From the D0 farm to the DataGRID

The NIKHEF D0 Farm is only a first step towards a much larger fabric which will eventually lead to the computing infrastructure for reconstruction and analysis for the LHC data. Further developments in this direction are done within the European DataGRID Project of which NIKHEF is one of the five principal partners. NIKHEF participates in several work packages one of which is farm management. In this project the D0 farm becomes part of a much larger farm where also jobs for ATLAS, ALICE and LHCb can run. Moreover NIKHEF is active in the network research work package, the particle physics application work package and in the test bed. In the DataGRID project the Amsterdam Computing Centre SARA and

the Dutch Meteorological Office KNMI are assistant contractors of NIKHEF; SARA to collaborate on networking, mass storage and the test-bed; and KNMI to provide the project with a different application to particle physics namely Earth Observation.

Much coordination is needed in projects of the size of the DataGRID which span the many countries and institutes and many different technologies.

3.4 ATLAS detector R&D spin-off

An experiment to determine G_N using RASNIK

The intended GRAPPA experiment employs a dual-pendulum set-up for the measurement of Newton's Gravitational constant G_N with a relative precision of about 1.0×10^{-4} . The pendulum motion is measured with RASNIK systems. A coded mask, the essential component for the RASNIK system in GRAPPA, was made. Its chess-board pattern ($1 \times 1 \text{ mm}^2$) consists of a million chess field squares of $1 \times 1 \mu\text{m}^2$ each. With state-of-the-art chip mask technology, contour position precision of 5 nm could be reached.

Recently, a publication by a group of the University of Washington claimed the measurement of G_N with a relative precision of 1.3×10^{-5} . In this experiment, the influence of the environmental gravitational field was eliminated by a slow rotation of the field masses. The torsion of the pendulum wire (a major error source) was eliminated by an active feedback method. The geometry of the field masses and the test mass has been chosen such that many first and second order errors are eliminated.

Since our present GRAPPA concept can not compete with the results of the group in Washington; we are investigating how to combine the excellent features of the Washington set-up with the high precision of the RASNIK system.

MediPix

MediPix is a collaboration between 15 European universities and research institutes. It is based at CERN, Geneva and it is an R&D activity approved by the CERN division for Education and Technology Transfer (ETT). Know-how obtained in designing semi conducting pixel detectors for high-energy physics is used to develop improved digital X-ray imagers, for use in medical, biological or analytical applications. Industrial partners have been identified, who are interested in commercial exploitation of these new imagers.

The MediPix detector is a sandwich structure of two

chips, one consisting of a matrix of reverse biased sensor diodes surrounded by a guard ring, the other containing a corresponding matrix of (deep)-submicron CMOS readout electronics. Every pixel electronics contains an amplifier, one or two individually tunable comparators and a digital counter. This CMOS circuit is bump-bonded in "flip-chip" technology to the sensor chip. For the sensor chip, high-resistivity silicon can be used with 100% conversion efficiency up to an X-ray energy of 10 keV. For higher energies GaAs and Cd(Zn)Te offer better conversion efficiencies.

At present, two versions of the CMOS readout circuit have been designed: Medipix-1 for the readout of 4096 pixels of $170 \times 170 \mu\text{m}^2$ each, and Medipix-2 for the readout of 65536 pixels of $55 \times 55 \mu\text{m}^2$ each. Medipix-1 has been tested primarily on GaAs sensors. Recently, our measurements on Medipix-1 with a silicon sensor have shown that the lower threshold in X-ray energy is about 5.5 keV, which opens up a range of interesting applications, especially because we hope and expect that the Medipix-2 circuit, which was submitted for production in December 2000, will show even less noise.

During a test-beam run at the European Synchrotron Radiation Facility (ESRF) in Grenoble, we have further characterised this Medipix-1 chip with a silicon sensor. Results are encouraging, especially the fine mapping with a pencil beam shows that full efficiency can be retained in the inter-pixel region, by suitable tuning the comparator levels. A high-speed test has shown an acquisition rate of 100 frames per second. No blooming or after-glow effects were seen.

Ongoing activities at NIKHEF include: deep submicron design for further versions of Medipix, especially to implement an ADC on the pixel level, wafer-probing of Medipix-1 and Medipix-2 wafers, I-V and C-V characterization of sensors, production of DAQ systems for MediPix-1, design of DAQ systems and chipboards for MediPix-2, and last but not least, combining several circuits in one larger sensor chip, to obtain large (about $3 \times 6 \text{ cm}^2$) uniform imagers without any intermediate dead area.

4 B Physics

4.1 Introduction

The B physics group at NIKHEF studies the breaking of charge-parity (\mathcal{CP}) symmetry. To accomplish this the group is involved in the HERA-B experiment at DESY and the LHCb experiment at CERN. The HERA-B experiment has been installed in 2000 and was partially commissioned before the shutdown in September 2000. The LHCb experiment at the LHC collider is planned to become operational in 2006. The development of detector components for LHCb is proceeding on schedule, while the same is true for software development and the study of data analysis methods.

4.2 HERA-B

Hardware

Most subsystems of HERA-B were installed and (partially) commissioned until the shutdown of HERA in early September 2000. Problematic units are the Outer Tracker (OTR) –to which NIKHEF contributed–, the Inner Tracker (installed, but not yet fully equipped) and the Muon chambers (of which the pad chambers, used for the pretrigger, show bad efficiency). The commissioning of the most important subsystem of HERA-B, the First Level Trigger (FLT), has been started, but is not yet complete. Below, we will give some details on the status of the OTR and of the FLT.

Outer Tracker

The installation of the OTR of HERA-B was completed in January 2000. Since then, the system has been available for more than 90% of the time. The high voltage and gas systems are operational and fully integrated with the global HERA-B slow control.

The following minor problems were identified and subsequently solved:

- Gas leaks. A lengthy search was carried out revealing dirt in the bellows of pumps, and loosening of gas fittings.
- About 2% (138) of the readout boards did not give signals, mostly caused by loose cables. Measures were taken to prevent this problem in the future. With two mechanical changes the cable weight is eliminated, and a more secure fixation of the plug itself is provided.
- Due to reflections between the TDC outputs and the FLT-Linkboards, the discriminator thresholds

of the first 4 superlayers had to be raised. The source of the problem –poor termination– has been identified, and measures are taken to eliminate the noise.

More important was the high rate of HV failures. When the chambers were opened during the HERA shutdown, it turned out that about 90% of these failures were due to radiation damage on the HV-distribution boards. This exclusively concerns the back of the distribution boards on which two capacitors are treated with another insulating film than those on the frontside. These boards are being corrected and replaced, and should restore 90% of the shortened HV channels.

The remainder of the shortages were mostly due to mechanical instabilities, and measures are being taken to improve this. The effectiveness of these actions is not easy to prove since the shortage rate is now already at such a low level, that in three months time no significant statistics has been build up.

First-Level Trigger

The analysis of the data taken allows some insight in the operation of the FLT. It must be noted that the low efficiency of the OTR chambers (only about 93%, due to higher discriminator thresholds than foreseen, and due to channels for which the HV was switched off) leads to a low efficiency of the FLT, and makes the result of this analysis rather uncertain. Since these problems are now solved –the cause of reflections has been eliminated, allowing lower TDC thresholds, and the cause for 90% of the HV failures has been eliminated– the input to the FLT will be of much better quality than before. Current estimates find Track-Finding- Efficiencies of the FLT including the OTR efficiency in the range of 50% to 80%. Since the FLT is geared to trigger on two leptons (electrons or muons) with an invariant mass of about the J/Ψ mass, the total trigger efficiency for the 2000-Run was much worse than the design value. This does not take into account that part of the acceptance was not yet fully equipped (the ITR), which reduces the FLT efficiency still more. The installation of the ITR is progressing steadily.

Physics Results

The analysis of the data taken until the shutdown yields about 3000 $J/\Psi \rightarrow \bar{\mu}\mu$ and 40000 $J/\Psi \rightarrow e^+e^-$ events. In the electron channel, the J/Ψ peak appears clearly only if one requires not only the electron hits in

the ECal, but also a hit from the bremsstrahlung photons. This cut reduces the number of analyzed J/Ψ 's in the e^+e^- channel to about 4000.

Nevertheless, it seems possible even with this sample to establish an A -dependence of the J/Ψ production cross sections.

Searches for detached vertices involving J/Ψ 's which are indicative of B -meson decays, have resulted until now only in very small numbers of candidates; The intriguing point is that more candidates are found than expected (one expects roughly 1 B per 1500 J/Ψ 's). However, given the large uncertainties in the b -production cross section, this is highly speculative.

In spite of a critical report of the Extended Scientific Council of DESY, the Directorate of DESY has decided on Dec. 22nd to continue HERA-B until the end of the year 2002. The physics program will encompass studies of heavy quarks, charmonium and Ypsilon production, Drell-Yan physics and rare decays such as $D \rightarrow \bar{\mu}\mu$. It is uncertain whether HERA-B will continue beyond the year 2002.

4.3 The LHCb Experiment

The B physics group at NIKHEF is heavily involved in the LHCb experiment at CERN. The group concentrates on tracking and has accepted various responsibilities such as the leadership for the Outer Tracker project and the coordination of Tracking Software activities. Moreover, NIKHEF is fully responsible for the pile-up detector and the mechanical design of the micro-vertex detector. In addition, NIKHEF participates in the development of radiation hard front-end read-out electronics of the vertex detector.

Outer Tracker

Given that the proton beams in LHC interact every 25 ns, it is important to restrict drift times to a narrow window: time overlap of signals from many bunch crossings would render pattern recognition unfeasible. Tests of prototype arrays of straw tubes have been carried out with pion beams from the CERN Proton Synchrotron.

Drift time spectra were measured for a large range of drift gas mixtures with varying CF_4 content. The admixture of CF_4 is essential for short signal collection times. Reduction of the CF_4 content however improves the resolution of the drift cell, allows for chamber operation at lower voltages and makes the detection gas cheaper. A drift gas mixture of $Ar/CF_4/CO_2$ (75/15/10) seems to be optimal with respect to low

CF_4 content and drift speed, even for magnetic fields up to 1.4 T. In the beam test measurements the observed drift cell efficiency and resolution have reached their design values, due to improved electronics and a better grounding scheme. See also Fig. 4.1.

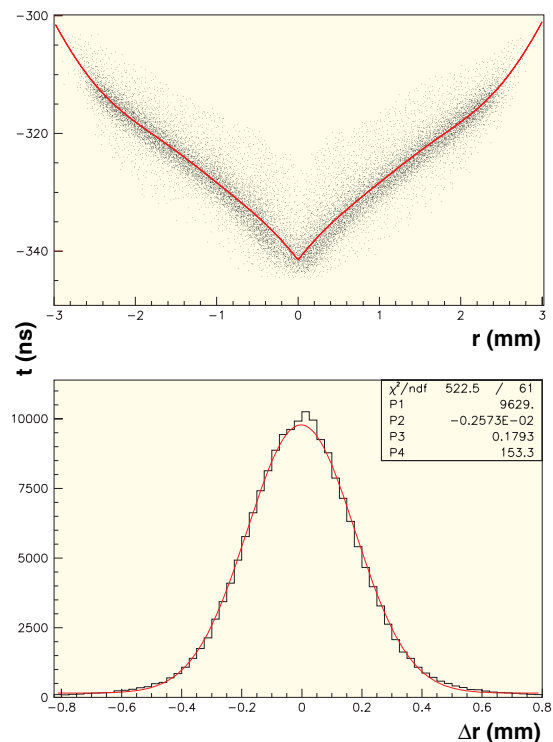


Figure 4.1: A fit of the $t(r)$ relation for a straw tube (upper graph) and resolution determination from the residuals histogram (lower graph) for: $Ar/CF_4/CO_2=75/15/10$, $B=0$, $HV=1600$ V.

Straw chambers of 2 m length have been incorporated in the beam test setup. The long anode wires have to be supported at intervals with positioning pieces (twistors) inside the straw tube. Measurements have shown that the twistors fix the wire within the required mechanical precision and cause an insensitive straw length of only 12 mm.

The amount of cross-talk between neighbouring straws is investigated both in beam test and laboratory conditions. Together with the detailed studies on electrical behaviour and shielding properties of straws with outer

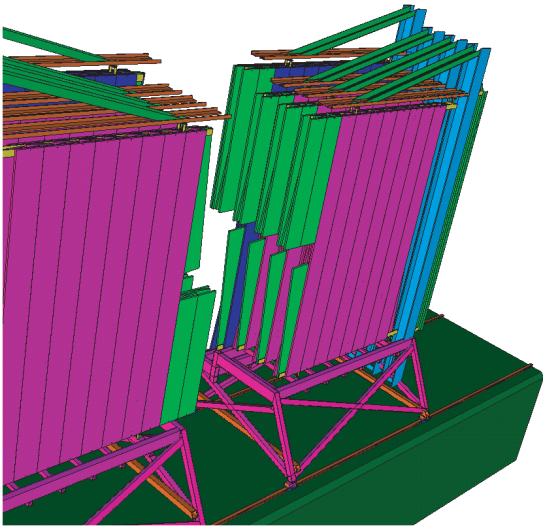


Figure 4.2: *Three-dimensional drawing of the frame containing stations T7 to T10.*

windings of various materials, the module design could be significantly improved.

Another 2 m long prototype straw chamber has been incorporated in the HERA-B detector during the 2000 physics run. The total dose received by the prototype equals 4 months of running in the hottest regions of the LHCb Outer Tracker. The chamber was operated with the standard HERA-B gas mixture, which is equal to the gas mixtures used in earlier ageing tests. During this ageing test, no deterioration of straw tube characteristics has been observed. This increases not only the confidence in the use of Kapton XC as a cathode material but also the selection of materials used in the module construction.

The frame design for the downstream stations T7 to T11 has made much progress. Detailed design work is done to integrate the modules into the station frame with high mechanical precision. In the design of support frames attention should not only be paid to the accessibility of station modules but also reaching the inner tracker stations or accessing the magnet tracking stations should be easily done. For these reasons a geometry is preferred that permits opening and closing. In Fig. 4.2 a three-dimensional model drawing of the station frames for T7 to T10 is depicted.

For a proper readout of the straw tube signals, extensive tests have been performed on the straw tube and ASDBLR preamplifier-discriminator combination. The

ASDBLR, originally developed for the ATLAS TRT detector, seems to match our needs entirely. Straw tubes with an aluminium outer winding have been selected as the baseline solution because of their low cross-talk characteristics.

A digital readout chain based on the HP-TDC chip is advancing to the prototype stage. Apart from this baseline the development of a new TDC has started at the ASIC lab in Heidelberg. This new TDC is designed for use in the LHCb Outer Tracker and therefore is better matching our needs; it offers better performance with a more compact data format. The TDC will be designed in a radiation-hard process which allows for integration of the chip in the on-detector electronics, thereby saving a large amount of cabling.

4.4 Vertex detector

The identification of detached vertices associated with B -meson decay (with an average track length of 7 mm) is an important feature of the LHCb detector. The vertex detector consists of 25 pairs of silicon strip detectors. During data taking the detectors have to be positioned at 8 mm from the beam, but during refill of the collider with protons from the SPS and the acceleration stage they have to be retracted over 3 cm.

NIKHEF is responsible for the vacuum vessel of the vertex detector, including the shielding and movement of the detector components. It is not possible to place the detectors directly in the ring vacuum system. In the first place the outgassing from the detectors with their associated electronics, support and cabling is in conflict with the ultra-high vacuum requirements of the ring. Furthermore, the detectors have to be shielded from the high electromagnetic fields that will be induced by the passage of the beam. And finally the rapid variation of the beam pipe dimension in the detector vessel will introduce strong wake fields that will cause beam blow-up.

Therefore, a design has been made in which the detectors are located in a secondary vacuum box, as is shown in Fig. 4.3. Since the detectors are partly overlapping, the construction of the separation foil is far from trivial. The physicists demand as little material as possible in order to diminish multiple scattering and unwanted particle production. For safety reasons one would like to have a sturdy separation between the primary ring vacuum and the secondary vacuum in which the silicons are located. As a compromise the separation foil will be made from 250 μm aluminum. The vulnerability of the foil puts strong safety requirements on venting and

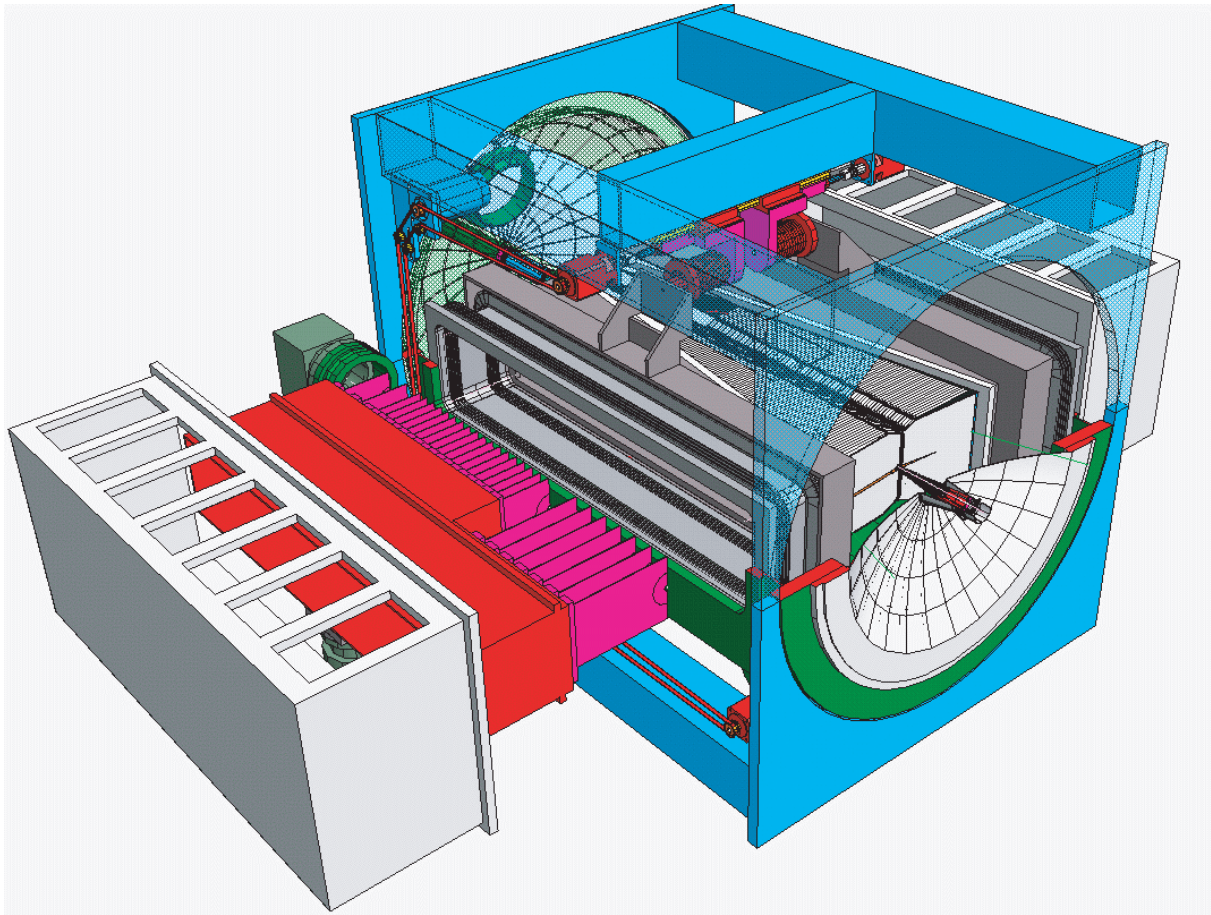


Figure 4.3: *The vacuum tank of the vertex detector. The silicons are placed in a secondary vacuum vessel. The figure shows the situation, in which the two secondary vacuum vessels are in the closed position. During injection the two secondary vacuum vessels will be moved apart. Each detector half is connected to the tank through a large rectangular bellow. In the figure one detector halve is visible outside the tank.*

evacuation of the vertex tank. A PLC-based control system has been designed to accomplish this task.

For the cooling of the silicons and the electronics a two-phase system with gaseous and liquid CO₂ has been proposed. The radiation resistance of CO₂ is excellent. In a first test set-up this system has shown to have the required cooling capacity.

Development of a radiation hard front-end chip for the vertex detector at LHCb

Special attention has to be given to the front-end chip of the silicon detectors due to the harsh environment, in which the hybrids will reside; at a distance of 5 cm from the LHC beams the expected radiation level amounts to 2 Mrad/year. In a collaboration between the ASIC-lab

in Heidelberg, Oxford University and NIKHEF various components of the front-end chip have been submitted in the 0.25 μm CMOS technology, which promises excellent radiation hardness if appropriate layout techniques, like enclosed transistors and guardrings, are used. These measures improve the behaviour under irradiation, especially with respect to leakage current and single event latchup. The performance of these test chips, containing a preamplifier and pulse shaper, LVDS output drivers, analog outputs and comparators has been tested and compared with simulations.

In September 2000 the first 128 channel 40 MHz full-size Beetle1.0 chips, featuring pipelines and I²C control logic, came back from the manufacturer. Since then measurements of the chip characteristics like pulse

shape and equivalent noise charge are performed. Also the radiation hardness is under investigation.

Further submissions of improved versions of the Beetle1.0 chip are foreseen to take place in 2001.

Pile-Up Veto System

A large fraction of the crossings at LHCb will contain multiple interactions. Since the processing of those events is time consuming and problematic in track reconstruction, their rejection is essential at the level-0 of event selection. Two dedicated Si-detector planes are placed in the backward region of the vertex detector vessel. The detector planes are identical to those used for the level-1 trigger in the rest of the vertex detector.

Hits in the two planes are correlated if they have the same origin. A correlation matrix provides a vertex origin histogram. The highest peak is ascribed to the true vertex. The hits correlated with that peak are masked and the peak search is performed once more. A second peak points to the second interaction. The effect of the Pile-Up Veto is shown in Fig. 4.4, the relative gain in "single" B -event statistics is about 30-40%.

The readout chip is the Beetle chip. The comparator outputs will produce a direct signal for a combination of 4 detector strips. Under study are the hybrid, cables, connectors and vacuum feedthroughs. Most design issues are similar to those for the level-1.

In Fig. 4.5 a schematic view of the layout of the Vertex Finder processor is given. Event data is sent to a

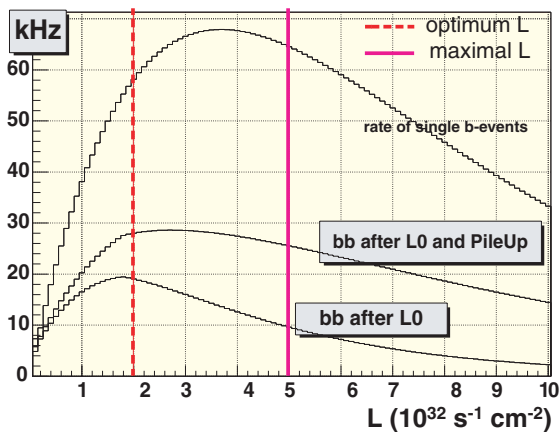


Figure 4.4: Number of "single" B -events as a function of luminosity: events produced (top), after level-0 high-pt trigger and pile-up veto (middle) and after level-0 trigger without pile-up veto (bottom).

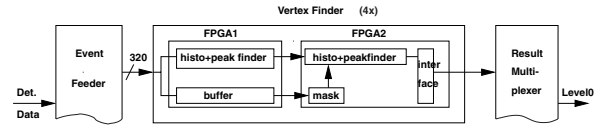


Figure 4.5: Schematic layout of the Pile-Up Veto electronics.

Vertex Finder module; the next (of four in total) will get the following event. For the processing tasks two Mgate XILINX FPGA's are foreseen. The results of the Vertex Finder modules are multiplexed and sent to the Level-0 supervisor. The conceptual design has been completed, a subdivision of the system and definition of the subcomponents is proceeding.

4.5 Track Reconstruction

The tracking system serves to find and measure all the tracks produced in a $B\bar{B}$ event. A typical event in the simulation program is depicted in Fig. 4.6. Besides a handful of B -decay particles on average a hundred additional particles are produced, either directly in the pp collision or as secondaries, in interactions of primary particles with the detector material.

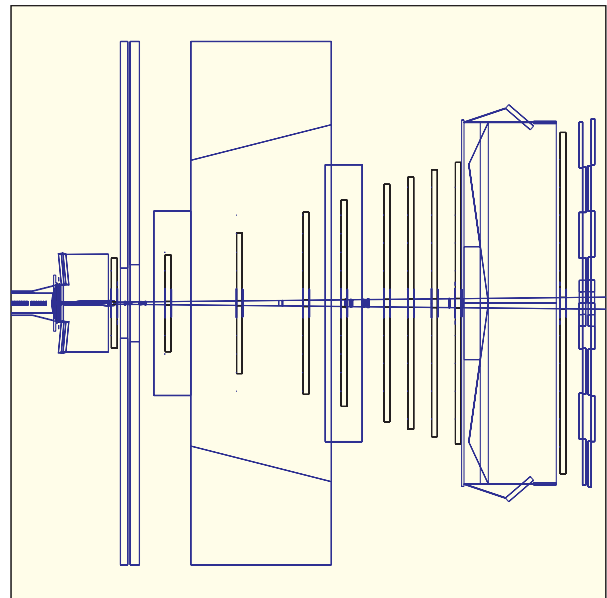


Figure 4.6: A simulated $B \rightarrow \pi^+ \pi^-$ event in the LHCb detector.

The LHCb software consists of a simulation program and a reconstruction program. In the GEANT simula-

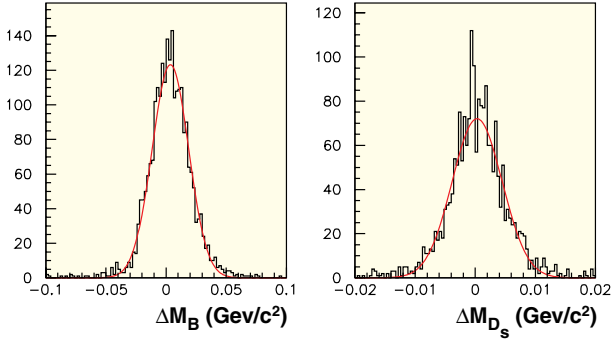


Figure 4.7: Reconstructed mass difference distributions for simulated $B \rightarrow \pi\pi$ events (15 MeV, left plot) and for $D_s \rightarrow KK\pi$ events (4 MeV, right plot).

tion program the detector response (the “hits”) to each traversing particle are simulated, in the reconstruction program the detector hits are again linked to form reconstructed tracks. Resolutions and efficiencies are calculated by comparing the reconstructed tracks to the original particle trajectories. The results of these studies are used to optimise the design of the LHCb detectors. For the tracking part the optimisations are mainly related to the optimal number and size of the tracking planes, the required granularity, the choice of the stereo angles, and the comparison of the relative importance of resolution vs. multiple scattering.

The NIKHEF group is responsible for the overall track reconstruction program, as well as for most of the tracking optimisation studies.

The track reconstruction program is an object oriented package in which algorithms for pattern recognition and the momentum refitting are implemented. Both algorithms use a Kalman fit method for track reconstruction, profiting from the iterative nature of the Kalman method in the pattern recognition task.

The pattern recognition algorithm itself consists of sub-algorithms of “track seeding”, *i.e.* finding initial segments of tracks in well suited areas of the detector, and of “track following”, *i.e.* following the tracks from the seed area into other parts of the spectrometer. The seed areas are the downstream region of tracking stations towards the end of the spectrometer and the region of the vertex detector. In both regions, due to absence of a strong magnetic field, track segments can be well approximated by straight lines.

Currently only the upstream tracking algorithm is im-

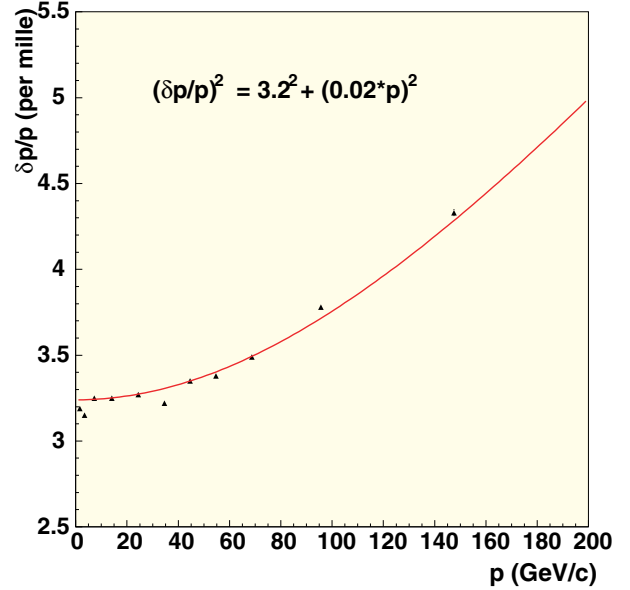


Figure 4.8: Reconstructed momentum resolution as a function of track momentum. The resolution is parametrised by: $\delta p/p = \sqrt{(0.32)^2 + (0.0002 \times p)^2}$.

plemented, leading to an efficiency of 90% to reconstruct the tracks in a $B \rightarrow \pi\pi$ event.

In the track refit, the particle trajectory is fitted from the vertex, through the dipole magnetic field, towards the calorimeters. The result of this fit is a precise prediction of the position, the direction and the momentum of the particle at each position along the trajectory. The momentum of the particle is mainly determined from the measurements of the main tracking system, while the position and direction at their production vertex are determined from the vertex detector hits. The momentum resolution of the reconstructed tracks is shown as a function of the true momentum of the track in Fig. 4.8. The average momentum resolution is $\delta p/p = 0.37\%$. For particles up to energies of 100 GeV, the precision of the momentum determination is limited by multiple scattering. Only for even higher energies, the measurement precision of the inner and outer trackers become important.

Precise measurements of the momentum and direction of B -decay particles lead to a precise measurement of the reconstructed mass of the resonance, which is subsequently important to obtain a background free selection of B -decays. In Fig. 4.7 the mass resolution distribution is shown for two benchmark decays: a decay of a B -meson into a $\pi\pi$ final state, and a decay

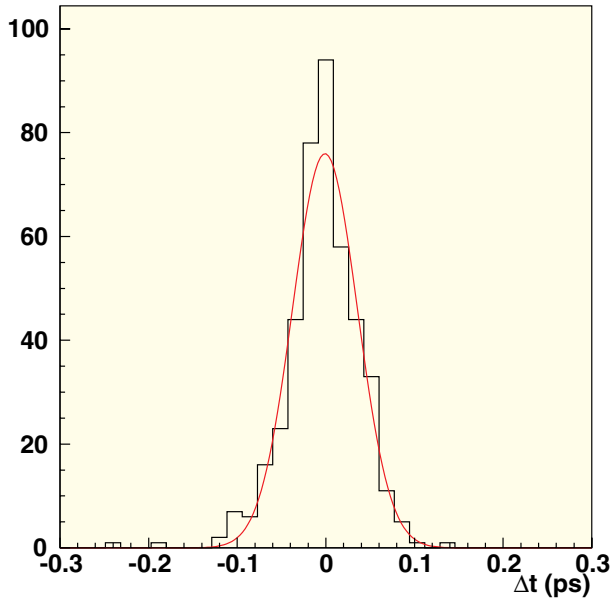


Figure 4.9: Decay time difference distribution for simulated $B_s \rightarrow D_s K$ events. The expected time resolution is 36.6 fs, or 3% of the B_s lifetime.

of a D_s -meson into a $KK\pi$ final state. The obtained resolutions are 15 MeV and 4 MeV respectively.

4.6 Physics Performance

In the physics performance studies NIKHEF focused on the decays of the B_s -meson. One of the main challenges of physics with the B_s -meson is to resolve the oscillation frequency of the $B_s - \bar{B}_s$ oscillations, for which the lower limit currently is $\delta m_s > 14 \text{ ps}^{-1}$. The expected decay time resolution for reconstructed B_s -mesons in LHCb is 3% (see Fig. 4.9).

The topics studied by NIKHEF are:

- Reconstruction of the decay-channel $B_s \rightarrow D_s^\mp \pi^\pm$. This channel can be used to measure the mixing frequency of B_s system, due to the fact that the charge configuration of the final state directly relates to the flavour of the B -meson at decay. Current studies indicate a sensitivity up to $\delta m_s = 60 \text{ ps}^{-1}$.
- Reconstruction of the decay-channel $B_s \rightarrow D_s^\mp K^\pm$. Contrary to the previous channel, in this decay each charge configuration of the final state can be reached by both flavour B -mesons, allowing for \mathcal{CP} violation to occur. This decay is optimally suited to study the angle γ in the

unitarity triangle of the CKM matrix. The reconstruction of this channel is very similar to the previous channel, the main experimental challenge is the suppression of backgrounds.

- Reconstruction of the channel $B_s \rightarrow J/\psi \phi$. The final state in this decay is a \mathcal{CP} eigenstate, such that it can be produced by decays of the \mathcal{CP} eigenstates of the B_s -meson: B_{heavy} and B_{light} . An angular analysis of the final state particles allows a measurement of the difference of the decay rate of the B_{heavy} and B_{light} -mesons and in particular of the \mathcal{CP} angle $\delta\gamma$. A value of $\delta\gamma$ different from zero indicates the presence of physics beyond the Standard model.

More information on HERA-B, LHCb and the NIKHEF participation in the two experiments can be found at <http://www-hera-b.desy.de>
<http://lhcb.cern.ch>
<http://www.nikhef.nl/pub/experiments/bfys>

5 CHORUS

5.1 Introduction

NIKHEF participates in the CHORUS (WA95) collaboration at CERN since 1992. The experiment has been designed to discover or exclude $\nu_\mu \leftrightarrow \nu_\tau$ oscillation with high sensitivity in the parameter region of small mixing ($< 10^{-3}$) and 'large' $\Delta m^2 (> 10(eV^2/c^4)^2)$. The results –even if only excluding neutrino oscillations in its region of sensitivity –severely constrain theoretical oscillation scenarios.

The CHORUS detector is 'hybrid', having electronic tracking components and an active nuclear emulsion target. This combination provides a powerful detection method for ν_τ charged current (CC) interactions. In the $\nu_\mu \leftrightarrow \nu_\tau$ channel, this method and the fact that the CERN-SPS ν_μ beam has a negligible ν_τ contamination (3.3×10^{-6}), allows in principle to claim the observation of neutrino oscillation in the case of a single recognised ν_τ CC interaction event.

In the emulsion target, charged particles produce –after development– silver grains with an average size of $1 \mu\text{m}$ and a density of 300 per mm. A τ can be recognised by its decay (kink) topology. This method allows a background free ν_τ CC interaction detection for leptonic τ -decays while bringing an almost negligible background for hadronic decay channels ('white kinks': hadron scattering without visible nuclear break-up or recoil, which can resemble τ -events).

Upon any event trigger in the electronic part of the detector, kinematic measurements are carried out using the muon and the hadron spectrometer, and the (118 ton) compensating lead-'spaghetti' calorimeter. Precise positions and directions of trajectories are deduced from fiber tracker planes. For events of interest, these trajectories are followed backward, pointing the way to the corresponding neutrino interaction vertices and possibly associated decay kinks of short lived particles in the emulsion.

5.2 Neutrino oscillation analysis

The first phase of the neutrino oscillation analysis has been completed (see Fig. 5.1). Results have been published [1]. No τ -candidates having been found, the oscillation probability has got an upper limit of $P(\nu_\mu \leftrightarrow \nu_\tau) \leq 3.4 \cdot 10^{-4}$ at 90% CL.

The second phase of scanning and analysis –in progress at present– aims at the full exploitation of the CHORUS potential for oscillation physics, and –as important

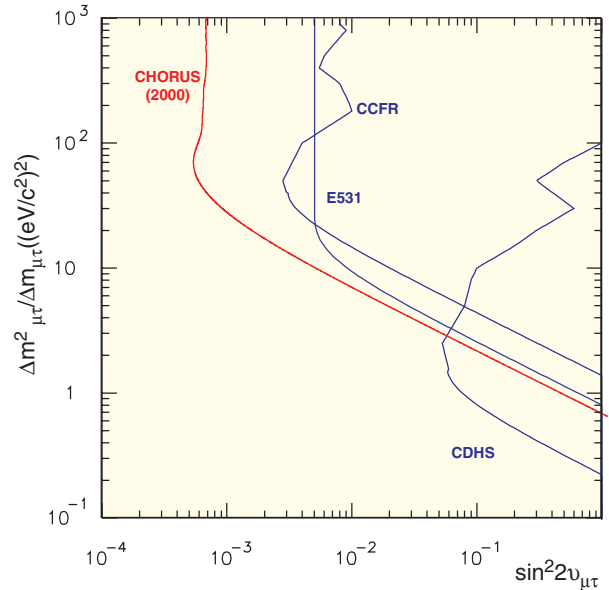


Figure 5.1: Exclusion plot for $(\nu_\mu \leftrightarrow \nu_\tau)$ oscillation with the CHORUS Phase-I analysis result [1].

additional research topic– charm physics. A major restructuring and upgrade of the analysis software, as well as a development of new methods in scanning (because of increasing scanning speed), has been accomplished. Developing this new software took more time than foreseen. Re-processing the data could be accelerated using Condor [2] on more than 100 Linux desktop PC's, partly compensating for the time delay.

The emulsion scanning is to a major extent performed in Japan. European institutes that have joined the scanning effort contribute increasingly. An automatic scanning facility (three microscope systems) with megapixel digital camera and digital signal processors has been set-up by CERN and NIKHEF for flexible –fully software controlled– track and vertex finding in the emulsion. A dedicated computer farm is used for on-line processing of the scanning data.

During the year 2000 the NIKHEF team was involved in emulsion scanning and analysis for neutrino oscillation physics. In addition a careful study for understanding the kinematic behaviour of the (marginally significant) 'white kink' background in hadronic τ decay channels was carried out. Simultaneously the analysis of CC ν_μ interactions, in the emulsion target as well as in the calorimeter was pursued.

5.3 Charm production

A pioneering study [3] has been made for charm production in the emulsion target. The search includes both deep inelastic and diffractive charm production. The use of emulsion allows to record different classes of ν -events with high precision. To suppress any background, the deep-inelastic charm production study concentrates on the muonic decay channels of the charmed hadrons. The first sample of 132 charm decay events has been analysed. It is a forebode of a much larger sample being collected in the phase-II analysis. Measurements have been obtained for charm production as a fraction of the CC cross section, the charm quark mass and the strangeness-down ratio of the nucleon. The methods developed for the analysis can be applied to the forthcoming more extensive charm studies. As an example, the neutral-to-charged charm production ratio for muonic decay events as a function of neutrino energy, compared with a previous emulsion experiment (E531), is shown in Fig. 5.2.

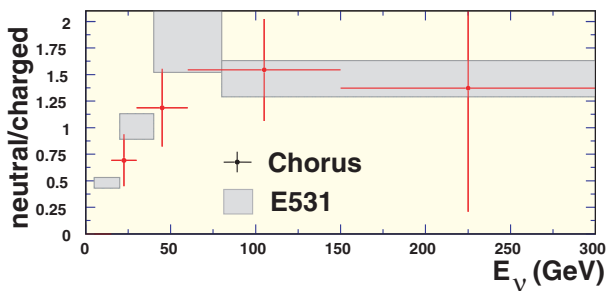


Figure 5.2: *Production ratio of neutral and charged charmed hadrons with muonic decay as a function of incoming muon-neutrino energy. The CHORUS data (statistical errors only) are compared with data from the earlier E531 Fermilab emulsion experiment.*

After a charm-production study [4] based on di-muon events from neutrino interactions in the (lead) calorimeter, a high statistics data sample with the CHORUS calorimeter as active target was obtained during a dedicated run in 1998 after the emulsion data taking had stopped. The analysis of these data provides a measurement [5] of neutrino-induced deep-inelastic differential cross sections on lead (see Fig. 5.3), from which $F_2(x, Q^2)$ and $xF_3(x, Q^2)$ structure functions can be extracted with a precision comparable to earlier results for iron targets. Neutrinos with an energy between 10 and 200 GeV were selected for the analysis. After cuts the data sample comprises about 1.1M ν -events and 230k $\bar{\nu}$ -events. A fast Monte Carlo simulation has been de-

veloped to correct for acceptance and the experimental resolution. The underlying cross section model is based on the GRV94LO parton distributions with modifications to allow for a non-zero longitudinal cross section and nuclear effects. A phenomenological correction is applied to improve the description of the data at low Q^2 .

Simultaneous measurements on four targets of widely different nuclear composition (polyethylene, marble, iron and lead) to measure the neutrino neutron-proton total cross section ratio are in an advanced state of analysis.

References

- [1] E. Eskut et al., Phys. Lett. **B497** (2000) 8
- [2] <http://www.cs.wisc.edu/condor/>
- [3] O. Melzer, PhD Thesis Univ. of Amsterdam, 2001
- [4] C.J.A.F. v/d Poel, PhD Thesis Univ. of Amsterdam 1999,
<http://choruswww.cern.ch/Reference/Theses/vanderpoel.ps.gz>
- [5] R.G.C. Oldeman, PhD Thesis Univ. of Amsterdam 2000,
<http://choruswww.cern.ch/Reference/Theses/oldeman.ps.gz>
and Proc. ICHEP2000, Osaka (World Scientific)

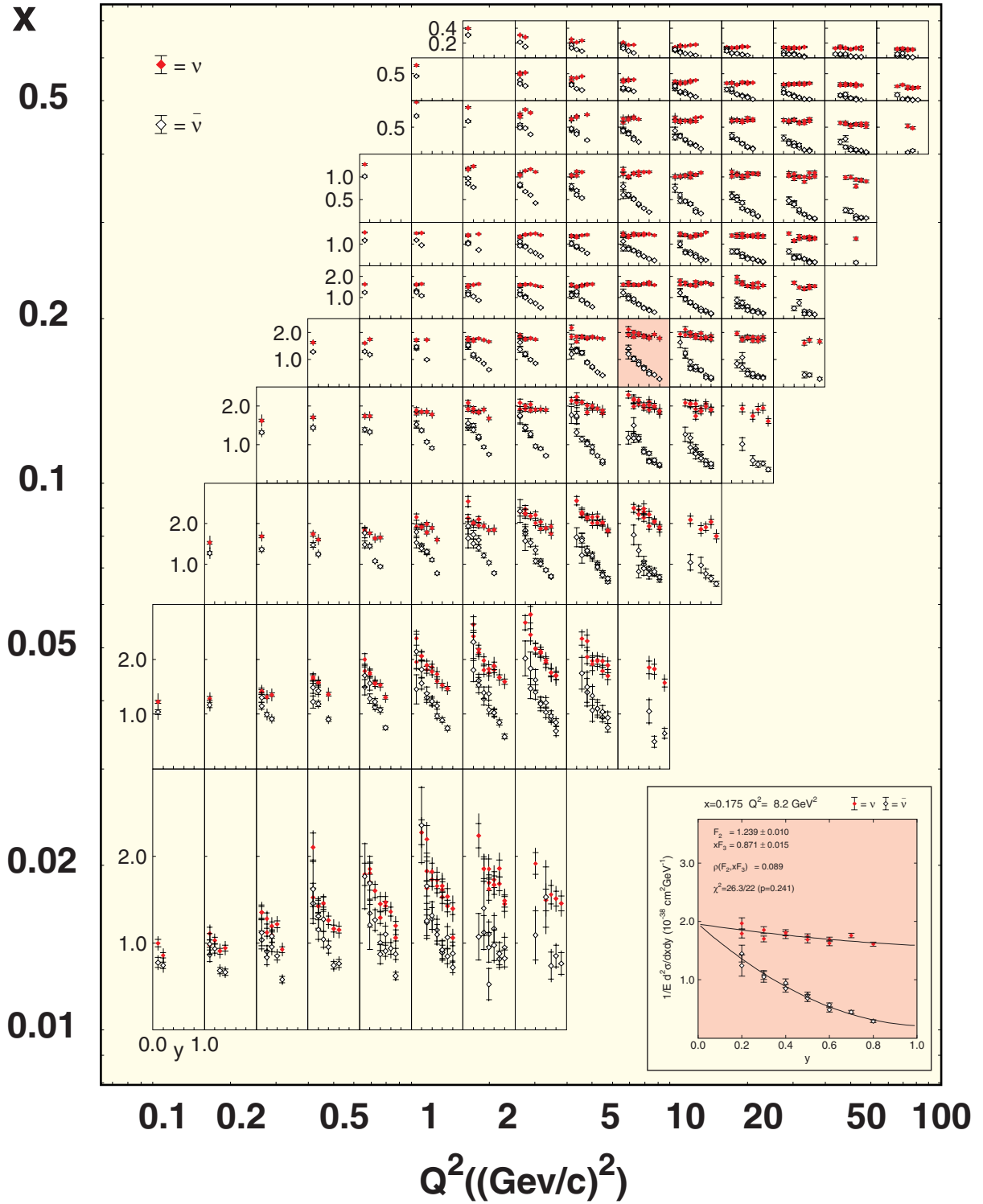
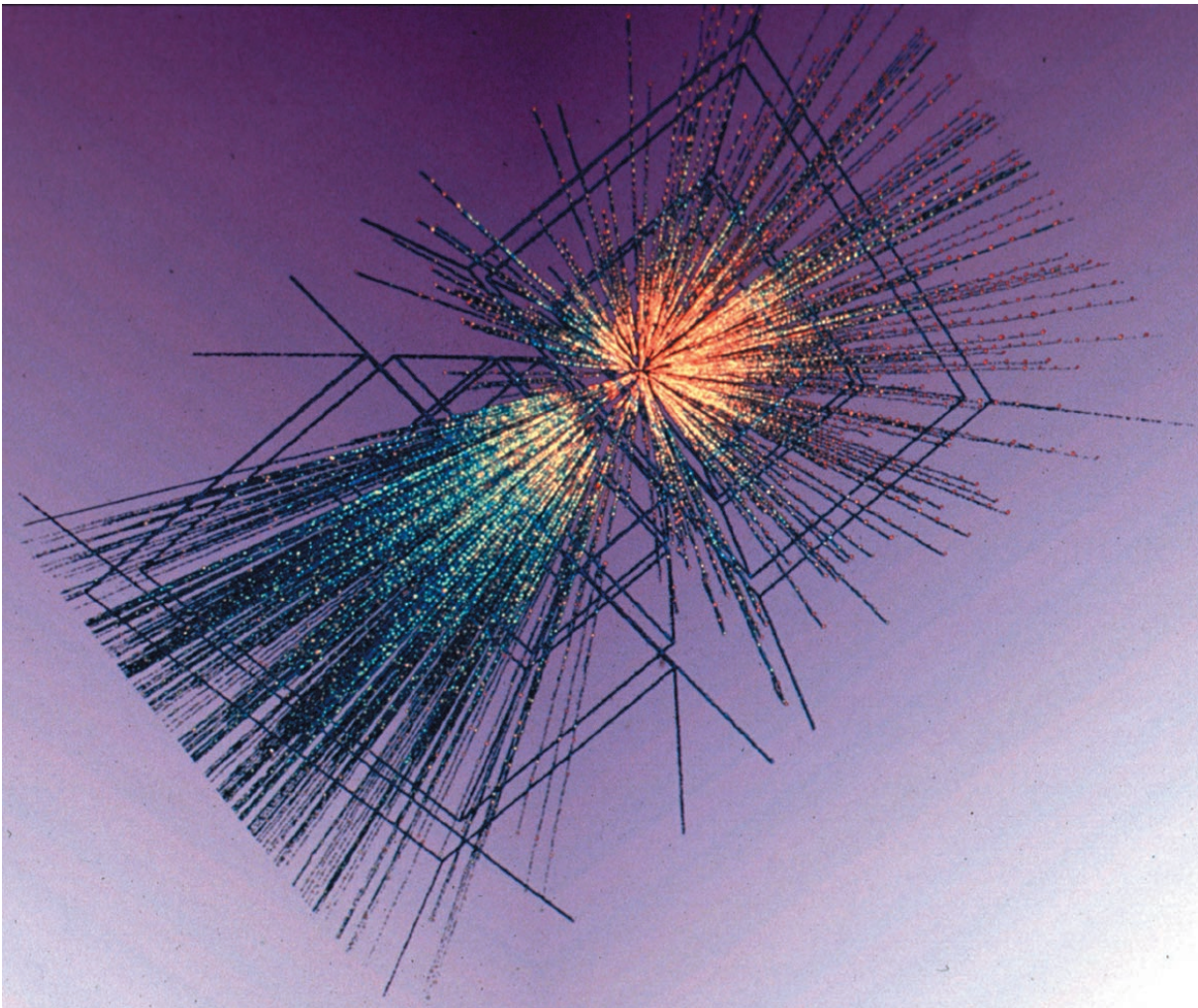


Figure 5.3: Measured CC differential cross section $\frac{1}{E} \frac{d^3\sigma}{dx dQ^2 dy}$ for ν_μ and $\bar{\nu}_\mu$ on lead. Insert: Example of a three-parameter structure function fit to the differential cross section for $x = 0.175$ and $Q^2 = 8.2 \text{ GeV}^2/c^2$. Errors are statistical only.



Lead ion collisions produced by the experiment NA49. (CERN photo-ex/9503044_13)

6 Heavy Ion Physics

6.1 Introduction

February 10th, 2000 marked the official announcement by CERN of the experimental observation of a new state of matter, the quark gluon plasma (QGP). This state, which is only produced for a fraction of a second in collisions of heavy nuclei, has a temperature that is sufficiently high to melt the protons and neutrons into their constituents, the quarks and gluons.

The experiments that confirmed the existence of the QGP, consisted of large particle detectors located at the end of lead beams extracted from CERN's super proton synchrotron, the SPS. The SPS delivered lead ions with maximum energies per nucleon of 158 GeV.

The experiments were for a large part dedicated to measuring only one aspect of the collisions: photons, leptons, charged hadrons, etc. Only a combination of the results of all experiments could exclude any explanation for the observed signal other than the quark gluon plasma.

The ultimate experiment where the properties of the quark gluon plasma will be measured is ALICE, a multi-purpose detector at the future LHC collider. The LHC will accelerate heavy ions, in addition to the regular proton-proton programme. Maximum energies will be 5 TeV per nucleon at the LHC, which will yield a totally baryon-free plasma in thermal equilibrium.

The joint-venture NIKHEF contributes to CERN's heavy-ion programme through a participation in three fixed-target experiments (WA98, NA49 and NA57) and a major participation in the ALICE experiment. In this report we describe recent results from the fixed-target experiments and the progress in the preparation of the ALICE detector.

6.2 Direct photons with WA98

One of the probes to study nuclear matter in heavy-ion collisions is the production of direct photons, as these photons decouple immediately after their production and are not affected by the hadronisation process. As such, direct photons are good indicators of the properties of the nuclear matter in the early stages of the interaction.

Direct photons are produced in both hard QCD processes, i.e. initial interactions of the constituents, and as thermal radiation from a deconfined (Quark Gluon Plasma) phase or a hadron phase. Photons from hard

processes dominate the spectrum at high p_{\perp} , while the thermal photons constitute the main part at the low end of the spectrum. Unfortunately, this low p_{\perp} regime, which is the most interesting domain in view of the search for the QGP, is not yet understood theoretically.

It is difficult to measure the presence of direct photons, as their yield amounts only to a few percent of the total number of photons produced in a collision at the conditions at the CERN-SPS accelerator. The large background of the detected photons originates from the decays of neutral mesons, mainly π^0 's and η 's. The accurate determination of the direct photon yield depends on the correct reconstruction of the background spectrum of these decay photons.

The first conclusive experimental evidence for direct photon production has been obtained by the WA98 experiment, in Pb+Pb collisions at the CERN-SPS [1]. The experimental set-up contains a large area lead-glass calorimeter, supplemented by a charged particle veto detector placed in front of it. Two calorimeters further downstream determine the centrality of the events by measuring forward and transverse energy flow, respectively.

As the first step in determining the direct photon spectrum, the π^0 and η spectra were determined by using a two-photon invariant mass analysis. The thus obtained spectra were then used to calculate the hadronic decay photon spectrum. Comparison of this calculated spectrum with the actually observed photon spectrum reveals an excess of photons due to direct photon production, as shown in Fig. 6.1.

Due to limitations imposed by the reconstruction of the parent mesons, the direct photon yield is only accurate at relatively high p_{\perp} . Since direct photons produced in hard initial scattering are expected to show up in this region, as indicated by the scaled p -A data in Fig. 6.1, no conclusion on the thermal contribution to the direct photon production can be drawn.

In order to investigate the thermal regime, the data of the WA98 experiment are being reanalysed in Utrecht, using an alternative method of analysis based on the inclusive photon spectra [2]. As this method uses ratios of central and peripheral photon and pion spectra, part of the systematical uncertainties encountered in the previous method partly cancel. Therefore, more accurate results are expected from this new analysis, especially in the lower p_{\perp} domain.

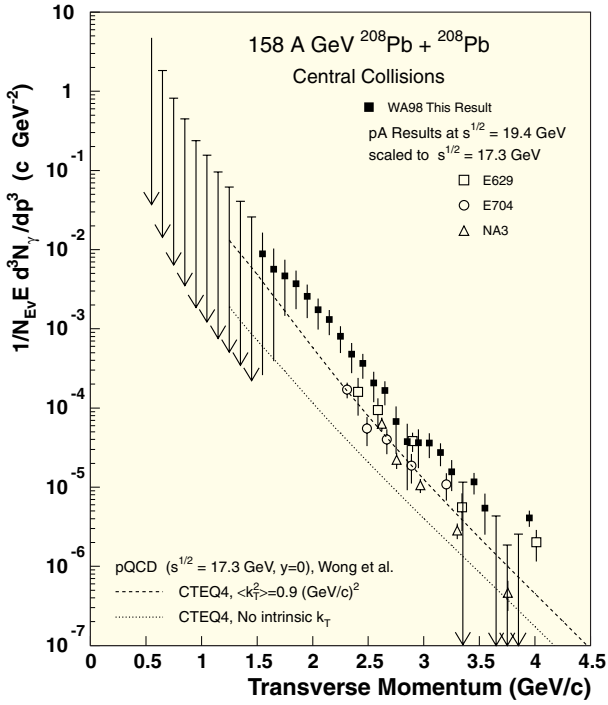


Figure 6.1: Invariant direct photon yield observed in central 158 AGeV Pb+Pb collisions by the WA98 experiment. Arrows indicate 90% confidence level upper limits.

A preliminary result for the photon yield, based on about 50% of the available data, obtained using the inclusive photon method is shown in Fig. 6.2. This first result is in good agreement with the earlier WA98 result. However, the necessary detailed study of the systematical errors in the direct photon yield is not yet completed, and consequently it is currently not possible to be conclusive concerning direct photons in the thermal regime.

6.3 Strangeness enhancement in NA57

The production of particles with one or more strange quarks has been proposed as a powerful probe for the transition of ordinary matter to the quark-gluon plasma.[3]

The WA97 experiment at CERN was designed to measure the production of strange baryons (Λ , Ξ , Ω). The yields of these strange particles were determined in both p -Be and Pb-Pb reactions at 158 AGeV. It was shown that the number of strange baryons per event in Pb-Pb collisions is enhanced with respect to the yield from p -Be collisions, scaled with the number of participants.

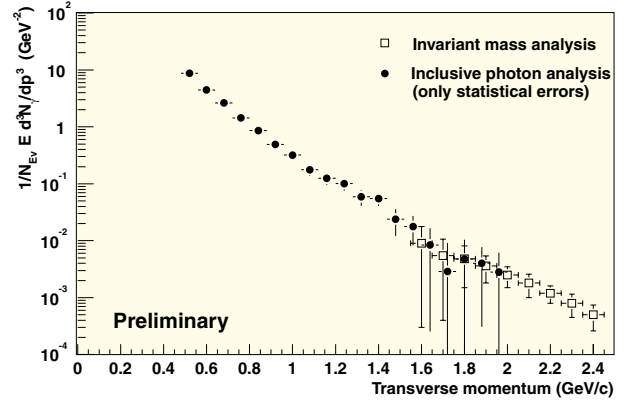


Figure 6.2: Preliminary result on the direct photon production in central 158 AGeV Pb+Pb collisions, obtained using the inclusive photon method. Only statistical errors are shown. For comparison, a part of the spectrum of Fig. 6.1 is included.

Furthermore, it was seen that this enhancement increases with the strangeness content of the particle [4]. This could be an indication of the creation of a state close to the phase transition.

The NA57 experiment is the successor of WA97 and extends its scope. In 1998 the measurements of WA97 for Pb-Pb reactions were repeated at 158 AGeV with an upgraded spectrometer: the silicon strip detectors of the tracking telescope were replaced by new, improved silicon pixel detectors. In this way together with the old silicon pixel detectors a high resolution pixel telescope was created. Furthermore the gas pad chambers in the lever arm of the spectrometer were replaced by silicon microstrip detectors. These microstrip detectors were developed by the department of Subatomic Physics of Utrecht University/NIKHEF and serve to improve the track momentum resolution of fast tracks. They have a size of $7.3 \times 4.0 \text{ cm}^2$ in horizontal and vertical directions, respectively. The strip detectors are double sided with a stereo angle of 35 mrad and have a thickness of $300 \mu\text{m}$. The pitch of the strips is $95 \mu\text{m}$ and the strips are orientated in vertical direction, such that the resolution is best in the bending direction of the particles. Due to the small stereo angle the vertical resolution is worse, in the order of 1 mm.

Together with improving the resolution of the tracking telescope, NA57 also made an effort to reduce various background sources in order to extend the covered centrality range towards more peripheral events. For those

events the created system will be smaller and the onset of the strangeness enhancement can be investigated.

In order to reduce the energy density of the system, NA57 took data in 1999 at a beam energy of 40 AGeV for both p -Pb and Pb-Pb interactions. By reducing the beam energy, we can search for a possible threshold effect in the yield curve. The 1998 experiment was repeated in 2000 to increase the statistics on the peripheral events. Besides taking data, NA57 also has started to publish their first papers in 2000, [5] and the analysis of the data collected in 1998 starts to give the first results.

In the 1998 experiment four double-sided microstrip detectors were placed along with four pixel detectors in the lever arm. In the 1999 experiments the lever arm comprised only the micro-strip detectors. The reconstruction software has been adapted for using the micro-strip detectors in the improvement of the fast track measurement. With this software the invariant mass spectra of the Λ for around 2 million events of the 1999 Pb-Pb data have been determined with and without the micro-strip lever arm (Fig. 6.3). For the invariant mass spectrum only those Λ 's were selected which had at least one decay particle in the lever arm. It can be seen that the mass spectrum resolution has improved from $\sigma = 44 \text{ MeV}/c^2$ to $\sigma = 36 \text{ MeV}/c^2$ and that more Λ 's are reconstructed by the analysing software. This improvement made that in the 2000 experiment two single-sided microstrip detectors were added in the lever-arm, because at 158 AGeV beam energy the momentum of the measured particles is higher and the lever arm is essential.

The reconstruction of the charged particle tracks and the first selection of V^0 decay candidates has already been completed for the 1998 and 1999 data. For the 1998 data the analysis of WA97 has been repeated in Utrecht and the yield per participant for the Λ and the $\bar{\Lambda}$ has been determined. Due to the improved trigger conditions an extra bin for peripheral events could be added next to the four centrality classes of WA97 [6]. This bin corresponds to a value of 62 for the number of participants. In Fig. 6.4 the relative yield per participant for the Λ and the $\bar{\Lambda}$ with respect to the proton induced reaction are shown for the five centrality classes of NA57. It can be seen that the most peripheral bin shows a drop in the relative yield per participant with respect to the more central bins for both particles. This drop in strangeness production could be an indication that in these peripheral collisions the system size has been too small to produce a QGP. This effect is also

seen in the Ξ and especially the $\bar{\Xi}$ relative yields as has been shown at the QM2001 conference [7].

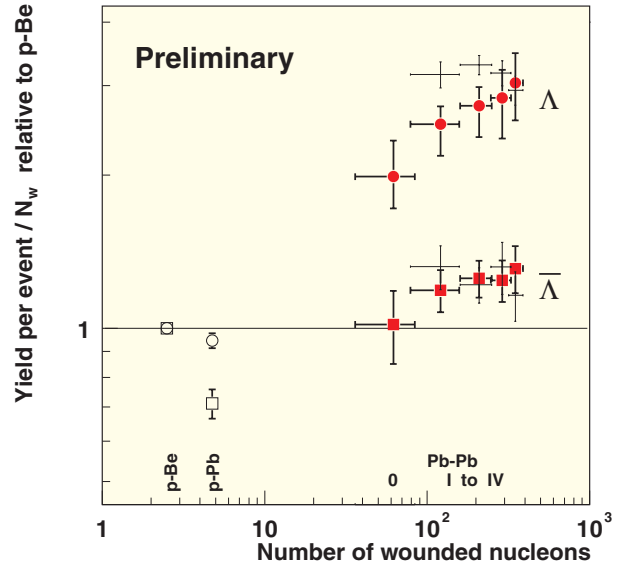


Figure 6.4: Yields per participant relative to the p -Be yield of Λ 's and $\bar{\Lambda}$'s. The error bars only indicate the WA97 results while the preliminary NA57 results from the analysis of the Pb-Pb 1998 data, are given by the squares and circles with error bars.

6.4 Charm and strangeness with NA49

The NA49 experiment studies the production of hadrons in collisions of protons and nuclei at the CERN SPS. NA49 is a fixed target experiment which uses a magnetic spectrometer, consisting of several large TPCs, to measure charge and momentum of the produced particles [8]. An additional time of flight system and the dE/dx information of the TPCs provide particle identification over a large part of the acceptance.

The physics programme of NA49 covers different subjects such as total production and spectra of many particles, ranging from pions to heavy strange baryons. In addition different types of correlations are studied, such as the Hanbury-Brown-Twiss (HBT) effect, stopping and even-by-event fluctuations. These phenomena can be studied as a function of system size and as a function of collision energy. For the study of the system size dependence, the following types of events have been recorded: $p - p$, C-C, Si-Si and Pb-Pb. For the study of the energy dependence, the following beam energies have been used: 40, 80 and 158 AGeV.

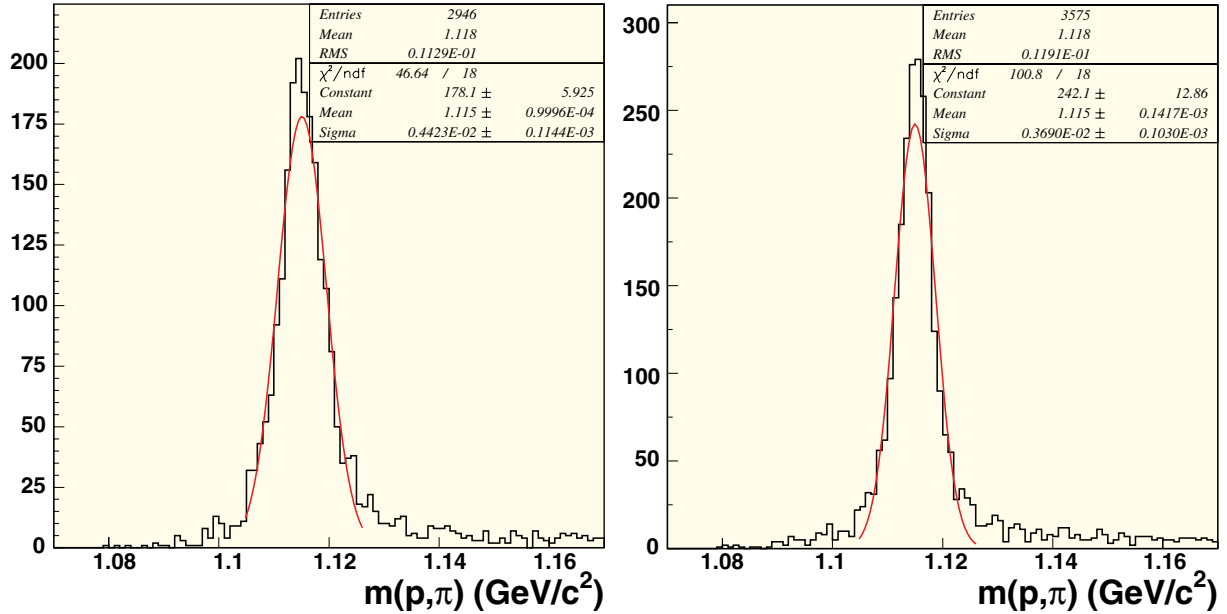


Figure 6.3: Invariant Λ mass distribution for the Λ 's which have at least one decay track in the lever arm. left: without the microstrips in the lever arm. right: with the microstrips in the lever arm.

The focus of the NIKHEF group in NA49 is the study of flavour (strangeness and charm) production in nuclear collisions. The analysis efforts are centred around measuring the total kaon and D -meson production in 158 AGeV Pb-Pb collisions.

Recently, a first result on kaon production at 40 AGeV beam energy has become available. In Fig. 6.5 this result is plotted together with published data from the AGS and an earlier preliminary result for kaon production at the highest SPS energy from NA49. In fact, what is plotted is the strangeness to entropy ratio as a function of Fermi's F variable, which is proportional to the expected energy density in the collision. Clearly the recent result at 40 AGeV indicates that the strangeness to entropy ratio does not rise monotonically as a function of energy density. Within a statistical picture of the collision, this can be attributed to the transition from a system where hadrons are the relevant degrees of freedom to a system where quarks and gluons are the degrees of freedom. The line in Fig. 6.5 was calculated using such a model [9].

We are currently finalising the analysis of the 40 AGeV data. The data which have been taken in September 2000 at 80 AGeV beam energy will be analysed in the near future, to better pin down the transition region.

The NIKHEF group is doing the re-analysis of the data at 158 AGeV beam energy.

In the near future the measurement of the kaon production in central Pb-Pb collisions at 40, 80 and 158 AGeV beam energy will be completed. Runs with 20 and 30 AGeV beams have been approved by CERN and will probably take place in 2002.

The next step for the NIKHEF group will be to search for D -mesons in central Pb-Pb collisions at 158 AGeV (cf. Ref. [10]). Last year's run has been used to accumulate statistics for this study and other studies which require large numbers of events.

6.5 Preparations for ALICE

The Dutch participation focuses its efforts on the development and construction of the two outer layers of the inner tracking system (ITS). These two layers consist of silicon strip detectors (SSD). The system is built together with groups from Turin, Strasbourg, Nantes, St. Petersburg, Kharkov, Kiev and Trieste.

In 1999 the design of the ITS was described in the technical design report, which was subsequently approved by the LHCC. However, during the year 2000 some adjustments to the design were found necessary. In order to bring the cost of the SSD layers down, both layers

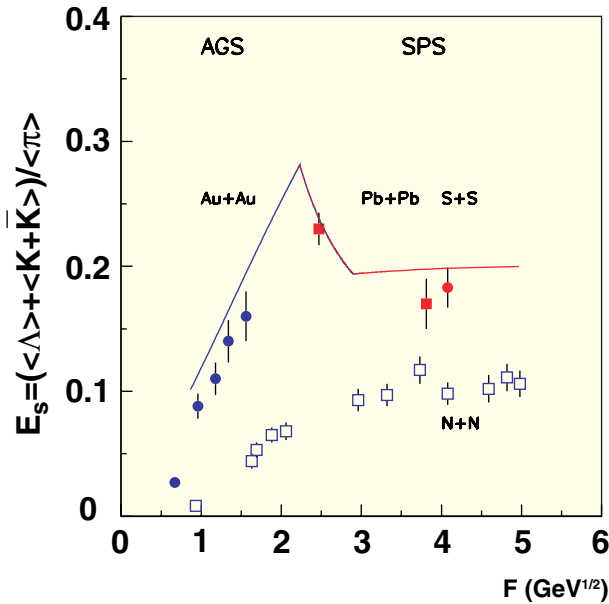


Figure 6.5: Dependence of the strangeness to entropy ratio on $F \propto s^{1/4}$.

were reduced in length by 4 cm. This reduction of acceptance was compensated by reducing also the radius at which the layers are mounted slightly. The effect on the physics performance of the ITS was shown, by simulation, to be small. During the LHCC review of the technical design report it was noticed that the tracking efficiency of the ITS could be improved by changing the stereo angles on the SSD. Formerly the orientations of the strips in the fifth and sixth layers of the ITS were symmetric with respect to the beam axis. This means that ambiguities encountered during track reconstruction in layer six are repeated in the fifth layer. The tracking efficiency was improved by making the SSD asymmetric and mounting the detectors differently in the two layers. In addition the collaboration has decided to replace the front-end ASIC (A128C) by a more radiation tolerant design. The new ASIC (HAL25) will also be designed by LEPSI in Strasbourg, but will use the IBM 0.25 μm technology with special libraries to make them radiation tolerant.

The changes in the design of the SSD layers have affected the work to be done by NIKHEF in a relatively modest way. The main consequence is a change in the end-cap design, which now has to be connected to the new front-end chip. Therefore NIKHEF has decided to develop a new ASIC, also in IBM 0.25 μm technology.

The most challenging parts of the new end-cap ASIC design will be prototyped in the first quarter of 2001.

The experience gained by making several prototypes of hybrids and detector modules during the year 2000 has demonstrated the advantages of the use of micro-cables for the SSD module design. Probing the limits of this technology has led to successive improvements, directed towards a reliable industrial production possibility. An important consequence of this experience has been the decision to use the opportunity given by the change of the front-end chip to change the positions of the bonding pads on this ASIC to better suit the properties of the micro-cables. It is expected that the final design of the SSD module can be finished during the year 2001.

NIKHEF has also started to design the assembly machine that will assemble SSD modules on their carbon support structures. The concepts were sufficiently developed to give the project to a commercial company, which will further develop the motion control software of the machine.

The ALICE collaboration has agreed upon a memorandum of understanding (MOU) which formally regulates the sharing of the work and the cost for the construction of the ALICE detector between the laboratories involved. At the end of 2000, the transition from the R&D phase towards the construction phase has begun for the SSD teams. The carbon support structures are already in production and the (CERN) procedure to order silicon detectors has started. Nearly all remaining hardware development work is expected to be completed during the year 2001.

References

- [1] WA98 collaboration, Phys. Rev. Lett. **85** (2000) 3595.
- [2] N. van Eijndhoven, Nucl. Phys. **A618** (1997) 330.
- [3] P.Koch, B.Müller and J.Rafelski, Phys. Rep. **142** (1986) 167.
- [4] E.Andersen *et al.*, CERN-EP/98-64.
- [5] F. Antinori *et al.*, Nucl. Inst. Meth. **A452** (2000) 323-337.
- [6] NA57 collaboration, Eur. Phys. J. **C18** (2000) 57-63.

- [7] N. Carrer for the NA57 collaboration, presented at the QM2001 conference and to be published.
- [8] NA49 Collaboration, Nucl. Instrum. Meth. **A430** (1999) 210.
- [9] M. Gazdzicki and M. I. Gorenstein, Acta Phys. Polon. **B30** (1999) 2705 [hep-ph/9803462].
- [10] NA49 Collaboration, CERN-SPSC-2000-011.

7 HERMES

7.1 Introduction

The year 2000 was a successful year for the HERMES experiment in general, and the NIKHEF group in particular. At DESY the HERMES experiment collected up to a factor of three more data as compared to any previous year. Moreover several important physics results were published, including the first determination of the gluon polarization in the proton.

For the NIKHEF group in HERMES the year 2000 was remarkable as well. Now that the first physics run of HERMES (1995 – 2000) has been concluded, the group has proposed to extend its involvement in HERMES until the end of HERA operations in 2006. After various reviews the proposal has been approved by the NIKHEF directorate. Furthermore, a dedicated proposal to study a newly discovered nuclear effect in deep-inelastic scattering was approved in the annual FOM project competition. This effect was first observed in an analysis of HERMES data carried out at NIKHEF in 1999. Apart from additional measurements on heavy nuclei at HERMES, this observation also gave rise to a new experiment at Jefferson Laboratory in Newport News, Virginia. This experiment, in which our group participates, was successfully carried out in the summer of the year 2000.

After the HERA luminosity upgrade, which is scheduled to be completed in the summer of the year 2001, data taking will be continued (“HERMES run II”). The average luminosity will be roughly a factor of 2 higher in run II as compared to (most of) run I. The physics objectives of the second data taking period include measurements of the polarization of strange quarks, gluons, and transversely oriented valence quarks.

In order to prepare for the future the HERMES spectrometer has been upgraded in various steps. In the last years a Ring-Imaging Cherenkov (RICH) detector, an iron wall with a scintillator hodoscope behind it to identify muons, a forward quadrupole spectrometer (FQS), a wide-angle muon hodoscope to detect muons passing through the iron of the spectrometer under a large angle, and a wheel-shaped silicon array downstream of the target to increase the acceptance for hyperon decay (known as the Lambda Wheels) have been developed. The Lambda Wheel project is led by the NIKHEF group. During the year 2000, a prototype silicon module was successfully operated for many months in the HERMES experiment. The series production of all 12

required modules was almost completed by the end of the year.

7.2 Data taking

The overall performance of the experiment during the years 1996 – 2000 is summarized in figure 7.1, in which the accumulated DIS events are plotted versus the number of days in that year since the start of the run. While the data taking conditions in the years 1996, 1997 and 1999 were quite comparable, the situation in 1998 and 2000 was different. In the year 1998 considerably less data were collected due to the late start of the run, and the relatively poor beam conditions when HERA changed over from positron to electron running that year. On the other hand running conditions in 2000 improved dramatically as compared to previous years. The storage cell containing the polarized target was replaced by one with a smaller diameter, resulting in an increase of the effective target density by 50%. A new (microwave) dissociator was used to feed the atomic beam source, and the HERA positron currents reached values as high as 50 mA on injection. Together these improvements represent an increase of the luminosity of the experiment by a factor of 2.5.

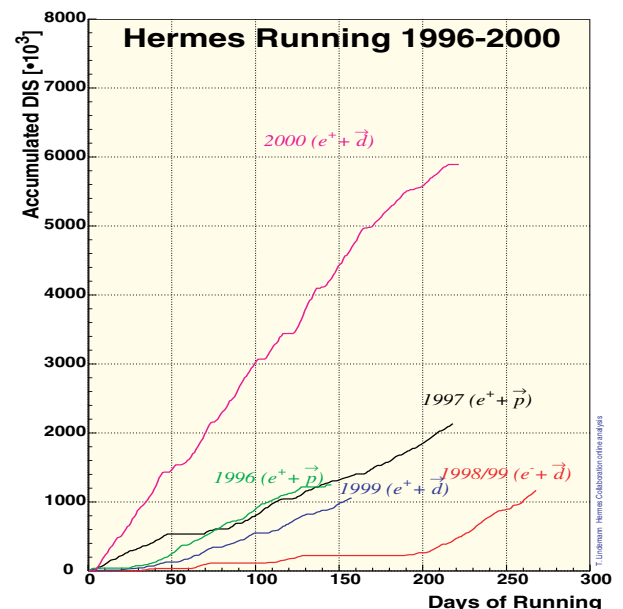


Figure 7.1: The integrated number of deep-inelastic scattering events collected by the HERMES experiment at DESY in the years 1996 – 2000.

During several months in 2000 the deuterium target was operated in both vector and tensor polarization states. Data collected on the tensor polarization states will enable the determination of the – so far unmeasured – structure function $b_1(x)$, which can be used to extract the quadrupole moment of the sea quarks in deuterium.

Apart from data collected on polarized deuterium, about 13 Million DIS events have been collected on various unpolarized targets. This large number of events has been obtained by injecting a dense stream of unpolarized gas into the beam during the last hour of each fill. In this way the life time of the HERA positron beam was reduced from typically 12 hours to about 1 hour, and luminosities as high as a few times 10^{33} N/cm²/s were reached.

Near the end of the data taking period, the HERA positron beam was operated for several days at a reduced incident energy of 12 GeV. It was possible to take data with the HERMES spectrometer during this low-energy run, which will make it possible to extend the kinematic coverage of many existing measurements that have been collected at 27.5 GeV.

7.3 Physics analysis

In this section some of the most prominent results are presented that have been obtained in the year 2000 by the HERMES collaboration.

The spin structure of the nucleon

The proton spin structure function $g_1^p(x, Q^2)$ was extracted from deep-inelastic scattering data collected on a polarized ¹H target in 1997. As compared to previous analyses, additional data at low x have been obtained by relaxing the requirements on Q^2 and y . The data are compared to measurements from SLAC (E143 and E155) and CERN (EMC and SMC) in Fig. 7.2. By fitting the Q^2 dependence of the data for separate x -bins, evidence is obtained for scaling violations of the polarized structure function $g_1^p(x, Q^2)$ at low x .

Using the inclusive and semi-inclusive target-spin asymmetries obtained on polarized ¹H (1996 and 1997) and ³He (1995) targets, the separate polarization of u , d and sea quarks in the nucleon was obtained. From the data (shown in fig. 7.3) it is seen that the u quarks are polarized parallel to the spin of the proton, which is partially canceled by the negative polarization of the d quarks. The polarization of the sea quarks is consistent with zero. The precision of the data displayed in fig. 7.3 is expected to improve considerably when

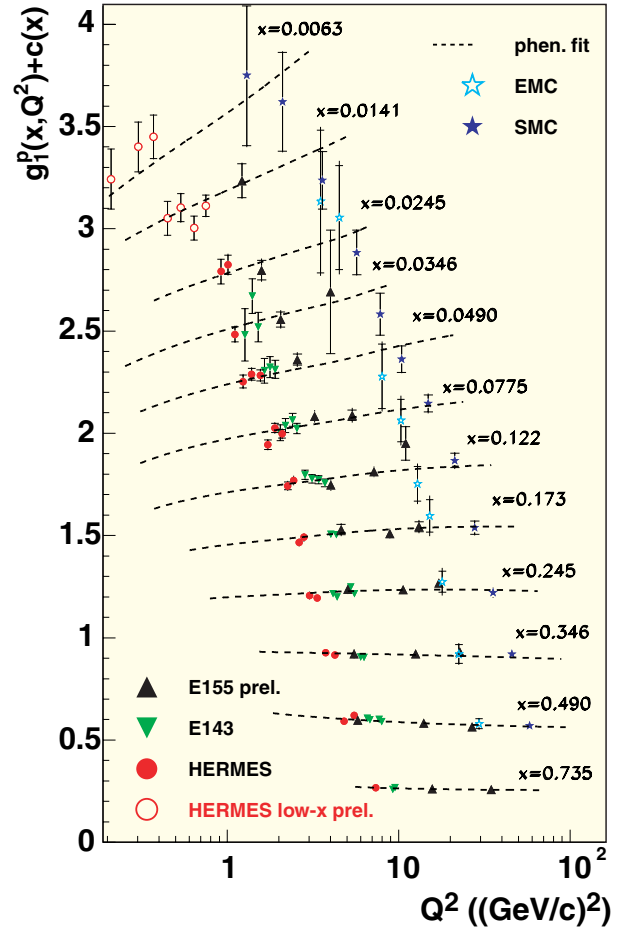


Figure 7.2: *The spin-dependent structure function g_1^p of the proton as a function of Q^2 . Data for different x -bins are connected by the dashed lines, which represent the results of phenomenological fits. The HERMES (closed and open circles) data are compared to data from SLAC (triangles) and CERN (stars).*

the polarized ²H data collected in 1998 – 2000 are also included in the analysis.

The formation time of pions and protons

Experimental information on the formation time of a particle can be obtained by producing such a particle in deep-inelastic lepton scattering inside the nucleus of an atom. In the nuclear environment the produced pion or proton will rescatter from any of the neighbouring nucleons. As a result the number of pions observed on a heavy nucleus will be reduced as compared to that number on a hydrogen or deuterium target. The reduction will be larger if the pion is formed sooner. Hence, the ratio of the number of pions produced on a

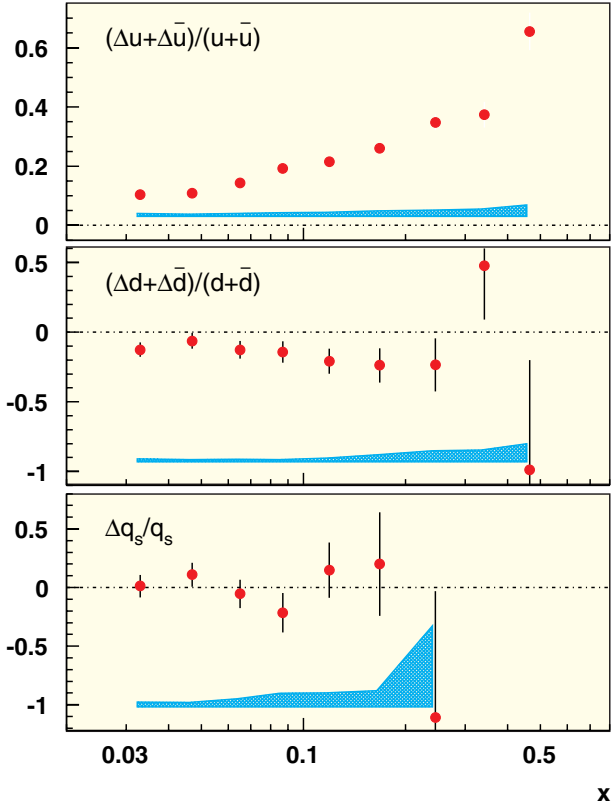


Figure 7.3: Results of the flavour decomposition of the nucleon spin. The results are derived from the 1995, 1996 and 1997 HERMES data on polarized ^1H and ^3He targets. The coloured areas near the bottom of each panel represent the systematic uncertainty of the data.

heavy nucleus to that on deuterium is a direct measure of the formation time.

The results of such measurements on ^{14}N and ^2D are shown in Fig. 7.4 as a function of the energy transfer ν . Whereas the reduction for positive and negative pions and negative hadrons is roughly the same, the reduction for positive hadrons is considerably less. As there are many more protons in the positive hadron sample than anti-protons in the negative hadron sample, this difference can be attributed to a formation time difference between protons and pions. The data seem to imply that the formation time of protons is considerably longer than that of pions.

Deep-Virtual Compton Scattering

Exclusive production of real photons in deep-inelastic scattering (known as deep virtual Compton scattering

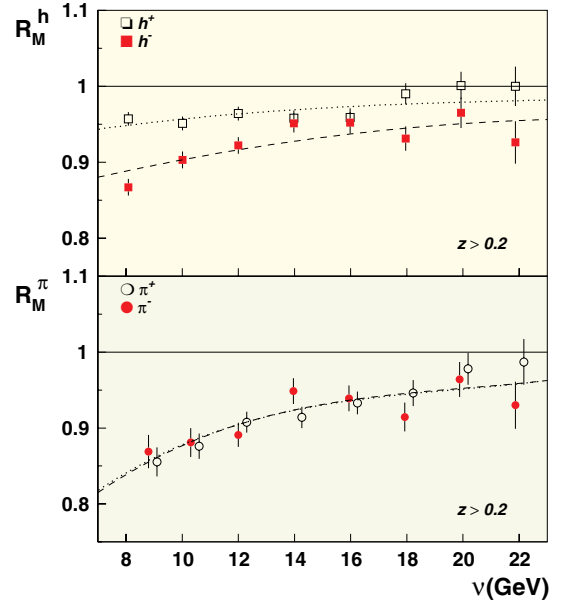


Figure 7.4: The ratio of the number of hadrons produced on ^{14}N and ^2D normalized by the number of scattered electrons. The data for hadrons (upper panel) and pions (lower panel) are separately displayed for the two charge states. The curves represent phenomenological fits of the data with the formation time as a free parameter.

– DVCS) is of considerable interest as it gives access to the recently introduced Skewed Parton Distributions (SPDs). The SPD's represent a generalization of the ordinary parton distributions by also taking into account the dynamical correlations between partons of different momenta. Most importantly DVCS might enable investigations of the role of the orbital angular momentum of the quarks L_q , although the relation between DVCS data and L_q is not beyond theoretical debate.

Experimentally it is difficult to observe DVCS events due to the dominance of photons originating from the Bethe-Heitler process. However, by determining single-spin azimuthal asymmetries using polarized lepton beams one can isolate the DVCS process, because this asymmetry is hardly affected by the Bethe-Heitler process.

At HERMES the electromagnetic calorimeter was used as a photon detector. The azimuthal asymmetry of the produced photons relative to the lepton scattering plane was determined in the exclusivity limit for two opposite helicity states of the incoming positron beam. The re-

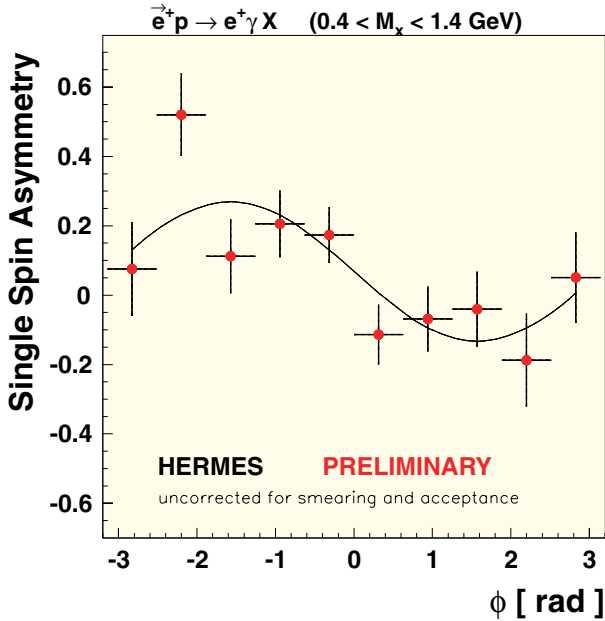


Figure 7.5: The asymmetry of real photons produced in deep-inelastic scattering (DVCS) with respect to the helicity of the positron beam as a function of the azimuthal angle ϕ . The data – collected in 1997 – have been obtained using an unpolarized hydrogen target. The curve represents a fit of the data assuming a simple $\sin(\phi)$ dependence of the asymmetry.

sults are displayed in Fig. 7.5. The $\sin(\phi)$ -weighted azimuthal asymmetry $A_{LU}^{\sin(\phi)}$ was measured to be $0.18 \pm 0.04(\text{stat}) \pm 0.02(\text{syst})$. By plotting the missing-mass dependence of the $\sin(\phi)$ -weighted asymmetry, it can be shown that non-zero values are only observed in the limit of $M_x \approx M_p$, i.e. for exclusively produced photons only. This is illustrated in Fig. 7.6. The result represents the first experimental observation of DVCS off a proton, and holds promise for future study of the total angular momentum of partons in the nucleon.

7.4 The JLab experiment

In order to investigate the unexpected nuclear effects observed in the inclusive Deep-Inelastic Scattering (DIS) data at HERMES, a dedicated experiment at Jefferson Laboratory (JLab) was carried out. The advantage of the experimental set-up in Hall C of JLab is that a high-luminosity DIS experiment can be performed at various energies of the incident electron beam. This makes it possible to separate the longitudinal and transverse components of the DIS

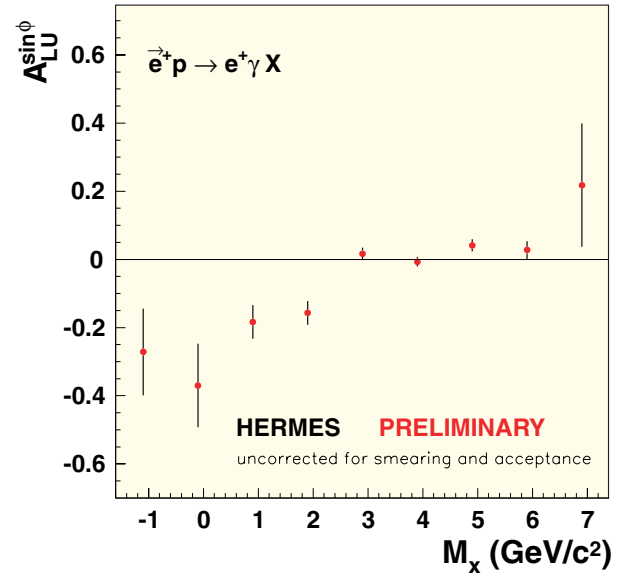


Figure 7.6: The $\sin(\phi)$ weighted azimuthal asymmetry A_{LU} for DVCS events at HERMES. The data are plotted versus the missing mass M_x . The non-zero asymmetries for $M_x < 0$ GeV are due to the finite resolution of the spectrometer.

cross section, whose ratio is supposedly enhanced in nuclei.

The experiment made use of 2.3, 3.4 and 5.6 GeV electron beams and the High Momentum magnetic Spectrometer (HMS) of Hall C. Data were taken at various scattering angles, ranging from 10 to 60 degrees, on targets of ^1H , ^2H , ^{12}C , Al, Cu, and Au, which makes it possible to perform a longitudinal-transverse separation for a range of x and Q^2 values as a function of the nuclear mass A .

The analysis of the data is in progress. Various efficiencies have been determined, the pion-electron separation has been optimised, and ‘positron’ contaminations have been determined. Special attention is being given to the radiative corrections, especially those due to elastic scattering which are important at these relatively low energies and Q^2 values.

7.5 The Lambda Wheel project

In the framework of the upgrade of the HERMES spectrometer, a new wheel-shaped silicon detector is being developed. The purpose of this detector is to increase the acceptance of the spectrometer for Λ^0 hyperons and charmed particles, such that the polarization of

strange quarks and gluons can be measured with improved precision. Most of the design and construction work related to the Lambda Wheel project is carried out at NIKHEF.

In the year 2000 extensive measurements have been carried out with a prototype detector module that was installed inside the beam vacuum just downstream of the internal target. The commissioning of the prototype module has shown that it is possible to operate such a silicon counter under ultra-high vacuum conditions close to the high-intensity electron beam of HERA. After some problems with the cooling systems (which were resolved), it has been possible to carry out a range of systematic studies. From these studies it was found that the efficiency of the prototype module ranged from 95 – 97%, depending on conditions. It was also found that the average track multiplicity amounted to only 1.2 tracks per module (after cuts). Hence, there are no concerns about possible tracking ambiguities.

During the year 2000 the HERA positron beam was unintentionally lost several times in the vicinity of the HERMES interaction point. As a result the leakage current of the prototype module increased dramatically. Such events will reduce the life time of the silicon detector and the readout chips. For that reason it has been decided to develop a Beam-Loss Monitor (BLM), which will create a trigger signal if the beam starts to diverge from its usual orbit. The trigger signal will be sent to a kicker magnet that will be installed in the HERA positron ring in 2001. A prototype BLM consisting of two simple ionization chambers was successfully tested during the last month of HERA operations in 2000.

The series production of the Lambda Wheel modules was started in the beginning of 2000, yielding 12 operational silicon modules near the end of the year. Of these modules five were successfully tested at DESY using a low-intensity electron beam. In Fig. 7.7 it is seen how one of the modules is installed in the wheel using a dedicated test set-up at NIKHEF.

7.6 Outlook

Data taking at HERMES will only be resumed after the HERA luminosity upgrade has been completed, i.e. in the fall of 2001. At that time the Lambda Wheels and all other upgrades of the HERMES spectrometer are expected to be fully operational.

The start of HERMES RUN II marks the beginning of a new hardware responsibility issues for the NIKHEF group, which was the result of a reallocation of tasks within the collaboration. As the vertex chambers



Figure 7.7: *Installation of a detector module in the new wheel-shaped silicon detector ('Lambda Wheels'). The picture was taken during a test of the installation procedure in the NIKHEF workshop.*

(based on the Multi-Strip Gas Chamber technology) will only be used as a spare detector in the front region in the coming years, manpower could be freed to take part in the operation and maintenance of the Longitudinal Polarimeter (LPOL). The LPOL measures the longitudinal polarisation of the HERA lepton beam to a precision of 2% close to the HERMES interaction point.



Installation of the Micro Vertex Detector (MVD) at ZEUS.

8 ZEUS

8.1 Introduction

The running conditions at HERA were extremely good in 2000 and the ZEUS experiment collected $\approx 50 \text{ pb}^{-1}$ out of the delivered 60 pb^{-1} . All running was with positrons of 27.5 GeV colliding with protons of 920 GeV, in spite of requests by the ZEUS collaboration for an increase in the amount of electron data. In the beginning of October 2000 the machine shut down to allow the modification of the accelerator to reach higher luminosity. The total integrated luminosity collected by ZEUS in the 'pre-upgrade' era is summarised in table 8.1

year	lepton charge	lepton energy (GeV)	proton energy (GeV)	integrated luminosity (pb^{-1})
2000	+	27.5	920	48
1999	+	27.5	920	20
1999	-	27.5	920	12
1998	-	27.5	920	4
1997	+	27.5	820	28
1996	+	27.5	820	11
1995	+	27.5	820	7
1994	+	27.5	820	4
1993	+	27.3	820	1

Table 8.1: Total collected luminosity.

The papers published by ZEUS in 2000 mainly concern the data collected up-to and including 1997, with some preliminary results dealing with differences between e^+p and e^-p using also the data from 1998 and 1999.

8.2 Physics highlights

The extraction of the F_2 structure function from the 820 GeV proton running, corresponding to data taking periods up-to and including 1997, was completed. Figure 8.1 shows the structure function for several different values of Q^2 (defined as minus the four-momentum transfer squared). The measurements extend to $Q^2 > 30000 \text{ GeV}^2/c^2$. Good agreement is obtained with a NLO QCD fit to the data for $Q^2 > 2.5 \text{ GeV}^2/c^2$. Figure 8.1 also shows the F_2 values obtained at low Q^2 using a special calorimeter and tracking system placed at very small angles to the electron direction. The marked increase of the structure function at low values of x (the fraction of the proton's four-momentum carried by the struck quark) is observed as Q^2 increases. In QCD this

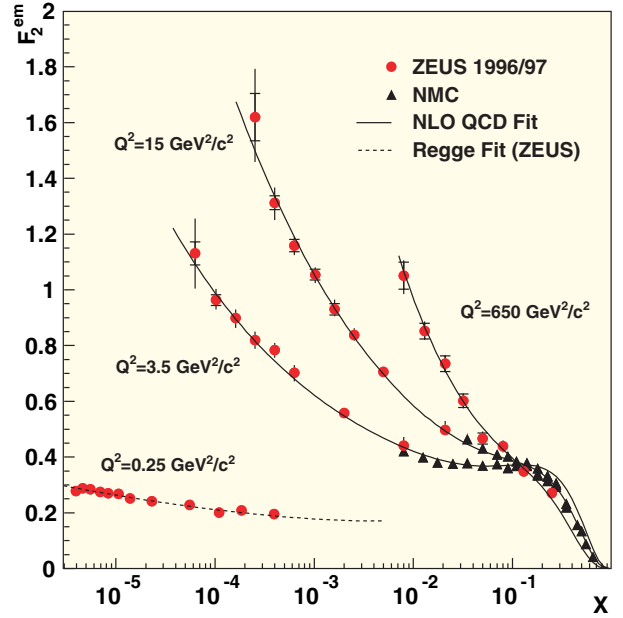


Figure 8.1: F_2 as a function of x for different values of Q^2 .

increase in the structure function is explained by the increase of the number of quarks and anti-quarks, due to the splitting of gluons to quark anti-quark pairs. The rate of increase is a measure of the gluon density inside the proton.

The structure function has now been measured with an accuracy of around 2% over a very large part of the available phase-space. Figure 8.2 shows the phase-space covered by the present measurements and the measurement accuracy obtained. The limiting factors for the accuracy are the estimate of the photo-production background (near the line $E = 8 \text{ GeV}$), the understanding of the acceptance of the detector near the rear beam-hole (the line $\theta = 177^\circ$) and the understanding of the proton remnant fragmentation (the line $W = 20 \text{ GeV}$). The statistical uncertainty begins to dominate the systematic uncertainty in the region of $Q^2 > 800 \text{ GeV}^2/c^2$. It is clear that the addition of the remaining data from 1999 and 2000 will be effective in reducing the error only above this value. Future post-upgrade running will concentrate on the high Q^2 range so that in effect the measurements below $Q^2 = 800 \text{ GeV}^2/c^2$ are the final ZEUS results.

The low Q^2 measurements of fig. 8.1 were not fitted

to the NLO QCD parameterisation but rather to a generalised vector meson dominance formalism (GVDM). At these low values of Q^2 perturbative QCD becomes unusable. Recently there has been considerable interest in the region where the transition takes place between the (hard) perturbative QCD description and the (soft) GVDM description. To investigate this region more systematically ZEUS has analysed their full Q^2 range in a

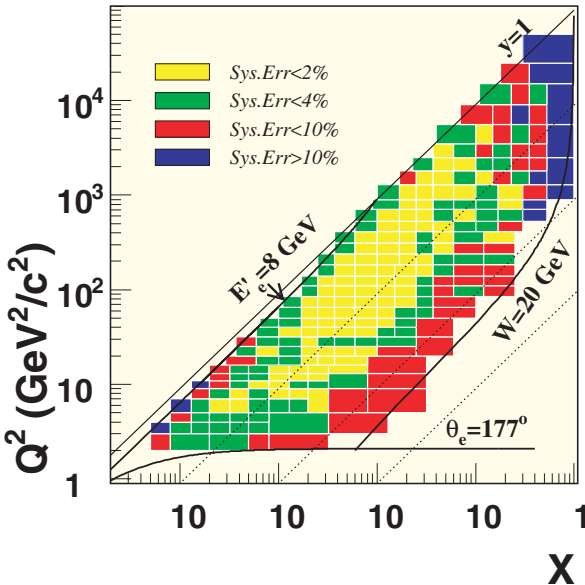
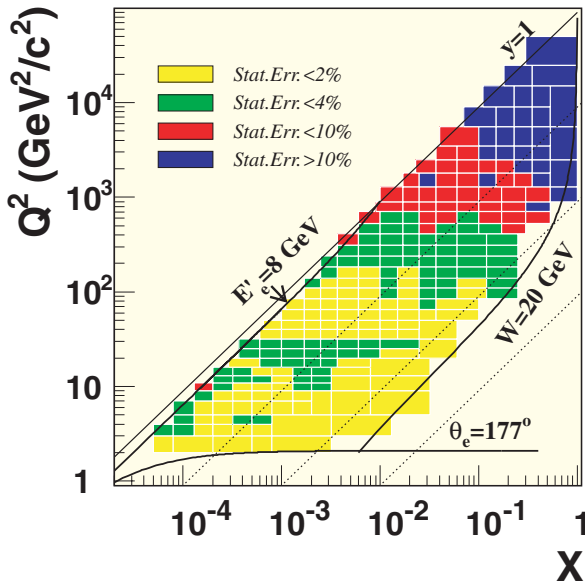


Figure 8.2: Statistical (top) and systematic (bottom) errors on F_2 .

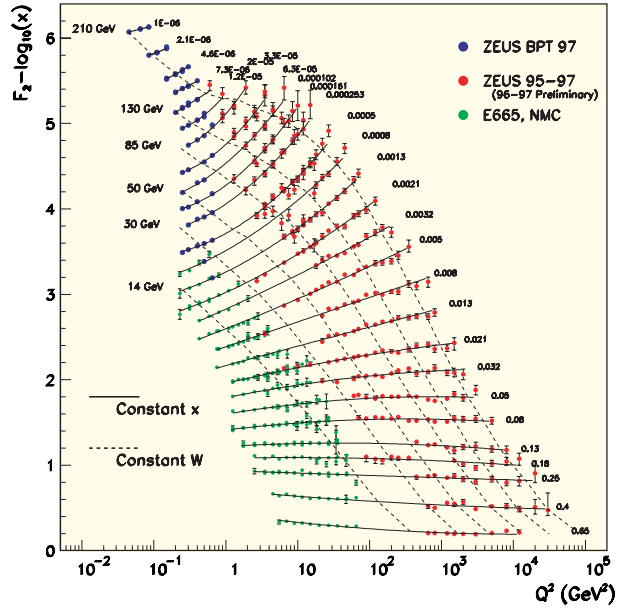


Figure 8.3: F_2 versus Q^2 for different values of x . Lines are second order polynomial fits in $\log F_2$.

somewhat different way. Fig. 8.3 shows the F_2 measurements as a function of Q^2 for different values of x . The lines are fits to F_2 according to a second order polynomial in $\log Q^2$. This allows the extraction of the derivative of the structure function with respect to $\log Q^2$, $dF_2/d \log Q^2$, at a fixed value of W . These logarithmic slopes are shown in fig. 8.4 as a function of Q^2 and of x for different values of W . A marked turnover is observed as Q^2 or x decreases. The point of turnover moves to lower values of x as W increases.

This turnover is also observed in the NLO QCD fits to the data, however the position of the turnover is not reproduced. The data on the logarithmic slopes can be described at least qualitatively in the context of a colour dipole model which includes saturation. Specifically the change of the turnover position in x with changing W is reproduced well. At present theoretical questions are how to smoothly make the transition from the dipole description to perturbative QCD, whereas experimentally different channels such as diffraction and elastic vector meson production are being investigated. In view of the importance of the low x region for colliders such as LHC a significant effort is being put into this investigation.

The final highlight was the extraction of α_s from comparison of the rates of events with two jets plus a rem-

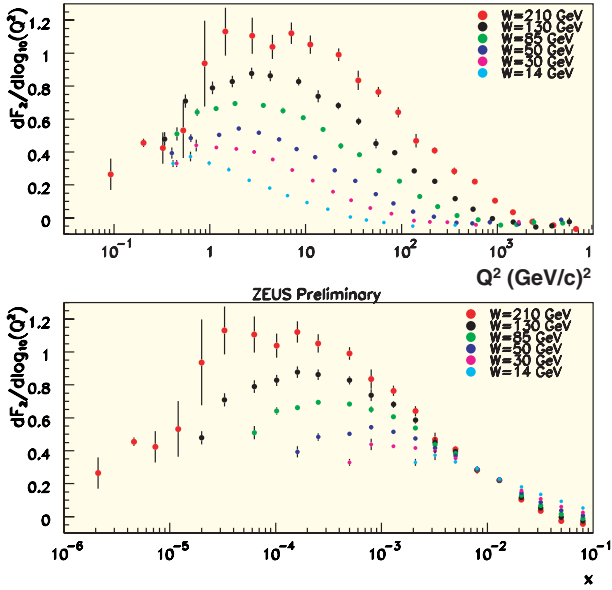


Figure 8.4: Logarithmic slopes of F_2 at fixed values of W versus Q^2 (top) and x (bottom).

nant jet (2+1 jet) and to those with one jet plus a remnant jet (1+1 jet). At HERA both the total jet production and the splitting into 1+1 and 2+1 jet events depends on α_s . A detailed analysis including the error propagation of the structure function, has allowed an extraction of the value of α_s . Fig. 8.5 shows the extracted values of α_s as a function of Q . The running of the strong coupling constant is clearly demonstrated, within one experiment. The value of the constant at $Q = cM_Z$ is found to be

$$\alpha_s(M_Z) = 0.1166 \pm 0.0019(\text{stat}) \\ +0.0024(\text{exp}) \pm 0.0057(\text{th}) \\ -0.0033(\text{exp}) - 0.0044(\text{th})$$

8.3 Microvertex Detector

The work on the microvertex detector has progressed well. In November the first half of the detector was shipped from NIKHEF to DESY for further tests. In the mean time the second half has also been shipped and preparations are taking place for a test using cosmic rays.

The detector is constructed of 30 ladders each containing 20 silicon strip detectors surrounding the beam (See fig 8.6).

In addition four wheels containing each 28 almost pie

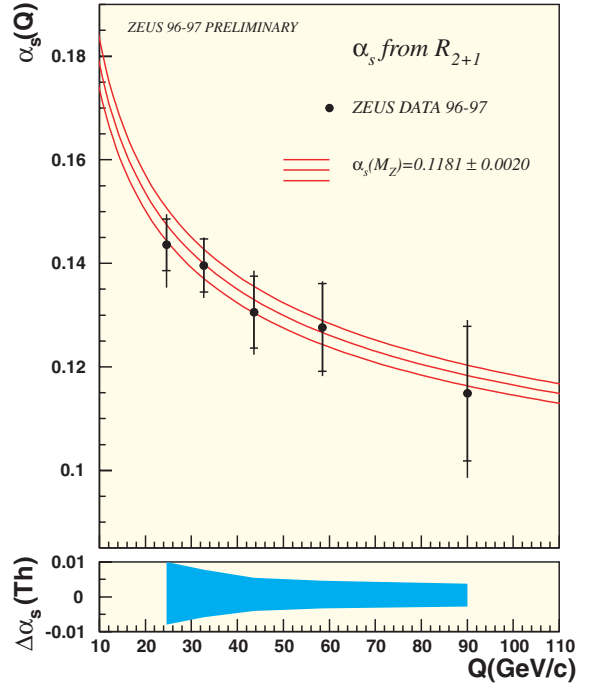


Figure 8.5: The strong coupling constant α_s as a function of Q .

shaped sensors are placed in the forward direction perpendicular to the beam (See fig 8.6).

The readout is organised in such a way that the sensors in the barrel are merged, combining a $r\phi$ strip with a neighbouring z strip. This method reduces the number of read out channels by a factor of two and, as has been verified, does not pose a significant problem in the pattern recognition. The strips in the wheel sensors are read out individually.

The analogue readout of the strips and the intermediate strip implantation allows a resolution of $7 \mu\text{m}$ for the coordinate perpendicular to the strip. This has rather severe consequences for the accuracy with which the detector has to be built. The ladder design is such that the stiffness avoids deflections of more than $20 \mu\text{m}$. Furthermore using moulds and positioning under microscope control allowed a positioning accuracy for the barrel sensors of the order of $5 \mu\text{m}$ within the ladder plane. The ladders themselves could be positioned to better than $20 \mu\text{m}$ in the microvertex support tube. All the positions were measured during the construction phase of the detector using a 2D and 3D measuring device. Fig 8.7 shows the result of one such measurement. Here the positions of the holes in the forward

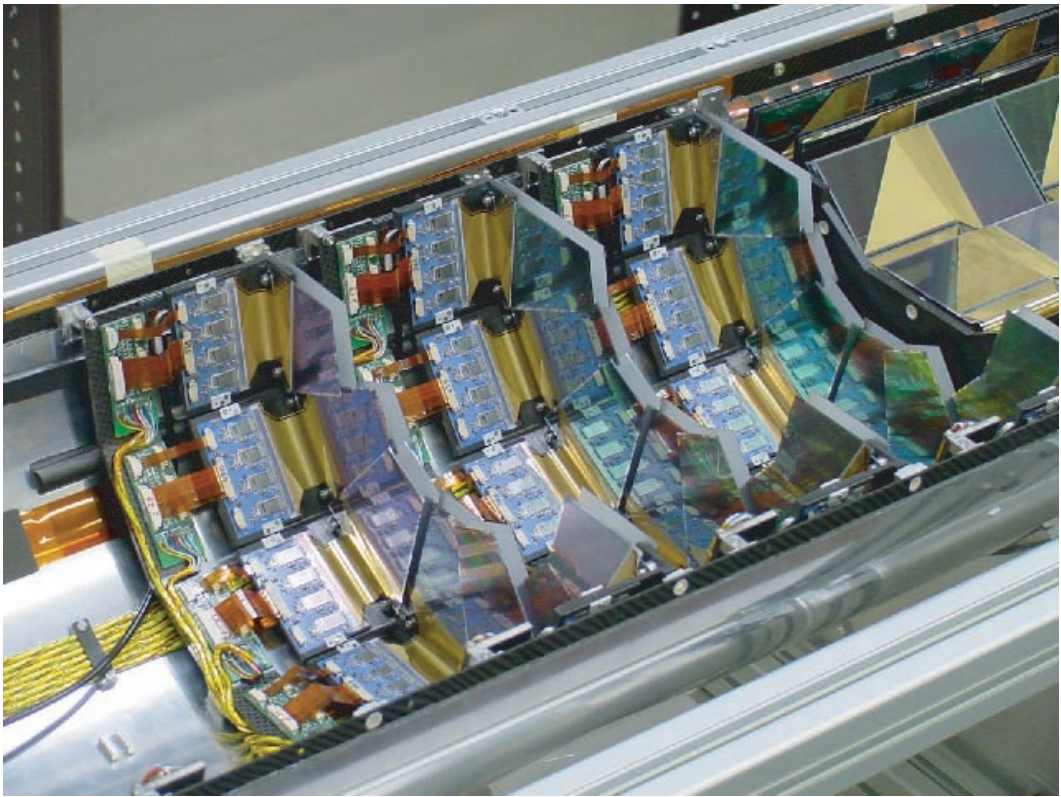
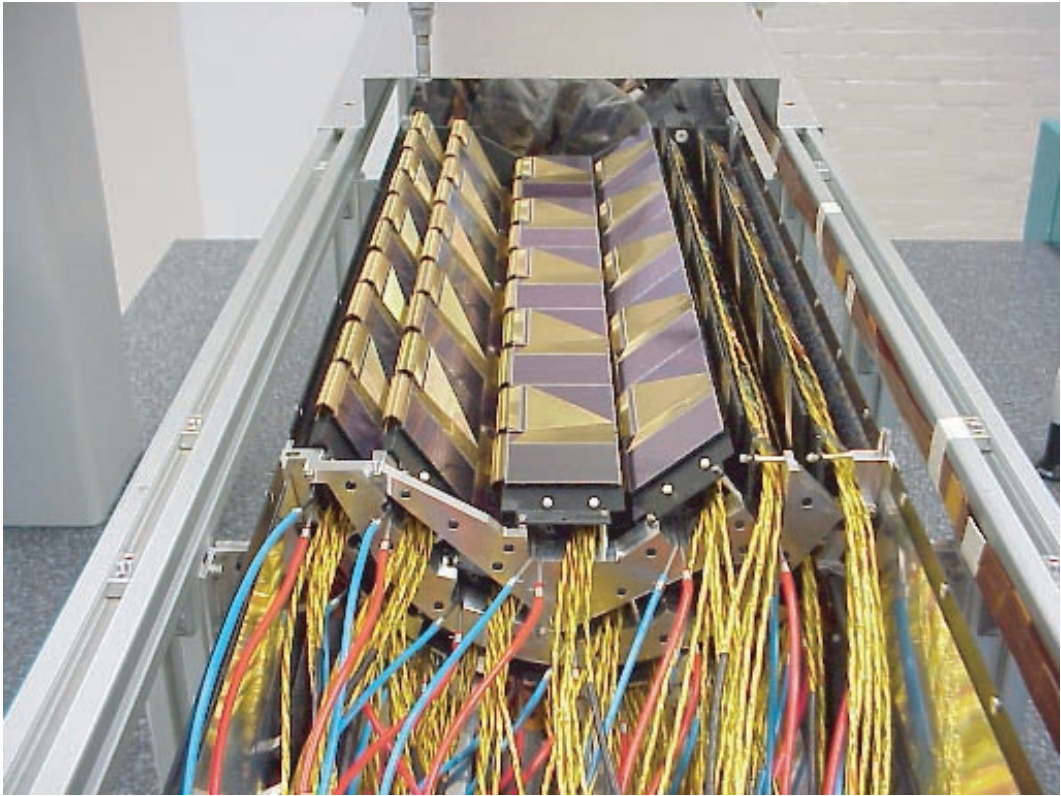


Figure 8.6: *Picture of the microvertex ladders (top) and forward wheels (bottom) positioned in the support tube.*

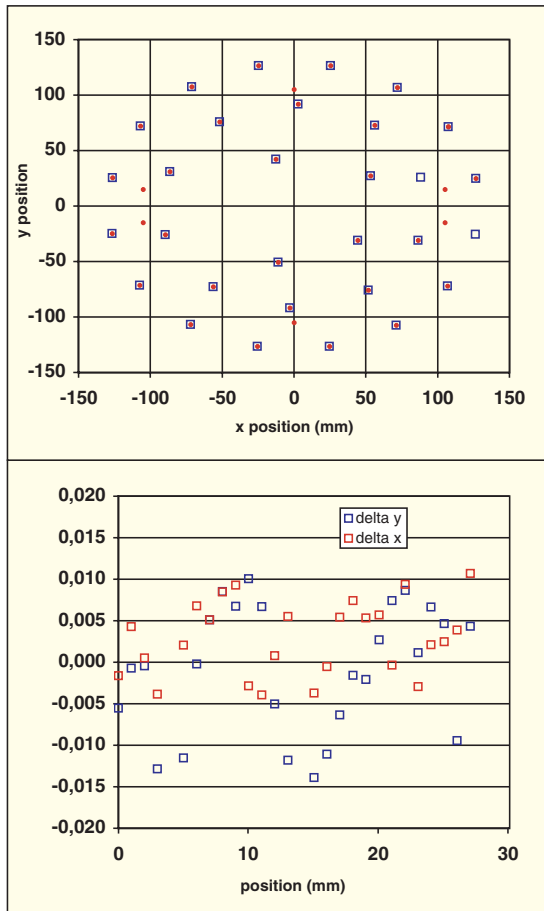


Figure 8.7: Top: The (x,y) positions of the ladder support holes (red dots) together with the design values (black squares). Bottom: differences between measurement and design positions.

barrel flange which provide the positioning accuracy for the ladders are shown together with the nominal design values. Also shown are the deviations from the design values for each of the holes. All values fall within a band of $\pm 15 \mu\text{m}$. This means that the final position of the ladders is known to better than the $\pm 10 \mu\text{m}$ as all measurement information is stored for future use in the track reconstruction.

In conclusion each sensor has been positioned inside the support tube to an accuracy which is known to about $5 \mu\text{m}$. This compares favourably to the intrinsic resolution of the detectors.

During construction and design care was taken to minimise the amount of material in the detector. However the final ladders do contain of the order of 2.8% of a

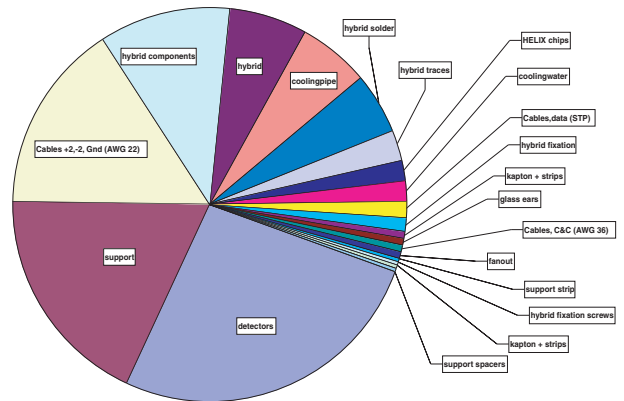


Figure 8.8: Breakdown of the material budget for the microvertex ladders. The total amount of material is equivalent to 2.8% X_0 . Sensors and readout account for more than 50% of this.

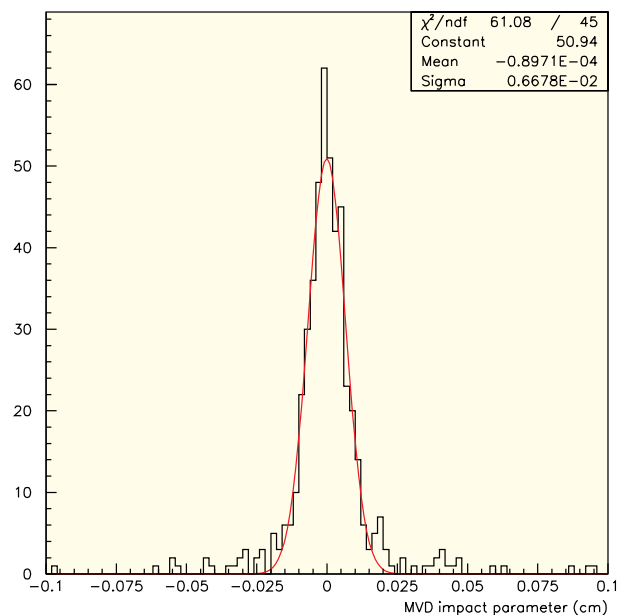


Figure 8.9: The impact parameter distribution obtained using the Kalman filter tracking and a simulation of the microvertex. All tracks originated from $(0,0,0)$. The r.m.s of the distribution is $65 \mu\text{m}$.

radiation length of material. Fig 8.8 shows the breakdown of different materials. By continuously keeping track of the dead material a detailed map of the material can be constructed for use in the reconstruction programme.

NIKHEF is also responsible for the track reconstruction

in the microvertex. A new programme has been created which makes use of the Kalman filter technique and has been coded in C++. First results on impact parameter resolution can be seen in fig. 8.9. The impact parameter has a typical resolution of $65 \mu\text{m}$ both in the $r\phi$ plane and in z . This is to be compared with a typical flight distance for a charm meson of about $300 \mu\text{m}$. The values obtained without microvertex are $300 \mu\text{m}$ in the $r\phi$ plane and 2.5 mm in z . The microvertex is thus on schedule to provide ZEUS with a significant improvement in charm tagging capability.

B LEP in 2000

1 Higgs search

In e^+e^- collisions at the highest available energies the Higgs particle, “*the missing link*” of the Standard Model, is mainly produced in association with a Z -boson. From the direct searches it was known at the end of 1999 that its mass had to be greater than $108 \text{ GeV}/c^2$. In its last year of operation, LEP the Large Electron Positron accelerator at CERN, and the four experiments ALEPH, DELPHI, L3 and OPAL (ADLO) were therefore optimized for a Higgs search. A special ramping scheme was introduced to boost the energy, so that for a period of about one hour per fill energies well above 103 GeV per beam were reached. The four experiments were sensitive to Higgs bosons up to masses of $115 \text{ GeV}/c^2$. NIKHEF participates in the DELPHI and L3 experiments. In Fig. 1.1 the collected luminosity of DELPHI as function of the beam energy is shown for the year 2000. As can be seen about half of the luminosity is collected above 206 GeV with a small but important amount around 208 GeV . The four LEP experiments collected about four times this luminosity. In what follows the results of the analysis of the combined data by the LEP Higgs group as reported in early November of 2000 are summarised.

The Higgs as well as the associated Z -boson are unstable and decay almost immediately. The three main decay modes of the Z -boson relevant for the search give a final state with: 1) a quark-antiquark pair producing two well separated jets of hadrons, 2) an undetectable neutrino-antineutrino pair and 3) a lepton-antilepton (electron, muon or tau) pair. Higgs bosons of $\sim 115 \text{ GeV}/c^2$ are expected to decay in almost all cases into a b -quark and a anti- b -quark. This $b\bar{b}$ pair forms two almost back to back jets each containing B -mesons, which travel a few millimeters before decaying into detectable hadrons.

Higgs candidates can therefore be characterized as so-called four-jet, two-jet + missing energy and two jets + two leptons events, where the associated Z -boson decays according to mode 1), 2) or 3) respectively. The Higgs search makes use of these typical features: a pair of jets or two leptons with an effective mass compatible with the mass of the Z -boson, or a missing mass (in the neutrino case) compatible with M_Z , in association with two jets with large invariant mass originating from a $b\bar{b}$ pair. The presence of b quarks can be deduced from the observation of tracks not coming from the

primary interaction point of the e^+e^- collisions but from a secondary vertex. In Fig. 1.4 a Higgs candidate of the type two-jet + missing energy is shown as it appeared in the L3 detector at the end of the 2000 data taking period. The reconstructed Higgs mass is about $114 \text{ GeV}/c^2$.

A variety of known processes, like the production of two Z bosons or a $b\bar{b}$ pair, form possible backgrounds to the Higgs signal. The experimental search techniques employed by the LEP experiments use a combination of cuts and neural networks to separate the signal from the background. The result is a number, the significance or signal to background ratio for each selected event.

In June 2000 the integrated luminosity at a center-of-mass energy in excess of 206.5 GeV became significant and a first event compatible with HZ production at $M_H = 115 \text{ GeV}/c^2$ was detected in the four-jet channel by the ALEPH Collaboration. By September several additional four-jet events were found. These tantalising signs led to LEP’s run being extended until the beginning of November. By the end of the running pe-

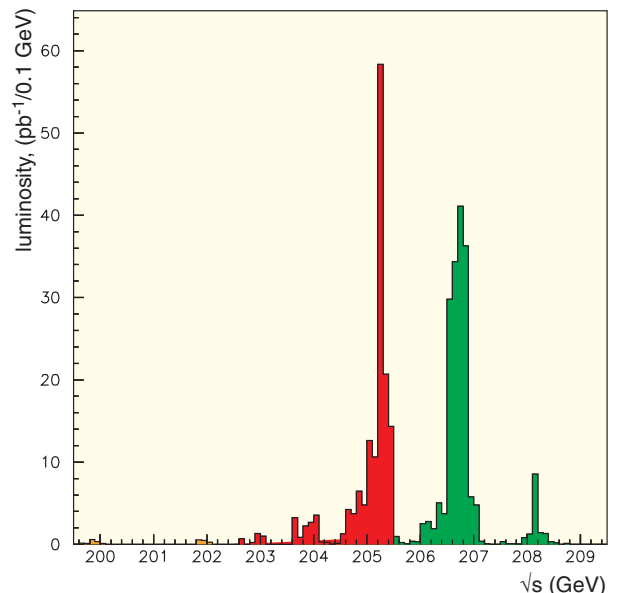


Figure 1.1: Collected luminosity as a function of the centre of mass energy for the DELPHI experiment.

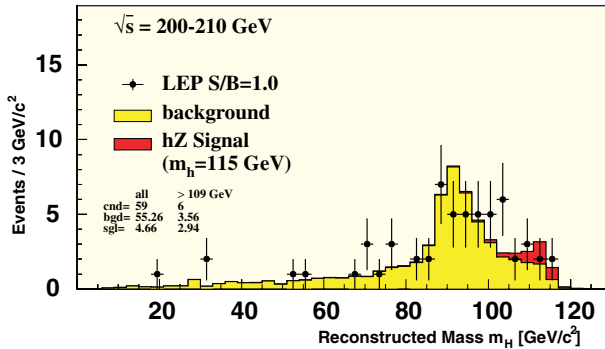


Figure 1.2: Number of events as a function of the reconstructed Higgs mass for a signal to background cut at 1. In red the signal of a Higgs mass of 115 GeV/c² is shown, in yellow the background.

riod four events have been reported with a high significance: three four-jet events from $H^0 q\bar{q}$ in ALEPH and one event compatible with $H^0 \nu\bar{\nu}$ in L3 (see Fig. 1.4).

In Fig. 1.2 the reconstructed Higgs mass distribution is shown for a signal to background cut at 1. The background shown in yellow has a clear peak around the Z mass due to ZZ production. The expected signal for a Higgs of 115 GeV/c² is shown in red. The data shown as points with error bars is well modelled by the simulation.

The combined results of the four experiments (ADLO) are in agreement with the hypothesis of a signal+background for a Higgs boson with a mass of $M_H = 115^{+0.7}_{-0.3}$ GeV/c² and 2.9 σ significance as shown in Figure 1.3. The top figure shows the negative log-likelihood ratio as function of the Higgs mass M_H . The green and yellow bands show the 68% and 95% compatibility bands for the background hypothesis only and the dashed line is the expectation in the presence of a signal. The red line shows the observed result. The compatibility of the data with the background-only hypothesis can also be given with $1 - CL_b$ as shown in the figure at the bottom. At the most probable Higgs mass of 115 GeV/c² the signal almost reaches the solid blue line of the 3 σ level. The probability that this minimum arises from a background statistical fluctuation amounts to only 0.4%.

Although the four LEP experiments requested one additional year of running to either confirm the background plus signal or the background-only hypothesis with a 5 σ significance, the representatives of the European community of high energy physicists were divided, and the

running in 2001 was not granted. The possible Higgs signal of the LEP experiments can only be confirmed or refuted by the Tevatron or LHC experiments, however, this will take at least till 2004 or even 2007.

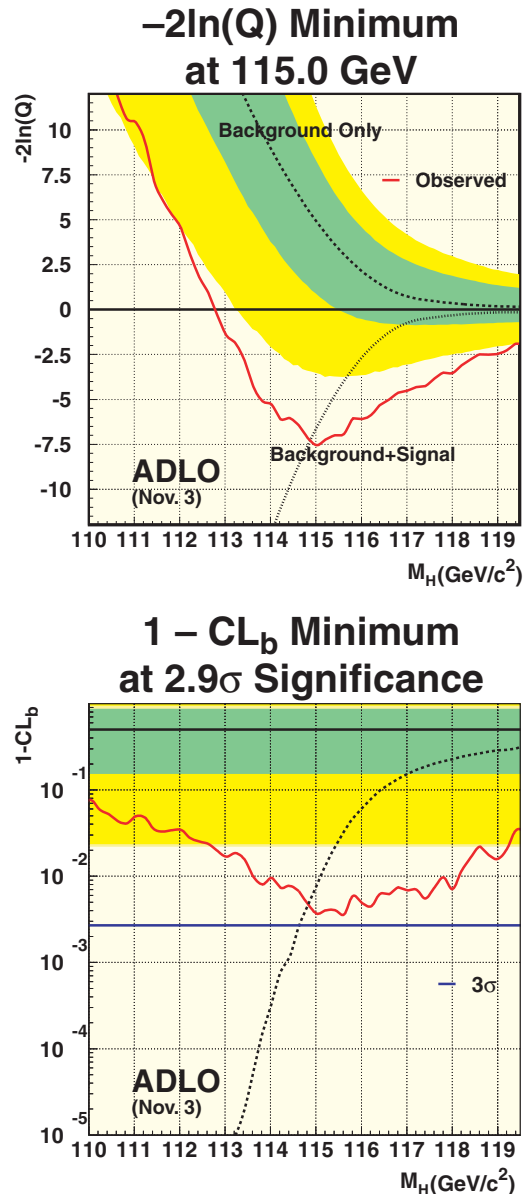


Figure 1.3: The probability curves as a function of the Higgs mass for combined LEP experiments (for explanation see text).

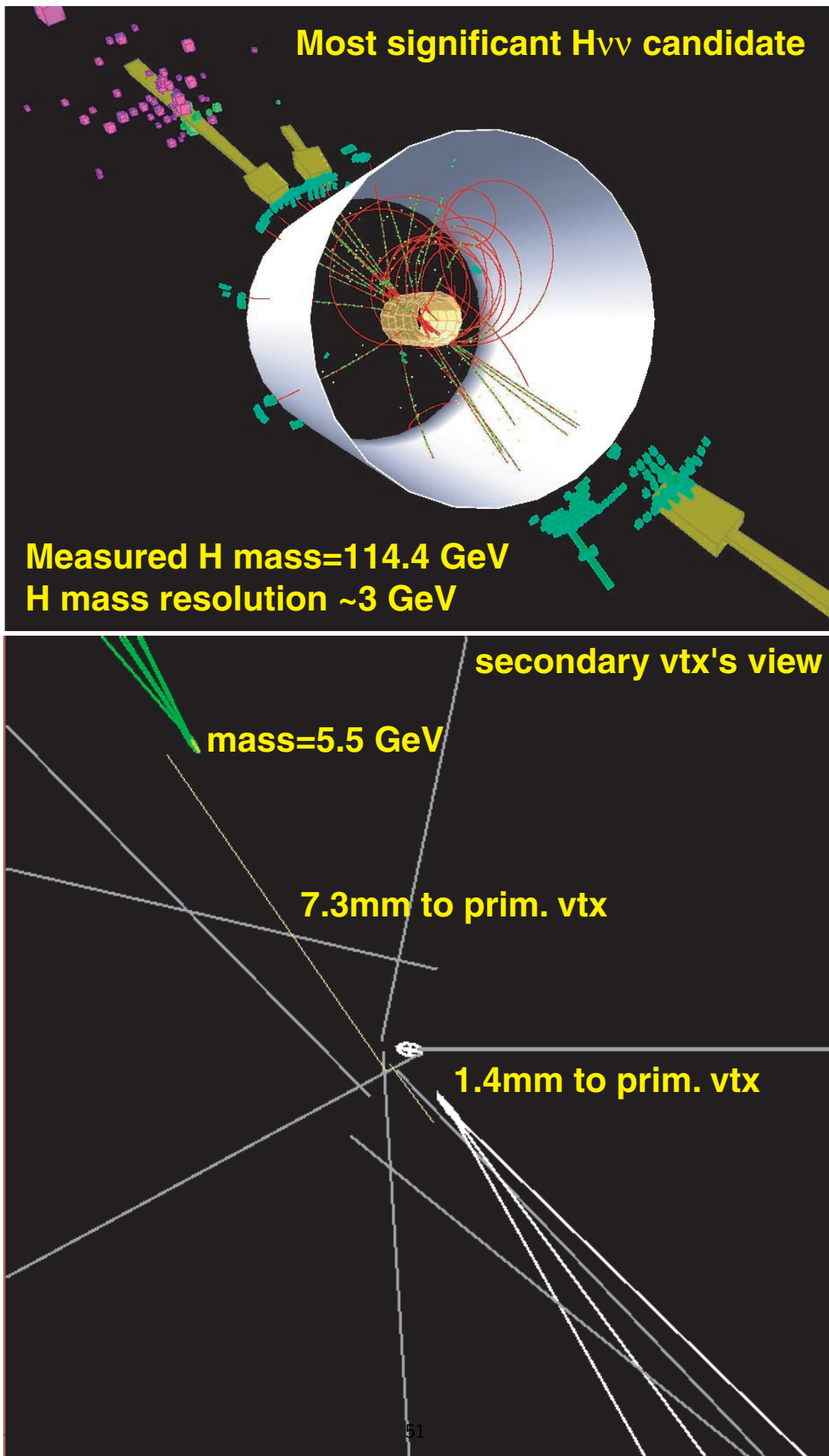


Figure 1.4: A display of the L3 Higgs candidate in the $H^0\nu\bar{\nu}$ channel.



Dismantling of the DELPHI detector.

2 DELPHI

2.1 Data taking and detector status

The year 2000 was a very successful year for LEP and the DELPHI experiment. In total an integrated luminosity of 226 pb^{-1} was collected. This brings the collected integrated luminosity to 688 pb^{-1} taken in the years 1996 through 2000 above the W pair threshold, well above expectation. Unfortunately, on the 1st of September 2000, one sector of the Time Projection Chamber was lost. This was due to a short circuit caused by a slack wire. One TPC sector corresponds to $1/12$ of the azimuthal angle. Other tracking detectors can partially compensate for this loss.

The average data taking efficiency in 2000 was further improved and amounted to 95.3%.

After the end of the run on the 3rd of November 2000, the dismantling of the detector has started. In 2001 a full reprocessing is planned for the data taken in the years 1996 to 2000 in order to obtain an improved, homogeneous data set.

2.2 Selected research topics

In total 30 papers were published in physics journals by the DELPHI Collaboration in 2000, 15 of which were based on data collected at LEP II energies. Half of the papers are based on the data from the Z running period. Some 62 contributions were submitted to the International Conference on High Energy Physics (ICHEP 2000) in Osaka.

The NIKHEF group contributed to the Higgs search, in particular the four-jet channel. The results were discussed in the previous section. A PhD thesis on the s quark asymmetry around the Z pole was finished. A few recent subjects, with contributions from our NIKHEF group, will be discussed here.

2.3 Tau topological branching ratios

Historically, there has been an inconsistency in the measured τ exclusive branching ratios: the measurements of exclusive branching ratios to decay modes containing one charged particle did not sum up to the inclusive branching ratio for a charged multiplicity of one. While this has been at least partly resolved in recent years, the current world average values from direct measurements of the topological branching ratios have uncertainties which are significantly larger than the values obtained through combined fits to all exclusive decay modes. For the case of the 1-prong branching ratio the difference

between the average and the fit value is more than two standard deviations.

An analysis has been performed of a dedicated simultaneous measurement of the decay rates, in $Z \rightarrow \tau^+\tau^-$ events, of the τ lepton to different final states as a function of the charged particle multiplicity. The τ topological branching ratios are defined as

$$\begin{aligned} B_1 &\equiv B(\tau^- \rightarrow (\text{particle})^- \geq 0 h^0 \nu_\tau (\bar{\nu})); \\ B_3 &\equiv B(\tau^- \rightarrow 2h^- h^+ \geq 0 h^0 \nu_\tau); \\ B_5 &\equiv B(\tau^- \rightarrow 3h^- 2h^+ \geq 0 h^0 \nu_\tau), \end{aligned}$$

where h is either a π or K meson.

In an initial step $Z \rightarrow \tau^+\tau^-$ events were selected with a high efficiency and low background with an emphasis on controlling the background contamination, which was estimated from the data themselves.

The DELPHI track reconstruction used four subdetectors: the vertex detector (VD), inner detector (ID), TPC and outer detector (OD). The pattern recognition was designed to minimise bad associations. The attachment of the VD to a track is important for rejection of secondaries of reinteractions in the detector material

Converted photons producing e^+e^- pairs in the tracking detectors were reconstructed using a kinematic algorithm based on the reconstructed tracks. This was complemented by conversion rejection based on an electron identification algorithm using TPC ionisation and calorimetry. The total conversion identification efficiency was 87%. Hadrons reinteracting inelastically in the material before the TPC gas volume were reconstructed by an algorithm which was 82% efficient.

After removal of tracks which were tagged as secondaries from material reinteractions, selection criteria for the different τ decay topologies were applied based on the multiplicity of tracks reconstructed in the TPC and OD and as a function of whether these tracks had associated VD hits. Further criteria were applied depending on the multiplicity of tracks reconstructed in only the VD and ID, and for 5-prong decays, based on the observed momentum of the 5-prong system. The $\tau^+\tau^-$ events were then classified according to both the hemisphere classifications. A fit was performed to the numbers of events estimated in each event topology.

Systematic effects accounted for included: $\tau^+\tau^-$ selection; tracking efficiency for isolated tracks and for tracks in the dense topologies of 3-prong and 5-prong

decays; the efficiency of the conversion and nuclear reinteraction reconstruction and the attendant misidentification probabilities; the material composition of the DELPHI detector; the efficiency and misidentification probability of the electron identification; the exclusive τ branching ratios; modelling of the 3-prong τ system; simulation statistics.

The results obtained for the topological branching ratios were

$$\begin{aligned} B_1 &= (85.316 \pm 0.093_{\text{stat}} \pm 0.049_{\text{sys}})\%, \\ B_3 &= (14.569 \pm 0.093_{\text{stat}} \pm 0.048_{\text{sys}})\%, \\ B_5 &= (0.115 \pm 0.013_{\text{stat}} \pm 0.006_{\text{sys}})\%. \end{aligned}$$

The B_1 and B_3 results are consistent with and more precise than the results obtained in the PDG2000 combined fit to all τ decay data: $B_1 = (85.32 \pm 0.13)\%$; $B_3 = (14.58 \pm 0.13)\%$, and more than twice as precise as the existing world averages of $(84.59 \pm 0.33)\%$ and $(14.63 \pm 0.25)\%$ respectively (see Fig. 2.1). The result on the 5-prong branching ratio is in good agreement with the world average of $(0.107 \pm 0.009)\%$.

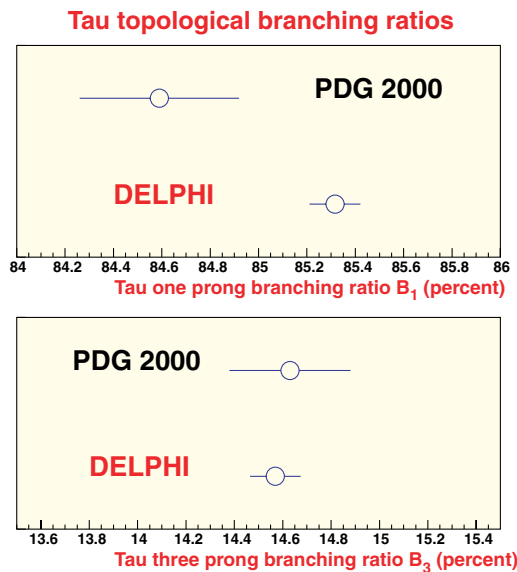


Figure 2.1: Measurements of the one and three prong tau branching ratio compared to the particle data book PDG 2000 average.

2.4 Other research topics

The analysis of $B_s^0 - \bar{B}_s^0$ oscillations is still continued, as well as the measurements on the tau lepton. Further,

the DELPHI group contributes to the measurements of the W mass and W production cross section. The analysis of the W mass for the 1998 data was finalized and published. For the above topics the reader is referred to the NIKHEF annual report of 1999 and the publication list.

2.5 Trilinear Gauge Boson Couplings

An important topic is the study of trilinear gauge boson couplings, i.e. the coupling of three bosons. Three processes were studied as shown in Fig. 2.2. Firstly, the production of a W^+W^- pair. Secondly, the production of a single W in the reaction $e^+e^- \rightarrow We\nu$. Finally, the process $e^+e^- \rightarrow \gamma\nu\nu$. These processes are sensitive to the ZWW or γWW couplings. The NIKHEF group contributes to the analysis of the single W process.

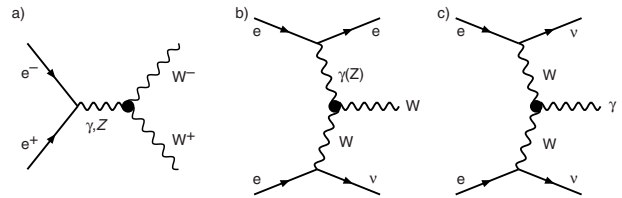


Figure 2.2: Diagrams involving three gauge bosons: a) $e^+e^- \rightarrow W^+W^-$, b) $e^+e^- \rightarrow We\nu$ and c) $e^+e^- \rightarrow \bar{\nu}\nu\gamma$.

The data are used to determine Δg_1^Z , the difference of the WWZ coupling strength and the Standard Model value, $\Delta\kappa_\gamma$, the difference of the value of the dipole coupling and the Standard Model value, and $\Delta\lambda_\gamma$, the $WW\gamma$ quadrupole parameter. In the Standard Model g_1^Z and κ_γ are equal to 1 and λ_γ is 0.

In the analysis an effective Lagrangian for the interaction of two W -bosons and a photon or Z is used imposing \mathcal{CP} conservation and $SU(2) \times SU(1)$ invariance. This leads to the following relation of the $WW\gamma$ and WWZ parameters $\Delta\kappa_Z = \Delta g_1^Z - s_w^2/c_w^2 \Delta\kappa_\gamma$ and $\lambda_Z = \lambda_\gamma$, where s_w and c_w denote respectively the sine and cosine of the electroweak mixing angle.

The 1998 data were fully analysed corresponding to a total integrated luminosity of 155 pb^{-1} . To study W pair production (process a), 621 events were selected where one W decayed leptonically and 1130 fully hadronic events. For the single W final state (process b), 10 events were selected where the W decayed leptonically and 64 hadronic events. In total 145 events with one final state photon were selected (process c).

For the extraction of the couplings the production cross

sections for the three final states were measured. To improve the sensitivity to the couplings in the W pair final state also the W^- production angle was used and the W decay angle for the leptonic final state.

From the data $\Delta g_1^Z, \Delta \kappa_\gamma$ and $\Delta \lambda_\gamma$ were fitted. The results including the results from previous years are shown in Fig. 2.3a-c and the table below.

parameter	value
Δg_1^Z	$-0.02^{+0.07}_{-0.07} \pm 0.01$
$\Delta \kappa_\gamma$	$0.25^{+0.21}_{-0.20} \pm 0.06$
$\Delta \lambda_\gamma$	$0.05^{+0.09}_{-0.09} \pm 0.01$

It is possible to translate these results into measurements of the the magnetic dipole moment μ_W and electric quadrupole moment q_W of the W -boson. Using the expressions:

$$\mu_W = \frac{e}{2 M_W} (g_1^\gamma + \kappa_\gamma + \lambda_\gamma) \quad (2.2)$$

$$q_W = -\frac{e}{M_W^2} (\kappa_\gamma - \lambda_\gamma) \quad (2.3)$$

This gives, assuming $g_1^\gamma = 1$:

$$\begin{aligned} \mu_W \frac{2 M_W}{e} &= 2.22^{+0.20}_{-0.19} \\ q_W \frac{M_W^2}{e} &= -1.18^{+0.27}_{-0.26} \end{aligned}$$

In the Standard Model one expects 2 and -1 respectively. The result is shown in Fig. 2.3d. All the results are compatible with the Standard Model expectation.

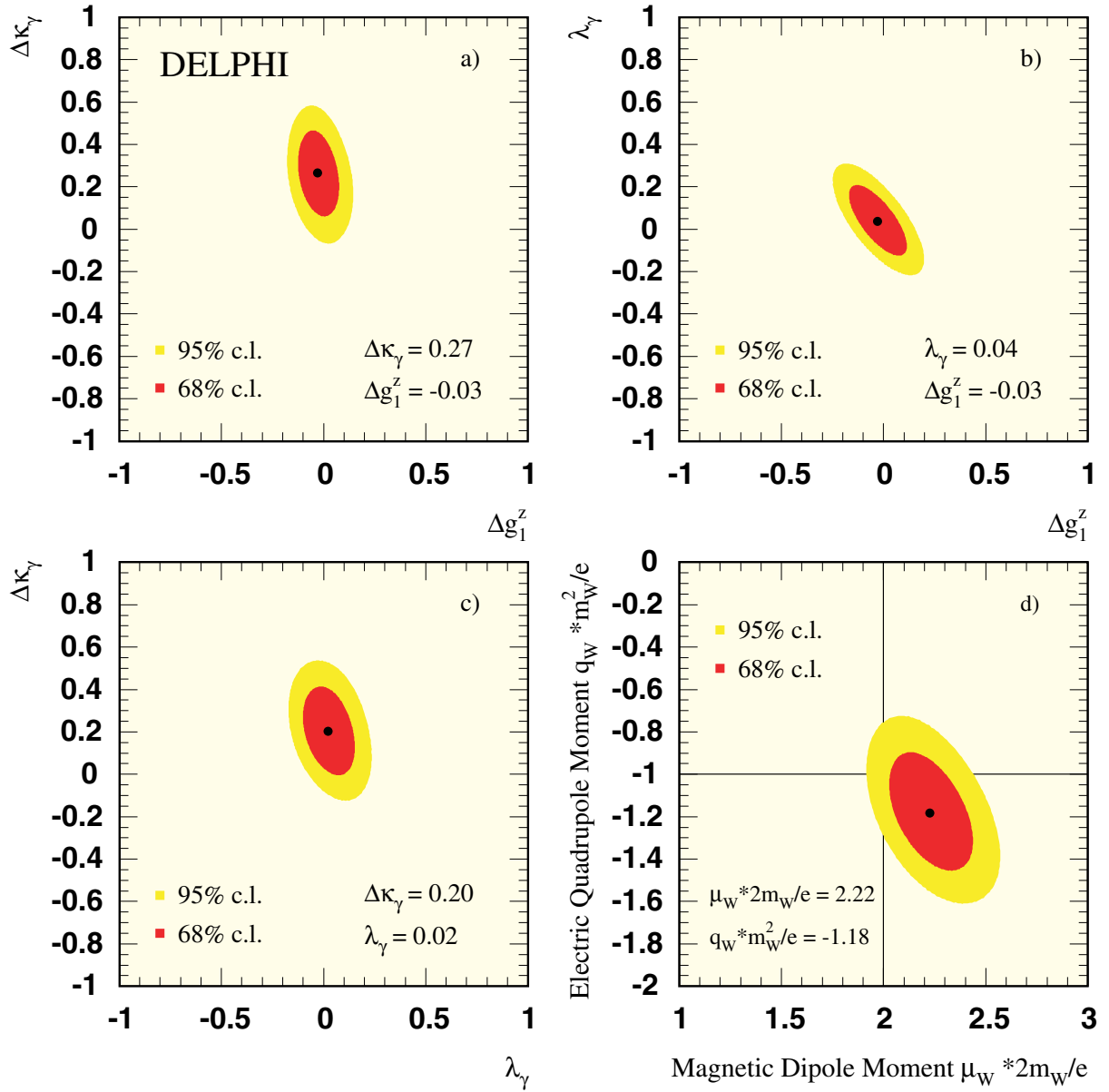


Figure 2.3: The results for the coupling constants $\Delta g_1^z, \Delta\kappa_\gamma$ and $\Delta\lambda_\gamma$ are shown in a)-c). The magnetic dipole momentum of the W versus the electric quadrupole moment is shown in d). The 68% and 95% CL contours are shown in red and yellow (dark and light shading).

3 L3

3.1 Introduction

The L3 detector is designed as a general purpose detection system with emphasis on the measurement with good spatial and energy resolution of electrons, photons, muons and jets produced in e^+e^- reactions.

During the 2000 LEP run, L3 accumulated 4.0 pb^{-1} of luminosity at the Z peak for calibration of the vertex detectors. At the highest LEP energies 217 pb^{-1} was collected with an on-line DAQ efficiency of 91%. This brings the total luminosity above the W^+W^- threshold collected with the L3 detector during 1996 to 2000 to 704 pb^{-1} . The analysis of the 2000 data is in progress; results given below are preliminary. The collaboration expects the analysis of the L3 data sample will last until 2003.

During 2000, 27 refereed papers were published by the collaboration, plus the contributions to the large winter and summer conferences in high energy physics, e.g. 58 papers were contributed to the XXX ICHEP conference in Osaka (Japan).

In the Netherlands the participation in the L3 experiment is from the FOM institute and the universities of Amsterdam, Nijmegen and Utrecht. In 2000, NIKHEF

physicists have contributed to the analyses of mass and couplings of the W -boson, production of τ pairs at high energies, charged multiplicity, moments of the multiplicity and Bose-Einstein correlations in hadronic Z and W decays, charmonium and bottomonium resonance production in two-photon collisions, searches for Standard Model Higgs production, and studies of the cosmic ray muon flux.

As in previous years the computer farm in Nijmegen has been generating Monte Carlo events. About 28 million events could be added to the pool of L3 Monte Carlo events, representing 40% of the total L3 production in 2000.

3.2 Searches

The main goal of the year 2000 LEP running was the search for the Higgs boson and Supersymmetric particles. The search for the Standard Model Higgs is described in section B1 and preliminary results of the Standard Model Higgs analysis of the year 2000 data have been published at the end of the data taking period. The cross-section for the production of a Standard Model Higgs of $114 \text{ GeV}/c^2$ mass in the reaction $e^+e^- \rightarrow ZH$ is compared in Figure 3.1 to hadronic production in various e^+e^- channels as measured with the L3 detector over the last 12 years.

Supersymmetric particles were searched for in many different channels and kinematical regions. No signal was observed and in many channels limits corresponding to the allowed kinematic phase space are established. An example is given in Figure 3.2 for the chargino mass limit.

By exploiting the complementarity of the different searches, an absolute limit on the mass of the lightest neutralino of $39.2 \text{ GeV}/c^2$ has been set.

3.3 W physics

One of the highlights of the LEP-2 program is the measurement of the properties of the W -boson. From the data taken in the 2000 LEP run, approximately 3000 $e^+e^- \rightarrow W^+W^-$ candidate events have been selected, bringing the size of the total WW sample acquired by L3 to some 10000 events.

The measured cross sections for $e^+e^- \rightarrow W^+W^-$ as a function of \sqrt{s} are shown in Figure 3.3 for the full L3 data sample. The measurements are in good agreement with recent Standard Model calculations including

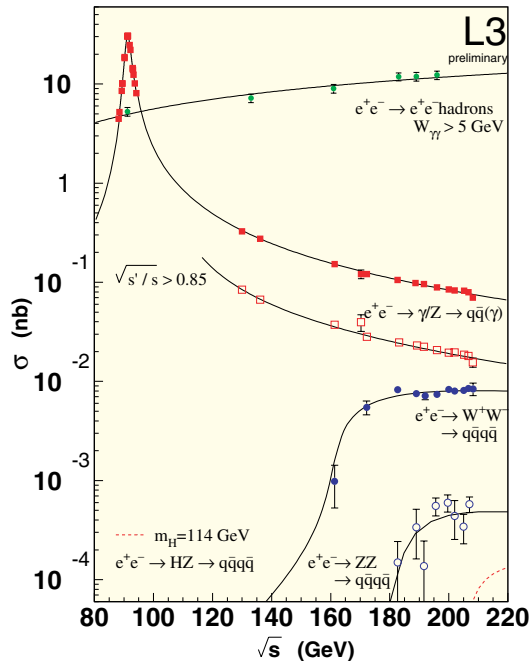


Figure 3.1: Hadronic production cross sections of various e^+e^- channels.

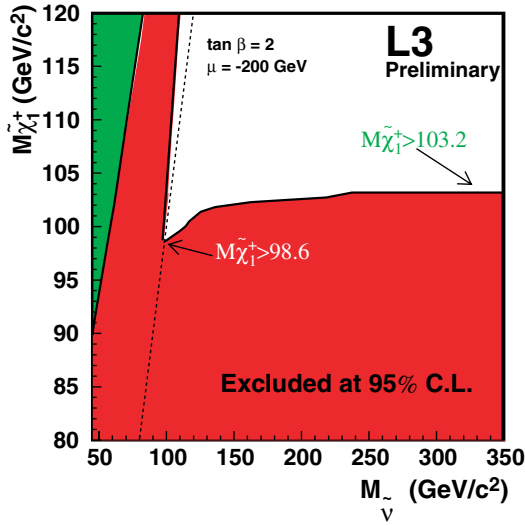


Figure 3.2: Chargino mass limits as a function of the sneutrino mass.

$\mathcal{O}(\alpha)$ radiative corrections in the double pole approximation.

The events selected in the various W decay topologies are used to determine the W branching fractions. The data are consistent with lepton universality. The branching fraction for hadronic W decay, $\text{Br}(W \rightarrow q\bar{q}')$ is measured to be $68.34 \pm 0.40(\text{stat.}) \pm 0.33(\text{sys.})\%$.

The differential production and decay cross sections of W -bosons, as well as their total production cross section, are used in fits to determine the WWZ and $WW\gamma$ couplings. These results are combined with information on W couplings obtained from analyses of single W production, $ee \rightarrow W\nu\gamma$, and single photon production, $ee \rightarrow \nu\nu\gamma$. The self-coupling between the electroweak vector bosons in the WWZ and $WW\gamma$ vertices plays a crucial role in the gauge structure of the Standard Model. Experimental tests of these couplings are sensitive to new physics beyond the Standard Model.

The results from the fits to the WWZ and $WW\gamma$ couplings are in agreement with the Standard Model predictions. Limits have been set on anomalous contributions to the \mathcal{CP} -conserving couplings g_5^Z , κ_γ , and λ_γ , which are 1, 1 and 0 respectively in the Standard Model. Some results are shown in Figure 3.4, where a theoretical relation between κ_γ and κ_Z , and λ_γ and λ_Z , based on a remaining $SU(2)$ symmetry, is assumed. In addition, more general fits without this assumption are performed. Furthermore, limits on the anomalous, \mathcal{C} - and \mathcal{P} -violating, coupling g_5^Z have been set.

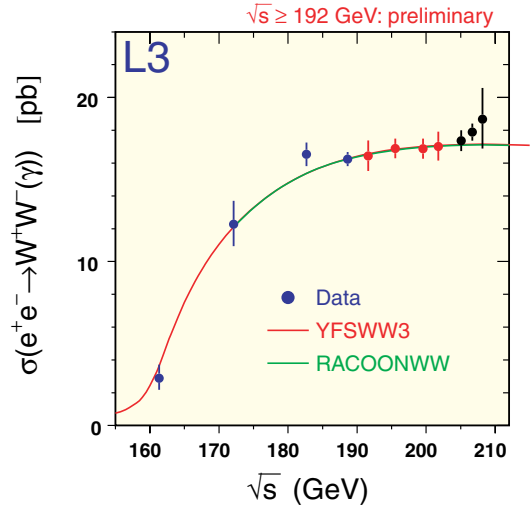


Figure 3.3: Cross sections for $e^+e^- \rightarrow W^+W^-$ as a function of \sqrt{s} .

Information on the polarisation of the produced W -bosons is gained by analysing the polar angle of the W decay products in the W rest frame. A fit to the distributions of these angles shows that, combining data at $\sqrt{s} = 183 - 202$ GeV, $25.9 \pm 3.5\%$ of the W -bosons are longitudinally polarised, in good agreement with the Standard Model expectation of 24.8%, whereas in the 2000 data at $\sqrt{s} = 204 - 209$ GeV these numbers are $21.6 \pm 5.3\%$ and 22.0% , respectively. \mathcal{CP} conservation demands that the helicity $\{-1, +1, 0\}$ fractions of the W^- are equal to the $\{+1, -1, 0\}$ fractions of the W^+ . This has been verified experimentally. In addition, correlations between the helicity of the W^- and the W^+ in a given event have been measured to agree with the SM prediction.

The cross section for the process $e^+e^- \rightarrow W^+W^- \gamma$ has been measured for isolated, energetic photons in the detector. This channel is sensitive to quartic gauge couplings of the type $WWZ\gamma$ or $WW\gamma\gamma$. The measured cross section agrees with the SM prediction, and limits have been set on anomalous contributions to these quartic couplings.

Above the WW production threshold, the W mass is most accurately measured from a fit to the invariant mass spectrum of W decay products. Events are reconstructed into four jets ($qqqq$ events), or two jets, a lepton (or τ "jet") and a missing momentum vector identified with an undetected neutrino ($qq\ell\nu$ events). A kinematic fit is applied to the measured event, demanding energy- and momentum-conservation. W mass is extracted in an unbinned maximum likelihood

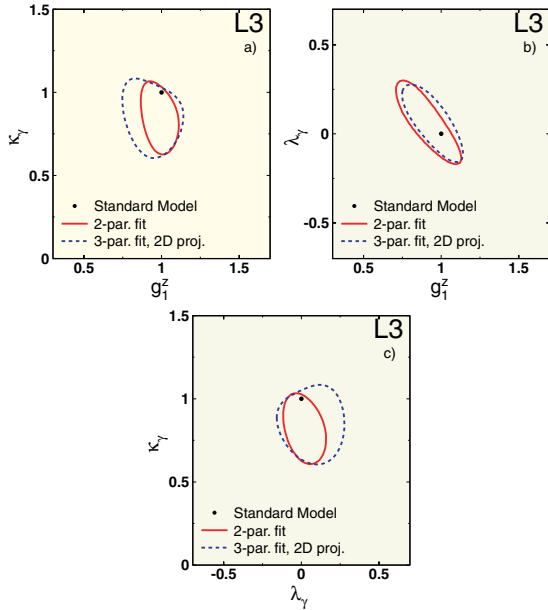


Figure 3.4: Allowed regions, at 68% confidence level, in the (κ_γ, g_1^Z) (a), (λ_γ, g_1^Z) (b), and $(\kappa_\gamma, \lambda_\gamma)$ (c) planes, resulting from fits to the 2 couplings shown, or to all 3 couplings.

fit by reweighting a fully reconstructed Monte Carlo sample. Combining the data taken at all center-of-mass energies, the W mass is measured to be $M_W = 80.398 \pm 0.048$ (stat.) ± 0.050 (syst.) GeV/c^2 .

From the width of the invariant mass spectrum of W decay products, the W width Γ_W is measured to be $2.24 \pm 0.19 \text{ GeV}/c^2$.

The dominant systematic error on the measurement of W mass and width in the $qqqq$ channel arises from final state interference effects such as reconfiguration of the colour flow (colour reconnection) between partons originating from different W 's, and Bose-Einstein correlations between identical bosons from different W 's. In 2000, significant progress has been made on experimental studies of these effects.

For the study of Bose-Einstein correlations (BEC), a method has been developed to isolate the correlations between bosons from different W 's. The two-particle density in $qqqq$ events is compared to a density constructed by mixing two independent $qq\ell\nu$ events. Figure 3.5 shows the ratio D' of these densities for like-sign particles in data and in Monte Carlo samples with and without inter- W BEC. The results show no evidence for

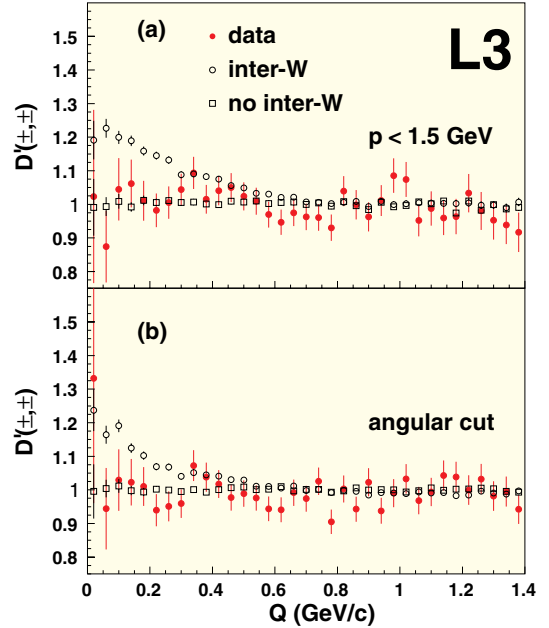


Figure 3.5: The ratio D' of two-particle densities in $qqqq$ events and mixed $qq\ell\nu$ events for like-sign particles in data and in Monte Carlo samples with and without inter- W BEC, as a function of four-momentum difference Q . In order to increase the sensitivity for inter- W BEC, only low momentum tracks have been used in (a), and only events with two jets from different W 's close together in (b).

such inter- W BEC in the data, and their implementation in various JETSET models is excluded. This result leads to a significant reduction of the systematic error on W mass and width due to BEC.

A study of particle- and energy flow between jets in selected $qqqq$ events has been found to be sensitive to predictions of various realistic models of colour reconnection. Preliminary results show moderate amounts of colour reconnection in data, as predicted by these models, and exclude very large amounts of reconnection. This procedure will be developed further, and will allow for a measurement of colour reconnection in actual data, and thus a well-motivated and limited systematic error from colour reconnection on W mass and width.

3.4 L3+Cosmics

The L3+Cosmics experiment takes advantage of the unique properties of the L3 muon spectrometer to get an accurate measurement of cosmic ray muons 30 m underground. The goal of this experiment is to measure the absolute cosmic ray muon flux and the muon

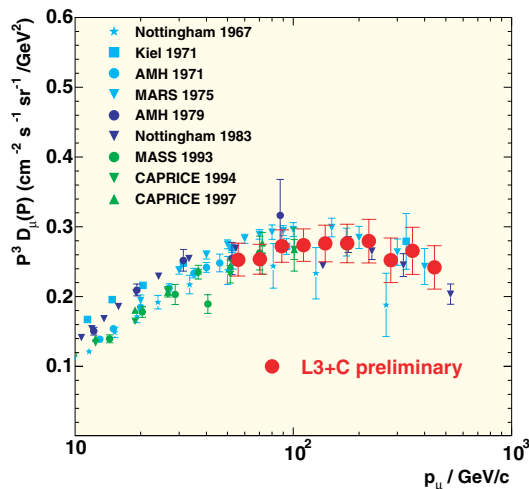


Figure 3.6: *The vertical muon flux of cosmic ray muons, multiplied by p^3 , as a function of muon momentum.*

charge ratio as a function of muon momentum, and to search for point sources. A new muon trigger, readout and DAQ system, (provided by NIKHEF and Nijmegen) has been installed, as well as 200 m² of scintillator covering the L3 magnet and is fully operational since the beginning of the 1999 run. Data taking started as soon as the L3 muon detector and magnet were operational at the end of March, and continued without interruptions to the middle of November. A total of 6.9×10^9 events were recorded. Together with the 5×10^9 of 1999, our total data set exceeds 10^{10} events.

In 2000 also the air shower array on top of the L3 building started taking data successfully. In total 33×10^6 air showers were recorded with 8×10^6 events triggered both in the air shower and the muon detector. The combination of the air shower array and the muon detector will enable studies of the chemical composition of the primaries.

In Figure 3.6, preliminary results on the measurement of the vertical muon flux are shown as a function of the muon momentum. The systematic uncertainty on this measurement has decreased from 20% in January to 10% in July 2000. Analysis is in progress to further reduce the error to a few percent.

The start of the dismantling of LEP and L3 implied the end of the L3+Cosmics experiment.

C Theoretical Physics

1 Theoretical Physics Group

1.1 Research program Theoretical Physics

The research in the NIKHEF Theory Group spans a wide range of subjects in subatomic physics. On the one hand, there is the reductionist effort to determine the most elementary building blocks of matter and to arrive at a unified and detailed description of the laws that govern their dynamics. This activity includes research in string theory, supersymmetry and conformal field theory. On the other hand, work is also going on along constructivist lines: given the present knowledge of the constituents of elementary particles and their dynamics, can we derive their structure or predict the outcome of high energy experiments? A large part of the research effort of the group goes in this direction, in particular into sophisticated perturbative QCD calculations.

Much of the research carried out is of direct interest to the experimental groups at NIKHEF. As a result, at present two positions for theoretical PhD students are being provided by experimental groups and several longer-term visitors to the group have been co-sponsored in the past year. The strong involvement of the Theory Group in the education of scientists has not been restricted to the supervision of the research of students pursuing their masters or PhD degree. The seniors in the group have taken on a sizeable course load at the universities that are represented in NIKHEF and have been heavily involved in the 'Special Topics' courses which are mandatory for all PhD students connected to NIKHEF. In 2000, J. W. van Holten was appointed as extra-ordinary professor of theoretical physics at the Free University of Amsterdam.

1.2 QCD

Within QCD there exists a well-defined framework for performing perturbative calculations. Higher order corrections to observables are crucial to obtain quantitative predictions for the strong force and the structure of hadrons. Vermaseren and co-workers have developed a new technique to evaluate the deep inelastic structure functions of the proton at the two- and three-loop level. The method relies heavily on the use of the computer-algebra program FORM (see below). The two-loop results have been published, while work on the three-loop calculation is in progress.

In some situations large quantum corrections remain which make perturbative calculations to only a finite order meaningless. The validity of the perturbative approach is restored through the analytic resummation methods, which have been studied by E. Laenen and co-workers over the past years. It was found that most resummations may be directly based on the fact that observables factorize into various functions corresponding to different effective degrees of freedom. Most recently, this approach has been extended to include recoil effects of quarks and gluons in the proton wave function. There are indications that this may resolve long-standing discrepancies between theory and experiment for prompt photon production.

Due to their large masses, processes involving heavy quarks with the flavor charm, bottom or top can be described in a perturbative approach. A perturbative description of the production of top quarks in high-energy colliders has been developed by E. Laenen and his group in close collaboration with the ATLAS/D0 group at NIKHEF. A Monte Carlo computer program for the simulation of single top production at hadron colliders was written which includes one-loop quantum corrections.

The phase structure of QCD is under intensive investigation by theorists and experimentalists. Evidence has been reported from studies with the CERN SPS that the transition from the hadronic phase, where the quarks and gluons are confined to hadrons, to a quark-gluon plasma may have been seen. Intensive research in this direction continues at the RHIC in Brookhaven and in the future at the LHC to firmly establish this transition and to study the properties of strongly interacting matter at high temperatures. J. Koch and collaborators are investigating to what extent the changing properties of hadrons, embedded in a medium of finite temperature, signal the approaching phase transition. Assuming thermal equilibrium, the electromagnetic form factor of a pion is being calculated for finite temperature. This is done by means of lattice gauge calculations in collaboration with E. Laermann (Bielefeld).

1.3 String theory

String theory goes beyond the quantum field theory framework, and its ideas are changing our view of nature at its most fundamental level. Recently, open

strings and higher-dimensional branes, on which their endpoints may lie, have been at the center of work in this field. Whereas closed strings can be described perturbatively through conformal field theory, this is not yet the case for open strings.

B. Schellekens and coworkers have studied open strings from the point of view of two-dimensional conformal field theory. The string theories of interest sweep out two-dimensional surfaces that have boundaries and that are not oriented, such as Moebius strips and Klein bottles. One of the objectives is to arrive at a general description for conformal field theories on such surfaces. This then can serve as a starting point for string spectroscopy and for a study of relations between different string theories.

1.4 Supersymmetry

A common feature of many models of physics beyond the standard model is supersymmetry. This symmetry concerns degeneracies between fermions and bosons. Groups of particles with integral and half-integral spin, respectively, which obey different statistics, have the same mass, charge and other quantum numbers. The combination of supersymmetry with other symmetries within a given particle physics model makes strong predictions for the properties of particles and can be tested by experiments. An interesting situation occurs when an ordinary (internal) symmetry is spontaneously broken at very high energies or short distances, where supersymmetry is still intact. Then massless Goldstone bosons, corresponding to the broken symmetry, are necessarily accompanied by massless fermions. If in turn also the supersymmetry is broken at the electroweak scale, then some of these massless fermions could be the relatively light quarks and leptons of the standard model.

Field theoretical work was carried out by members of the group along these lines. It was cast in a geometrical language, appropriate to the discussion of symmetries. Models of quarks and leptons were constructed, based on the symmetries of unified gauge theories with gauge groups such as $SU(5)$, $SO(10)$ or E_6 . Anomaly cancellations in these models, ensuring their quantum consistency, were examined. Several of the results obtained are contained in the dissertation of S. Groot-Nibbelink, entitled 'Supersymmetric non-linear unification in particle physics'.

1.5 Computational Physics

To test and improve our understanding of field theories such as QCD by comparing to experiments, it is crucial

to have powerful computational techniques. In this respect the computer-algebra program FORM developed by J. Vermaseren has become an indispensable tool for higher order perturbative calculations. The program is used worldwide and has been optimized with respect to the speed and the size of the formulas it can manipulate. FORM can perform complex calculations and has been used, for example, for the interpretation of experiments at HERA, the Tevatron and for predictions for the future LHC. In order to keep up with theoretical developments, an effort had been started several years ago to adjust and extend FORM. In 2000 version 3 of this program was released, which has a variety of completely new features. Among other things, this version has interesting aspects for parallel processing. In collaboration with the Universität Karlsruhe a version of FORM is being developed which works with several processors.

D Technical Departments

1 Computer Technology

1.1 Introduction

In April 2000 we were shocked by the sudden death of our colleague Eric Wassenaar, who was responsible for an important part of the system management, such as mail, DNS configuration and similar network services. Eric has contributed in programming of network tools as `host` and `traceroute` since the early days of the Internet in the late seventies of the past century. This was illustrated by many reactions on his death from the Internet community.

Fearing many, but in reality not dangerous at all: the millennium bug did not attack the NIKHEF computer and network infrastructure when the clock stroke twelve January first of the year 2000.

The year 2000 has been the start of the era of LHC computing. This can be characterized by two projects that are described in some more detail in this chapter: the implementation of a gigabit network infrastructure and the installation of a Linux PC-based compute farm for D0 event simulation and reconstruction. On January 20 the first meeting on a subject called Datagrid was held at CERN, with participation from representatives of IT departments of CERN and associated institutes. By the end of the year the Datagrid project was well on its way and NIKHEF has committed itself to participate in both a European and a Dutch Datagrid program.

Obviously, regular CT activities have been performed throughout the year 2000 as well. Software contributions were made to the data-acquisition, detector control and production systems for the ATLAS detector and to some minor extent for the LHCb outer tracker. Design studies and prototyping have been started for the data-acquisition system of the ANTARES neutrino telescope.

Linux is without any doubt the preferred choice for scientific end users. The Open Source products, the Linux system itself and a wealth of applications, are reliable and match perfectly the requirements of the scientific users for desk top computing. In the year 2000 Linux became a favorite system for embedded applications for data acquisition and control systems of the LHC detectors, where strong requirements are put on performance and real-time deterministic behavior.

WTCWnet: high-bandwidth campus network

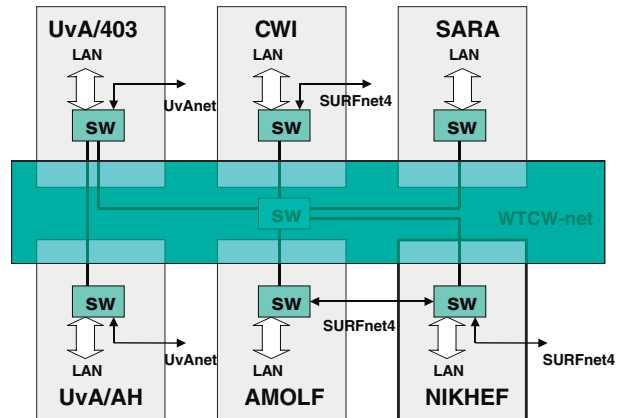


Figure 1.1: The WTCW campus high bandwidth network.

1.2 Upgrade network infrastructure

The NIKHEF local area network and the external connections have been upgraded to Gigabit ethernet. This upgrade has been driven and partially financed by the ICES-KIS projects that were started in 1999 at the institutes of the Science & Technology Centre Watergraafsmeer (WTCW). Typical for these projects is the challenging demand for a high bandwidth between the locations where the participating scientists reside. Based on the already existing fiber cable infrastructure, a Gigabit network has been implemented, called WTCW-net, to distinguish it from its predecessor the WCW-lan. This network interconnects the institutes CWI, AMOLF, NIKHEF, SARA and the University of Amsterdam to a 'core switch' with gigabit ethernet links (see Fig. 1.1).

After the definition of the requirements and a survey of the market for Gigabit ethernet switching routers, a testbed has been setup with the routers of four selected suppliers. On the basis of the results of this testbed and the best price/performance ratio, the BigIron switching routers from a company called Foundry Networks have been purchased. The NIKHEF configuration consists of two modules with eight gigabit ports each and one module with twenty-four fast-ethernet ports (100 Mbit/s). Figure 1.2 illustrates the two basic functions of this

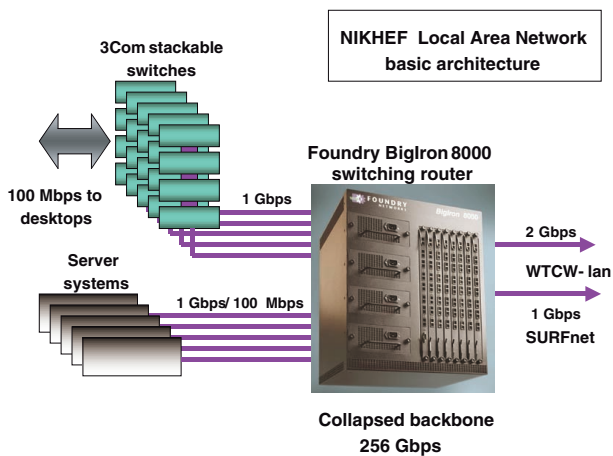


Figure 1.2: The NIKHEF high bandwidth LAN.

switching router: the firewall to the external world and the collapsed gigabit backbone for the NIKHEF internal networks. The connection to our Internet Service Provider SURFnet, has been upgraded to 1 Gbit/s, by linking the NIKHEF router to the SURFnet-4 point of presence (PoP) at SARA. Full capacity of this link will be obtained as soon as the SURFnet-5 infrastructure is available at the WTCW. The connection from NIKHEF to the core switch of the WTCW-net has a capacity of 2 Gbit/s, realized by configuring two gigabit links in parallel (trunking).

1.3 Compute farms for off-line analysis

Commodity PC's, running Linux and loosely coupled by fast ethernet switches, are scalable and flexible resources to run simulation and reconstruction analysis by distributing the compute jobs to these PC's. Each compute job analyses one event and runs on one single PC and is completely independent from similar jobs executed at other PC's in the network. The results of the analysis are written on disks and packed together for further analysis and/or transport to other locations. In theory this distributed batch system can be implemented on ordinary desktop PC's, scattered around the building. However, there are some drawbacks in allocating these desktop PC's for compute jobs. The first one is obviously that the owners of PC's do not want their resources to be exhausted by heavy compute jobs running in parallel with their own jobs on the system. However, distributed batch systems exist that overcome this drawback by checking system parameters before and during executing of batch jobs (e.g. Condor). The second drawback of using desktop PC's is

probably more serious and is caused by the differences in the hardware and software configurations of the systems, such as different versions of operating systems, available memory and disk space, processor power and so on.

The arguments mentioned above justify a substantial investment in money and manpower to install powerful PC's for event simulation and reconstruction and to interconnect these systems in a dedicated switched network environment. This kind of powerful compute servers are usually referred to as 'compute farms'. These farms are flexible and scalable: the number of 'nodes' in the farm can be extended anytime whenever extra compute power is needed and older nodes can easily be replaced by newer, more powerful PC's.

Apart from the compute nodes, farms usually contain special nodes for management and file services. To be able to deal with a large number of compute nodes, automation of system and application software and tools for continuously monitoring are demanded. A flexible 'farm management' system allows partitioning the farm into sectors where per sector different versions of the operating system and applications can be loaded. By doing this, the resources of the farm can be dynamically shared amongst more than one analysis environment.

Compute farms are expected to be heavily used for the simulation and (in a later stage) the reconstruction of LHC detector event data. To gain experience with this technology it has been decided to make a contribution to the analysis of event data of the D0 experiment at

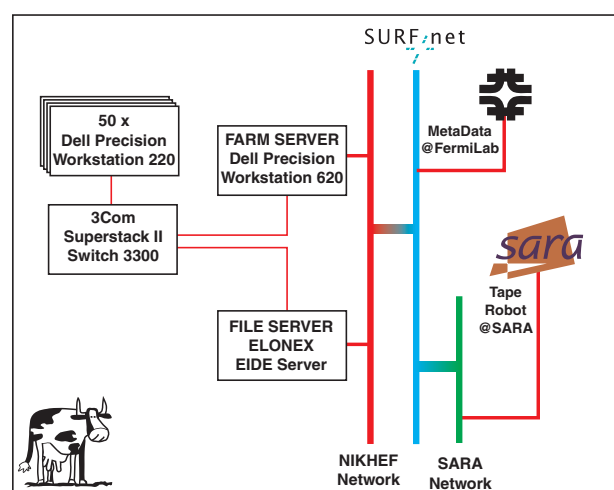


Figure 1.3: Schematic overview of the D0 farm.



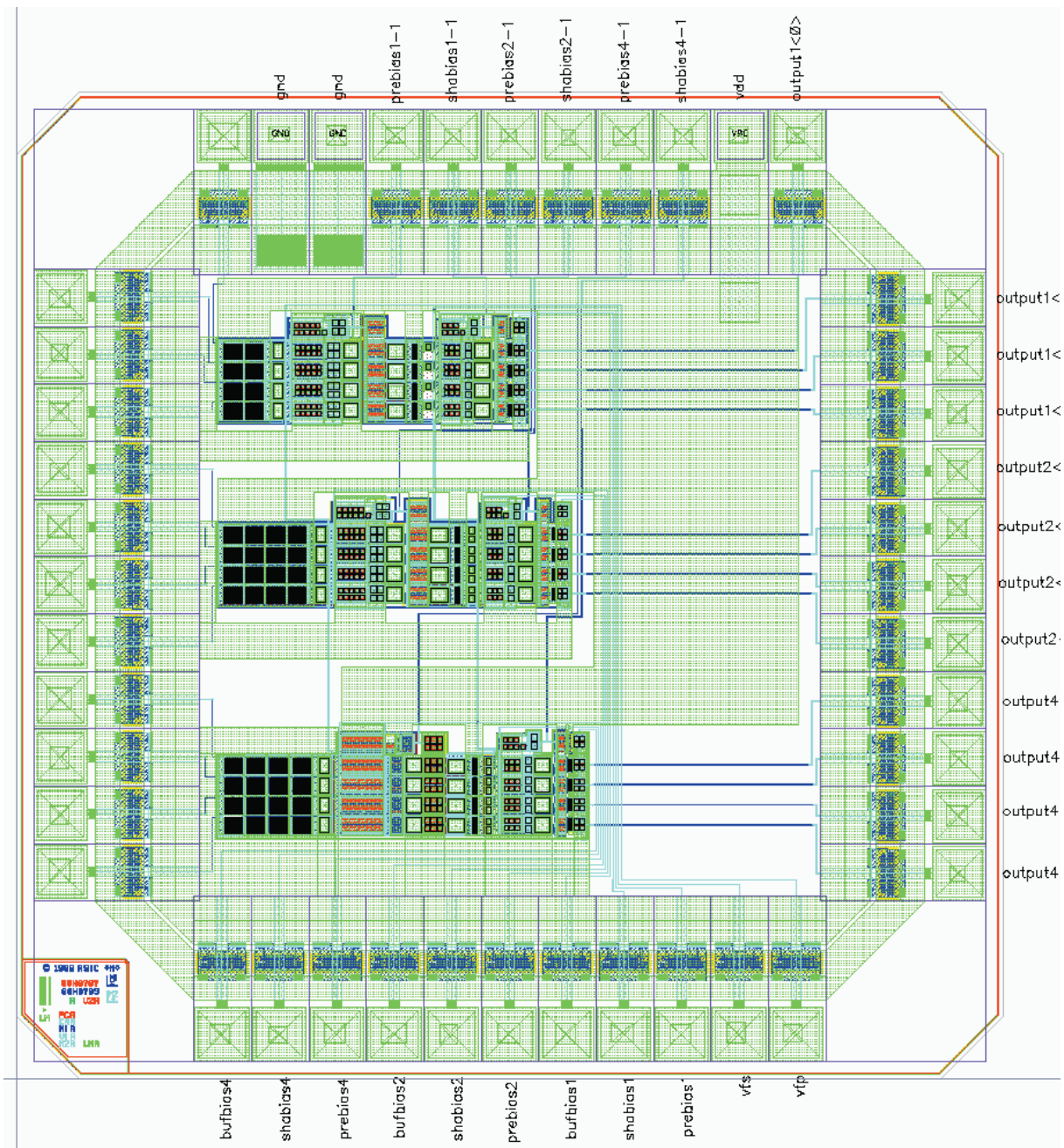
Figure 1.4: *The D0 farm at NIKHEF.*

FNAL by installing a compute farm equipped with 50 dual-processor PC's (see Figs. 1.3 and 1.4).

Each PC, a DELL Precision Workstation 220, is configured with two 800 MHz Pentium III processors, 512 Mbyte of RDRAM memory and an internal hard disk of 40 Gbyte. This configuration is tuned to run the D0 analysis software. The operating system used is version 6.1 of the Red Hat Linux distribution. To be as flexible as possible the operating system is loaded on the nodes during start up from an image on the farm server by a mechanism called 'netboot'. The farm server is also used to distribute the application jobs to the farm.

For the Monte Carlo simulations of the D0 detector, dedicated software developed at FNAL, has been installed to manage jobs and associated data files. Special effort has been put into an optimisation of the transport of the generated data files to the mass stor-

age facilities at FNAL over the wide-area network. This project benefits from the high bandwidth to the SURFnet PoP at SARA and of the good quality of the transatlantic 155 Mbps connection to the STAR TAP in Chicago. Performance tests demonstrated that the transport of data was not limited by the available bandwidth, but by the network protocols TCP/IP and FTP.



The BEETLE test chip with four front-ends with different amplifiers.

2 Electronics Technology

2.1 Introduction

The Electronic's Department has a staff of 35. The main assignments are in the area of design and engineering of electronics for the experiments. The ever increasing number of read out channels, clock rates and radiation loads affect the connection and simulation techniques. In order to facilitate this, the group maintains several Electronic Design Automation (EDA) software suites, such as VHDL, Cadence, Pspice, Mentor, which are used by both engineers and PhD students. Education is essential for using all these utilities successfully, and the development of skills is of continuous concern.

Although 'first time right design' would be ideal, in practice intensive prototyping is necessary to achieve the ultimate 'best design'. Therefore the group has high standard instrumentation like signal analyzers, oscilloscopes, power meters and surface mounting devices handling tools.

In addition there are a number of specialized laboratory rooms (one with a probe station for micro-electronics test, another is an electrically isolated Faraday-caged room, to mention some examples). On detector production sites the department supports various controls, such as temperature sensing and logging, gluing machines, local control systems.

2.2 Projects

We briefly describe the department's involvement in projects. Manpower was distributed over these projects as given in Fig. 2.1. The projects themselves are described elsewhere and further information on most of these can be found on the NIKHEF website <http://www.nikhef.nl> and <http://www.nikhef.nl/pub/departments/et>

2.2.1 ZEUS

Cooling system

In order to maintain a stable temperature inside the Zeus Micro Vertex Detector (MVD), a cooling system for this sub-detector has been designed and built. The system cools with water running through stainless steel pipes inside the MVD. The pipes are mounted in such a way that contact is made with the hybrids on which the front-end chips are placed. Power dissipated from

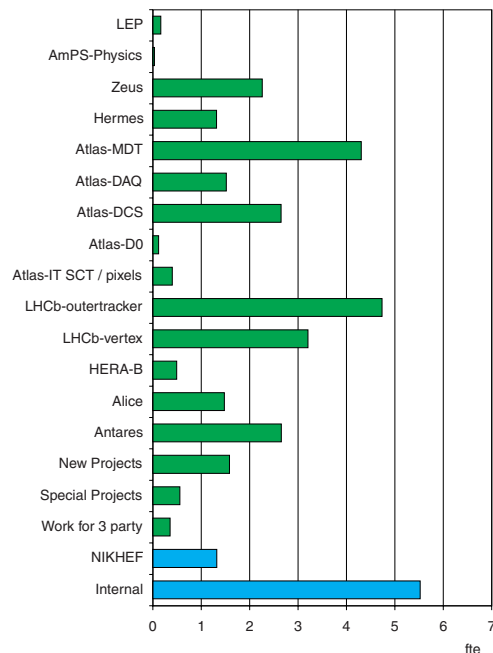


Figure 2.1: ET manpower distribution in 2000.

the chips is effectively transported out of the detector volume.

The system is normally controlled via a CAN field-bus, but can also be controlled via RS-232 for maintenance. The temperature, water pressure, air humidity and the possible existence of water in the bottom of the MVD are continuously monitored. The cooling system is currently being used at DESY

Electromagnetic compatibility constraints

The analogue signal from the front-end chips is transported over a distance of typically 30 m. To avoid accumulation of noise or other interference a special receiver module was developed which restores the signal using knowledge of the cable shortcomings. Modules were built and are being tested and installed at the experiment at DESY.

Related to the analog signal treatment, proper connections to 'earth' and 'ground' potential are important. Erroneous signal or return currents may cause interference with other channels or even other sub-detectors. Also the mechanics, which consists of a conducting aluminum structure, is part of the consideration for which

special shielding and electric insulation was sometimes necessary.

Irradiation tests of the front-end chips

In order to check whether the front-end chips will survive high radiation doses, a number of HELIX128 (v3.0) front-end chips have been irradiated up to 500 krad. No dramatic changes showed up, indicating that the chips can be used during the entire lifetime of the ZEUS experiment.

2.2.2 HERMES

The first (prototype) silicon module of the lambda wheels was exposed to normal operation throughout the complete period of beam in 2000. Radiation damage was detected; caused mainly by unexpected electron beam losses. Therefore a Beam Loss Monitor (BLM), which triggers the HERA beam dump system, was developed. The prototype of the BLM consisted of 2 small ionization chambers with electronics and a pc-based stand-alone data acquisition. This was installed in July 2000. Based on experience gained with this prototype a full scale BLM of 8 ionization chambers is currently being developed.

2.2.3 ATLAS

Most work for the ATLAS-project concerned electronics for the large Muon Drift Tube (MDT) precision chambers. Some parts are in the production phase, in parallel with the chambers themselves. Parts of the readout systems are still in the design phase.

Detector control system

The design of the MDT Detector Control System (DCS) is now in the final stage. The system is furnished with an Embedded Local Monitor Box (ELMB). This is a joint design of CERN and NIKHEF and exists of a mezzanine card with a micro-controller, a CANbus interface and a 64 channel ADC. The hardware is designed by CERN and the software has been developed by NIKHEF.

The MDT DCS is capable of measuring and controlling 32 temperature sensor channels, two magnetic-field sensor channels, two interface channels and one 8-bit digital I/O channel.

Red alignment system Nikhef

The Red Alignment System of the NIKHEF (Rasnik) is

used for the alignment of the MDT chambers in ATLAS. The system design, with all of its components, was finalized. This includes the RasCaM, RasLeD and RasMuX on the chambers, the MasterMuX in USX15 and the read-out and control electronics with PC's in USA15. See also Fig. 2.2 for the various components.

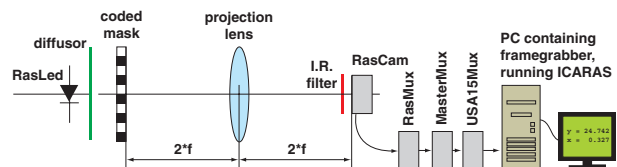


Figure 2.2: System overview of RASNIK.

The production of RasCaMs and RasLeDs has been started and first delivery of these parts is expected in January 2001. The department installed the two dedicated Go/NoGo test set-ups at the manufactures plant to check the production of these.

The final RasMuX prototype, with 8 RasCam and 16 RasLeD connections, was designed. For its testing, a MiniMasterMux with a microprocessor was designed. This microprocessor can handle 4 RasMuXs and combines the MasterMuX and USA15-Mux functionality for PC readout and control.

Muon Readout Driver

After the successful tests of a first Muon Radout Driver (MROD) prototype-0, the design of a second, more sophisticated MROD prototype has started. This prototype, called MROD-1, supports six S-Link inputs, each arriving from a Chamber Service Module (CSM) on the MDT-chamber. The CSM converts serial data-bits from a maximum of 18 TDC's on one layer of the chamber into 32-bits data-words. The MROD groups these words for each TDC and subsequently checks whether all data of the same event has arrived. The data is then formatted and send via a S-Link output to the Read-Out Buffer (ROB) for further processing by the central Data Acquisition System. The use of Digital Signal Processors (DSP) makes extensive error checking and recovering possible.

Most of the logic functions of the MROD-1 are implemented with five DSP's from Analog Devices in combination with seven APEX FPGA devices from Altera. These devices require the use of the latest software. Since the software is not error free, this design developed some delay. The design of APEX FPGA's of the MROD-1 is largely finished.

2.2.4 B-Physics

LHCb-Outer tracker

In the past year, development focussed on longer chambers (up to 2 m). We have investigated the electrical properties of different straws and chamber constructions, such as signal transport, cross talk, pickup and resonances. This investigation included beam-tests. The department further supports high-speed data acquisition system and the installation of electronics for additional chamber beam-tests at CERN. We also investigated the properties of the ASDBLR front-end chip and boards for the detector. The ASDBLR chips provide the complete front-end signal processing for eight straw tubes. Cross talk, double pulse resolution, stable operation and proper shaping of the selected gas mixture in the straw tube are currently under study. Improvements have to be incorporated in the second, pre-production amplifier prototype, which will also include a more radhard version of the chips.

In collaboration with the Institute of Nuclear Physics in Krakow (Poland) we made proposals for a baseline data acquisition solution for the outer tracker. These are now accepted and worked out. New TDC boards are in development including two levels of data reduction, the so-called "B-timizer". In Krakow work is done on a data-concentrator that with a S-LINK output. The department also contributed to the technical design report of the LHCb outer tracker, by preparing documents about e.g. high voltage system and detector control.

2.2.5 LHCb-Vertex

RF-investigations

Various calculations were made on the shielding between the silicon strips and the proton beam. The thickness of this aluminum foil shielding needs to be 250 μm . The electrical field strength close to the foil at the side of the silicon strips will then be 1V/m for the 40 MHz frequency component in the beam. The attenuation of the electromagnetic field by thin aluminum foils will be verified.

Pile-up detector

The pile-up trigger of LHCb will provide a veto for the acquisition of events with multiple primary vertices. The pile-up trigger identifies vertices by correlating the binary hit signals of two silicon detector wheels. Because of the large number of inputs (2000) into the trigger, and the requirement to operate at the

full (40 MHz) bunch crossing frequency, the use of "million gate" FPGA's is indispensable. Currently FPGA's from Altera and Xilinx are being evaluated by synthesizing a central part of the vertex trigger processor. The fact that these new devices require the use of the latest software, which is not error-free, makes this evaluation a far from trivial task. After selection of the FPGA that fits the trigger algorithm best, detailed design of a prototype will start.

Front-end chip

The front-end chip (BEETLE) is a development of the ASIC Laboratory in Heidelberg. It is an analogue readout chip with 128 preamplifiers, shapers, comparators, analogue pipelines and an analogue multiplexer. NIKHEF participated in this project by designing the comparator and the analogue output buffer after the multiplexer. The chip is developed in a 0.25 μm radiation tolerant CMOS technology. First prototypes of a complete chip have been processed and tested. The results and improvements will be implemented in a next version in 2001.

Detector control system

We identify two control systems in the design phase: the vacuum system and the motion control. The vacuum system consists of two parts, a primary and a secondary system. The primary system is part of the LHC vacuum with a pressure better than 10^{-8} mbar. The secondary system contains the detectors. The vacuum in the secondary system will not be better the 10^{-4} mbar, due to the out-gassing of the detector units. A thin aluminum foil of 250 μm thick (also for RF shielding; see above) will separate the two vacuum systems. The foil can withstand a pressure difference of 10 mbar. A control and safety mechanism should keep the pressure difference within 5 mbar at any circumstances. The system will be controlled, including automatic venting and de-venting, by a Simatic PLC. The PLC will be connected to the standard SCADA-system of LHCb. A manual control panel will be available during set-up of the system. The PLC is also hard-wired to the LHC machine safety systems and the LHC machine group can monitor the state of the vacuum system.

The complete vertex detector consists of two detector halves, which have to move with respect to the beam, with respect to each other and as entire system. The operator has to know the positions of the detector at any time. Therefore the position readout of the detector will be carried out by two independent methods. A Simatic PLC will control this system.

2.2.6 ALICE

The design of the EndCap electronics for the ALICE Silicon Strip Detector layer in the ALICE Inner Tracker has started. At the end of each Silicon detector ladder inside the detector, a control module is placed. Due to the radiation, power and space requirements, the use of ASIC's is necessary instead of using commercially available discrete components. A radiation tolerant $0.25\ \mu\text{m}$ CMOS technology is used for this purpose. Each module needs to control 14 double-sided detector modules, for power, control signals and analogue readout buffering. Analogue multiplexing, distribution of the serial control bus and regulation the power for the hybrids are some of the functions of the EndCap module.

2.2.7 ANTARES

Optical links

For the 'All-Data-to-Shore' concept, an optical system using Dense Wavelength Division Multiplexing (DWDM) was further detailed. DWDM systems employ high spectral purity lasers in the 1550 nm band. Laser wavelengths can be spaced as closely as 1.6 nm and multiplexed onto a single fiber with passive optical DWDM components. For Antares seven wavelengths on a single fiber will be used. The DWDM concept was verified with optical simulations. Within limitations this solution will work in Antares. First drafts outlining the Passive Optical Network and the Active Opto-Electrical circuits were written. Commercial 2.5 Gb/s components like lasers and optical receivers will be used as transport layer for the 50 km fiber-optic 1 Gigabit Ethernet connection from the deep-sea experimental set-up to the Shore Station.

An engineering firm specialized in this type of optical networks has been invited to evaluate the preliminary outlines of the final optical designs. Special attention is given to long term stability –10 years experiment life– and testability.

2.2.8 Several small projects

RIPE-NCC

The ET is asked for help design an interface for RIPE-NCC. This GPS interface was needed for test traffic measurements on Internet. The interface is connected to a smart GPS antenna. Together with a dedicated computer with the appropriate software installed, an

accurate timestamp can be generated. This is useful for measuring network performance and time delays. The main advantage of the GPS time is the high accuracy anywhere on the world. These interfaces (200) are being build and will be placed, all over the world, at Internet network servers. The interface consists of an isolated power-supply and level converters (RS485 \leftrightarrow RS232). All the electronics are placed on one PCI-card. The computer PCI-bus powers the interface. The smart GPS antenna is powered by the interface, which has an isolated output. Standard CAT5 computer network cable can be used for connecting the antenna; this facilitates installation.

Zero Iron Power Supply

A DC-DC converter has been developed for use in a magnetic field as a proof of concept. This can be useful in big detectors like ATLAS to save thousands of power cables, transmission losses and stabilization losses. The converter has a special transformer without ferrite or iron to achieve isolation and the right outputs. This transformer is realized on an 8 layer PCB (Fig. 2.3). An efficiency of 76% has been achieved at 3 W. Special attention needs the RF-field emission.

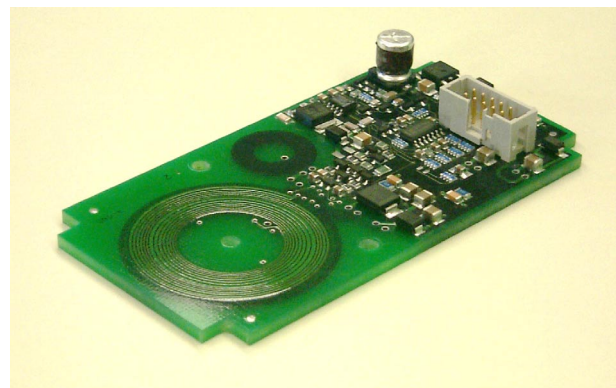


Figure 2.3: Zero Iron Power Supply.

Low Noise Amplifier for Capacitive Detectors

This amplifier was designed in $0.6\ \mu\text{m}$ CMOS technology from AMS. Two versions have been realized, a 'radiation tolerant' (gate-around FET's) and a 'rectangular' version. The main difference in behavior seems to be the linearity.

Medipix

An interface has been developed for the control and readout of the Medipix IC, designed for medical X-ray imaging applications. This system (MUROS-1) is

based on standard commercial analogue and digital I/O boards and a simple dedicated interface. The interface (Fig. 2.4) has three main functions:

- Power supply for the Medipix circuit
- Clamping of the TTL signals to CMOS level
- Simple test pulse generator

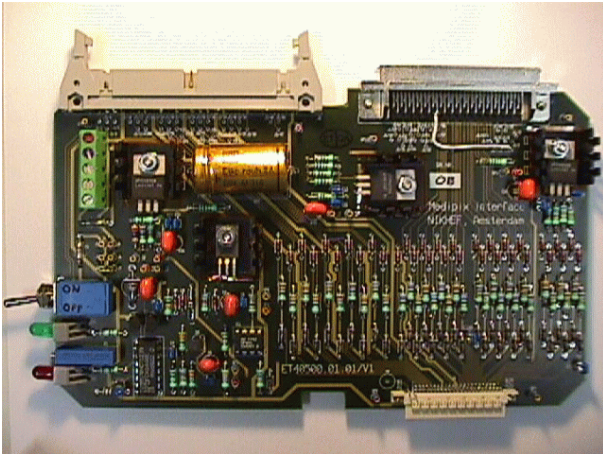


Figure 2.4: *MUROS-1 interface.*

NIKHEF-infrastructure

The internal information system of the NIKHEF institute has been upgraded. Whereas the previous one was based on an Amiga-computer, the new system is based on a personal computer running MS PowerPoint. The PC is connected to a video broadcasting system, and the information is displayed on various TV screens in the institute.

2.3 Department development

The ET department identifies three main items; connection techniques, microelectronics and electronic design automation. In the first, the department investigates the suppression of induced electromagnetic effects, which often have a link also to the mechanics of a system. Throughout the field, signal transfer over any reasonable distance is being replaced from electrical to optical connections. Compactification leads to changes in inter IC connection techniques. For example, we presently use field programmable arrays (FPGA) with over 600 inputs and outputs in ATLAS and LHCb electronics

Microelectronics is a vast area of activity. After several years of education, 15% of the engineers are working in

the field of VLSI design. The design of IC's (in particular deep sub-micron) is now frequently done in-house. There are close international collaborations with European ASIC laboratories (University Twente, Heidelberg, CERN).

Finally, design automation is connected to the exponential growth of the number of cells in e.g. FPGA's and consequently to the design of printed circuit boards. The computing group (CT) is instrumental in the application of embedded software in digital signal processors (DSP).



Milling of parts for the ATLAS Silicon Tracker.

3 Mechanical Technology

3.1 Introduction

The group Mechanical Technology has been involved in 12 projects in the year 2000. In Fig. 3.1 the manpower invested in the most demanding projects is listed.

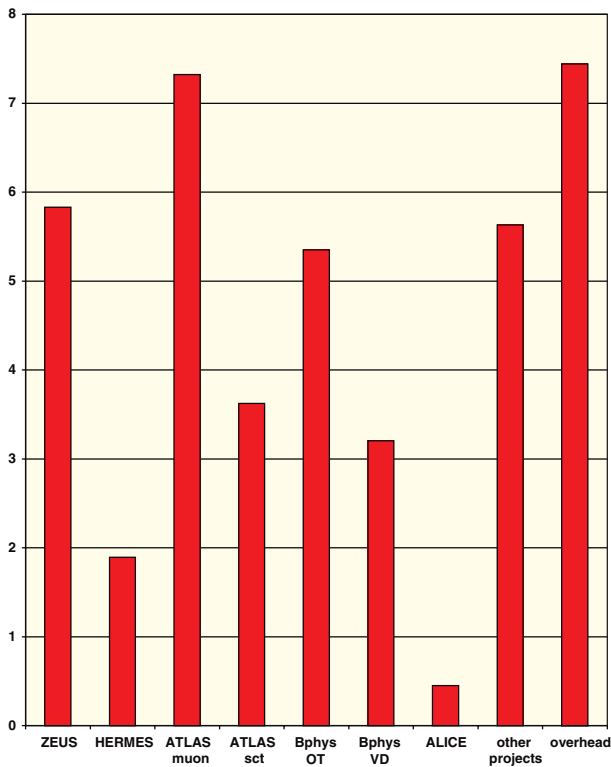


Figure 3.1: Distribution of manpower of MT in 2000 over the most important projects.

3.2 Projects in exploitation

DUBBLE

The group took care of service aspects of the equipment delivered in the past to ESRF in Grenoble. In 2000 we completed many experimental set ups for the SAX/WAX experiments.

COLDEX

Measurements of desorption effects of the LHC vacuum wall are in full progress. The apparatus that we have designed, built and tested is, at present implemented in the electron positron accumulator EPA at CERN, producing data with which the conditions in the future accelerator can be simulated.

D0

At Fermi lab the mechanics of the Roman pots, produced by NIKHEF, were revised because an accident with a baking procedure caused a major failure.

MEA/AmPS

Support has been given to permit an adequate transfer of the last accelerator parts of MEA/AmPS to JINR at Dubna.

3.3 Projects in development

ATLAS Muon chambers

Major progress has been made in finalizing the tooling, that is necessary to produce 96 of the largest muon chambers of the ATLAS detector. The assembly machine of the tubes, developed by CERN is commissioned and fulfills its purpose. Quality control after assembly is obtained with a wire position and tension control apparatus. The first space frame is manufactured and checked on the 3D survey machine. The leak tightness of the tubes has been checked in first instance by the so-called coffin method. Afterwards we concluded that the test method used by Frascati has to be preferred, because it is less sensitive to the background of helium. The decision was made that a new test set up based on this principle will be developed. The gluing machine has been realized and tested, resulting in a good quality joint between the MDT tubes and the center frame. Finally, the assembled chamber without gas flow system

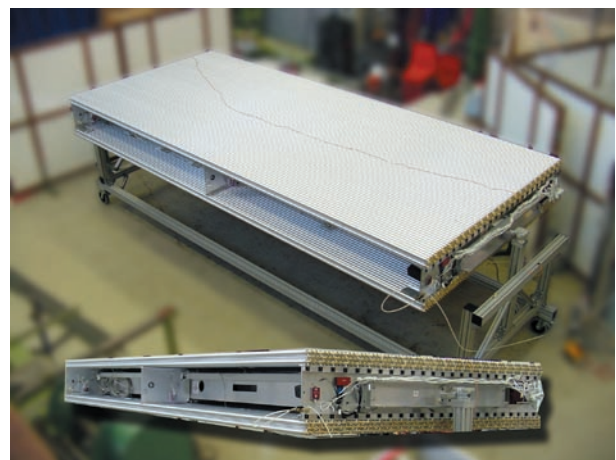


Figure 3.2: The ATLAS Muon chamber.

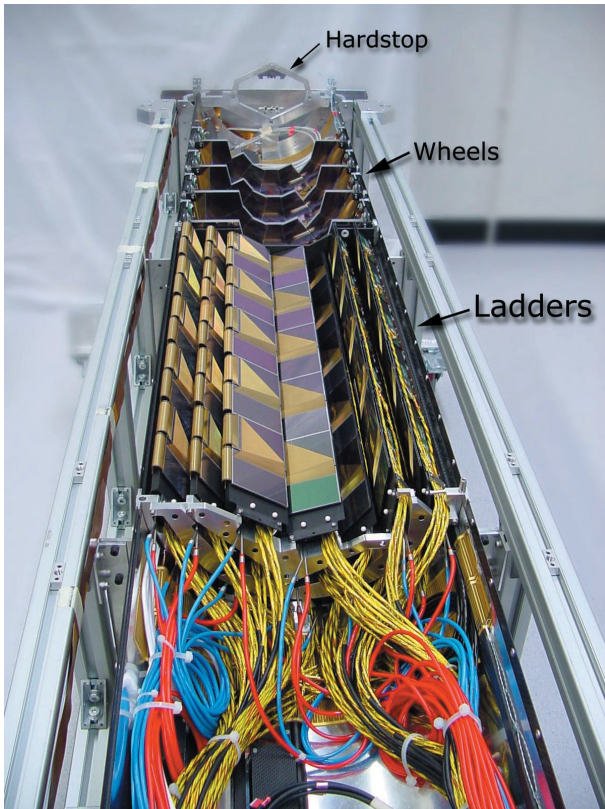


Figure 3.3: *Half of the ZEUS micro vertex detector.*

has been transported to CERN in order to be checked in the X-ray tomograph.

ATLAS-SCT

Prototype carbon fiber honeycomb constructions have been designed and manufactured in industry in order to measure stiffness, gluing properties and eigen frequencies. The fact that the final assembly and quality control of the position of the silicon detectors on the discs will be done at NIKHEF urged us to develop positioning equipment with an accuracy of $2 \mu\text{m}$. An apparatus with which we are able to study the heat conduction problems between the source (the electronics) and the cooling fluid was built. With this apparatus it is possible to optimize the amount of material while choosing between minimum multiple scattering and maximum stability. The machining of the inserts had to be developed in such a way that the modules are in one plane within an accuracy of $2 \mu\text{m}$. Stiffening rings in epoxy have been designed and manufactured in industry.

LHCb Outertracker

Three prototype straw chambers have been built and subsequently tested with beam at CERN and DESY in order to study stability, signal quality and radiation hardness. We varied the length (1.6 meter has proven to function well) in order to study the stiffness. We studied the electrical conductivity of 3 types of straw tube material. Tests were performed with several grades of humidity in order to find out what the consequences are for the deformation of the straw. Two manufacturing methods for the modules were developed in parallel to find out what the mass production consequences will be. We concluded that aluminum straws directly glued on a honeycomb material of 10 mm thickness covered with conductive foil, fulfill the specifications. The detection wire locators in the straw still need development, especially in view of the large number of straws that has to be dealt with. Design studies of the stations, in which the modules have to be mounted in front of the analyzing magnet, are finalized. Optimization of installation aspects and dismantling and cabling problems are important criteria that were determined in this study.

LHCb Vertex detector

Regular discussions with CERN have resulted in an increasing confidence in the design of the detector tank and the vacuum system. The secondary vacuum system and its safety aspects, issues of great concern of the LHC machine people, have been discussed thoroughly at various occasions. Progress has been made in a new design based on bellows constructions. The CO_2 cooling, the selection of feedthroughs (22000) and the rf shielding are to be determined soon. Prototypes of the interaction chamber and differential vacuum containment are being constructed. Finite element studies are being done on the thin-walled separation foil between the secondary and the primary vacuum.

HERMES

The bonding of all silicon modules was done and tested. A test mounting in HERA has been successfully performed and the positions of the modules in the lambda wheels are checked. The cooling set up is revised. The final assembly in HERA will be realized in the beginning of 2001.

ZEUS micro vertex detector

The silicon layers, a cooling system and many support structures for the fragile silicon wafers have been manufactured. Problems encountered with the form stability

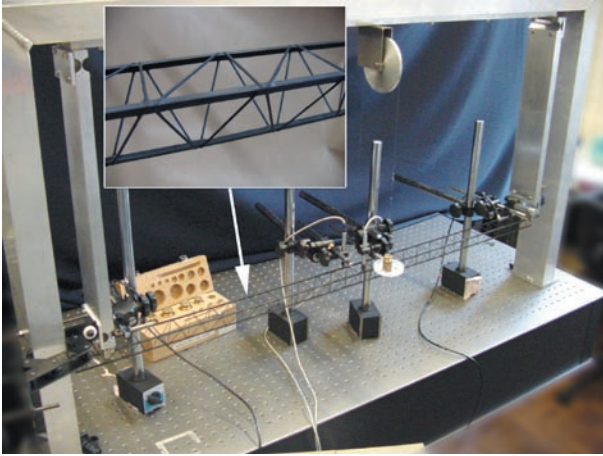


Figure 3.4: *Ladder assembly tooling for ALICE.*



Figure 3.5: *One of the ATLAS end cap toroids during the manufacturing stage. Photo: Courtesy Eddie Towndrow*

of the carbon fiber constructions were solved. A positioning system has been fabricated and tested in order to mount the modules in a precise way on the ladders. The final assembly in the supporting carbon fiber cylinder, followed by control measurements with the 3-D survey machine, is completed. Also the mounting of the cooling channels and the cabling was a delicate and time-consuming job. Every part in the detector has been thoroughly designed in order to minimize multiple scattering effects. The installation of the detector will take place in the beginning of 2001.

ALICE

In collaboration with the University of Utrecht we are contributing to the ALICE detector. Especially we delivered the design of the ladder assembly tooling. A preliminary study has been done and resulted in accepted ideas for an automated positioning of the silicon detectors. We have generated ideas about the overall integration of the detector that are being discussed in the collaboration.

3.4 Projects for third parties

ATLAS end cap

NIKHEF will deliver as an inkind contribution the vacuum vessels of the end cap toroids of ATLAS to CERN. The Royal Schelde is manufacturing these huge (diameter 10 meter and a height of 5 meter) aluminum vacuum constructions (see Fig 3.5). People from our group were and will be involved in the assembly and test phases of these vessels. Vacuum test procedures have

been agreed upon between NIKHEF, Royal Schelde and the designers of RAL.

Supersymmetric non-linear unification in particle physics

**Kähler manifolds, bundles for matter
representations and anomaly cancellation**



Stefan Groot Nibbelink

Stefan Groot Nibbelink's PhD Thesis; one of the twelve theses finalized in 2000.

E Publications, Theses and Talks

1 Publications

- [1] Abbiendi, G. *et al.*; Bentvelsen, S.; Opal Collaboration
Investigation of the decay of orbitally excited B mesons and first measurement of the branching ratio $BR(B^ \rightarrow B^*\pi(X))$*
Eur.Phys.Journal, (2000), 47 pp.
- [2] Abbiendi, G. *et al.*; Bentvelsen, S.; Opal Collaboration
Measurement of the B^0 lifetime and oscillation frequency using $\bar{B}^0 \rightarrow D^ + L$ - anti-neutrino decays*
Phys.Lett. **B 493** (2000) 266-280
- [3] Abbiendi, G. *et al.*; Bentvelsen, S.; Opal Collaboration
A measurement of the rate of charm production in W decays
Phys.Lett. **B 490** (2000) 71-86
- [4] Abbiendi, G. *et al.*; Bentvelsen, S.; Opal Collaboration
 W^+W^- production cross-section and W branching fractions in e^+e^- -collisions at 189 GeV
Phys.Lett. **B 493** (2000) 249-265
- [5] Abbiendi, G. *et al.*; Bentvelsen, S.; Opal Collaboration
Measurement of the low X behavior of the photon structure function $F_{2\gamma}$
Eur.Phys.Journal **C 18** (2000) 15-39
- [6] Abbiendi, G. *et al.*; Bentvelsen, S.; Opal Collaboration
Multiplicities of π^0, η, K^0 and of charged particles in quark and gluon jets
Eur.Phys.Journal **C 17** (2000) 373-387
- [7] Abbiendi, G. *et al.*; Bentvelsen, S.; Opal Collaboration
Search for trilinear neutral gauge boson couplings in Z-gamma production at $\sqrt{s} = 189$ GeV at LEP
Eur.Phys.Journal **C 17** (2000) 553-566
- [8] Abbiendi, G. *et al.*; Bentvelsen, S.; Opal Collaboration
First measurement of the inclusive branching ratio of B hadrons to phi mesons in Z^0 decays
Phys.Lett. **B 492** (2000) 13-22
- [9] Abbiendi, G. *et al.*; Bentvelsen, S.; Opal Collaboration
A Measurement of the τ mass and the first CPT test with τ leptons
Phys.Lett. **B 492** (2000) 23-31
- [10] Abbiendi, G. *et al.*; Bentvelsen, S.; Opal Collaboration
Photonic events with missing energy in e^+e^- -collisions at $\sqrt{s} = 189$ GeV
Eur.Phys.Journal **C 18** (2000) 253-272
- [11] Abbiendi, G. *et al.*; Bentvelsen, S.; Opal Collaboration
Z boson pair production in e^+e^- -collisions at $\sqrt{s} = 183$ GeV and 189 GeV
Phys.Lett. **B 476** (2000) 256-272
- [12] Abbiendi, G. *et al.*; Bentvelsen, S.; Opal Collaboration
Measurement of $|V_{cb}|$ using $\bar{B}^0 \rightarrow D^ +$ lepton- anti-neutrino decays*
Phys.Lett. **B 482** (2000) 15-30
- [13] Abbiendi, G. *et al.*; Bentvelsen, S.; Opal Collaboration
Transverse and longitudinal bose Einstein correlations in hadronic Z^0 decays
Eur.Phys.J. **C 16** (2000) 423-433
- [14] Abbiendi, G. *et al.*; Bentvelsen, S.; Opal Collaboration
Bose-Einstein correlations in $K^\pm K^\pm$ pairs from Z^0 decays into two hadronic jets
Submitted to Eur.Phys.Journal (2000) 25 pp.
- [15] Abbott, B. *et al.*; Filthaut, F.; D0 Collaboration
Search for New Physics in $e\mu X$ Data at D0 Using Sleuth: A Quasi-Model-Independent Search Strategy for New Physics
Phys. Rev. **D 62** (2000) 092004
- [16] Abreu, P. *et al.*; Blom, H.M.; Boudinov, E.; Kjaer, N.; Kluit, P.; Mulders, M.; Reid, D.; Timmermans, J.; Apeldoorn, G.W. van; Dam, P. van; Eldik, J. van; Vulpen, I. van; DELPHI Collaboration
A study of the Lorentz structure in τ decays
Eur. Phys. J. **C 16** (2000) 229-252
- [17] Abreu, P. *et al.*; Blom, H.M.; Boudinov, E.; Kjaer, N.; Kluit, P.; Mulders, M.; Reid, D.; Timmermans, J.; Apeldoorn, G.W. van; Dam, P. van; Eldik, J. van; Vulpen, I. van; DELPHI Collaboration
Determination of $\frac{|V_{ub}|}{|V_{cb}|}$ with DELPHI at LEP
Phys. Lett. **B 478** (2000) 14-30
- [18] Abreu, P. *et al.*; Blom, H.M.; Boudinov, E.; Kjaer, N.; Kluit, P.; Mulders, M.; Reid, D.; Timmermans, J.; Apeldoorn, G.W. van; Dam, P. van; Eldik, J. van; Vulpen, I. van; DELPHI Collaboration
Search for heavy stable and long-lived particles in e^+e^- collisions at $\sqrt{s} = 9$ GeV
Phys. Lett. **B 478** (2000) 65-72
- [19] Abreu, P. *et al.*; Blom, H.M.; Boudinov, E.; Kjaer, N.; Kluit, P.; Mulders, M.; Reid, D.; Timmermans, J.; Apeldoorn, G.W. van; Dam, P. van; Eldik, J. van; Vulpen, I. van; DELPHI Collaboration
Two-dimensional analysis of the Bose-Einstein correlations in e^+e^- annihilation at the Z^0 peak
Phys. Lett. **B 471** (2000) 460-470
- [20] Abreu, P. *et al.*; Blom, H.M.; Boudinov, E.; Kjaer, N.; Kluit, P.; Mulders, M.; Reid, D.; Timmermans, J.; Apeldoorn, G.W. van; Dam, P. van; Eldik, J. van; Vulpen, I. van; DELPHI Collaboration
W pair production cross-section and W branching fractions in e^+e^- interactions at 189 GeV
Phys. Lett. **B 479** (2000) 089-100
- [21] Abreu, P. *et al.*; Blom, H.M.; Boudinov, E.; Kjaer, N.; Kluit, P.; Mulders, M.; Reid, D.; Timmermans, J.; Apeldoorn, G.W. van; Dam, P. van; Eldik, J. van; Vulpen, I. van; DELPHI Collaboration
Hadronization properties of b quarks compared to light quarks in $e^+e^- \rightarrow q\bar{q}$ from 183 to 200 GeV
Phys. Lett. **B 479** (2000) 118-128
- [22] Abreu, P. *et al.*; Blom, H.M.; Boudinov, E.; Kjaer, N.; Kluit, P.; Mulders, M.; Reid, D.; Timmermans, J.; Apeldoorn, G.W. van; Dam, P. van; Eldik, J. van; Vulpen, I. van; DELPHI Collaboration
Search for charginos in e^+e^- interactions at $\sqrt{s} = 189$ GeV
Phys. Lett. **B 479** (2000) 129-143
- [23] Abreu, P. *et al.*; Blom, H.M.; Boudinov, E.; Kjaer, N.; Kluit, P.; Mulders, M.; Reid, D.; Timmermans, J.; Apeldoorn, G.W. van; Dam, P. van; Eldik, J. van; Vulpen, I. van; DELPHI Collaboration
Measurement of the gluon fragmentation function and a comparison of the scaling violation in gluon and quark jets
Eur. Phys. J. **C 13** (2000) 573-589

- [24] Abreu, P. *et al.*; Blom, H.M.; Boudinov, E.; Kjaer, N.; Kluit, P.; Mulders, M.; Reid, D.; Timmermans, J.; Apeldoorn, G.W. van; Dam, P. van; Eldik, J. van; Vulpen, I. van; DELPHI Collaboration
Search for supersymmetry with R-parity violating $LL\bar{E}$ couplings at $\sqrt{s} = 183$ GeV
Eur. Phys. J. C **13** (2000) 591-608
- [25] Abreu, P. *et al.*; Blom, H.M.; Boudinov, E.; Kjaer, N.; Kluit, P.; Mulders, M.; Reid, D.; Timmermans, J.; Apeldoorn, G.W. van; Dam, P. van; Eldik, J. van; Vulpen, I. van; DELPHI Collaboration
Consistent measurements of α_s from precise oriented event shape distributions
Eur. Phys. J. C **14** (2000) 557-584
- [26] Abreu, P. *et al.*; Blom, H.M.; Boudinov, E.; Kjaer, N.; Kluit, P.; Mulders, M.; Reid, D.; Timmermans, J.; Apeldoorn, G.W. van; Dam, P. van; Eldik, J. van; Vulpen, I. van; DELPHI Collaboration
Measurement of the strange quark forward-backward asymmetry at the Z^0 Peak
Eur. Phys. J. C **14** (2000) 613-631
- [27] Abreu, P. *et al.*; Blom, H.M.; Boudinov, E.; Kjaer, N.; Kluit, P.; Mulders, M.; Reid, D.; Timmermans, J.; Apeldoorn, G.W. van; Dam, P. van; Eldik, J. van; Vulpen, I. van; DELPHI Collaboration
Precise measurement of the τ polarisation at LEP-1
Eur. Phys. J. C **14** (2000) 585-611
- [28] Abreu, P. *et al.*; Blom, H.M.; Boudinov, E.; Kjaer, N.; Kluit, P.; Mulders, M.; Reid, D.; Timmermans, J.; Apeldoorn, G.W. van; Dam, P. van; Eldik, J. van; Vulpen, I. van; DELPHI Collaboration
Measurement and interpretation of fermion-pair production at LEP energies of 183 and 189 GeV
Phys. Lett. **B 485** (2000) 45-61
- [29] Abreu, P. *et al.*; Blom, H.M.; Boudinov, E.; Kjaer, N.; Kluit, P.; Mulders, M.; Reid, D.; Timmermans, J.; Apeldoorn, G.W. van; Dam, P. van; Eldik, J. van; Vulpen, I. van; DELPHI Collaboration
Update of the search for charginos nearly mass-degenerate with the lightest neutralino
Phys. Lett. **B 485** (2000) 95-106
- [30] Abreu, P. *et al.*; Blom, H.M.; Boudinov, E.; Kjaer, N.; Kluit, P.; Mulders, M.; Reid, D.; Timmermans, J.; Apeldoorn, G.W. van; Dam, P. van; Eldik, J. van; Vulpen, I. van; DELPHI Collaboration
Search for supersymmetric particles in scenarios with a gravitino LSP and $\tilde{\tau}$ NLSP
Eur. Phys. J. C **16** (2000) 211-228
- [31] Abreu, P. *et al.*; Blom, H.M.; Boudinov, E.; Kjaer, N.; Kluit, P.; Mulders, M.; Reid, D.; Timmermans, J.; Apeldoorn, G.W. van; Dam, P. van; Eldik, J. van; Vulpen, I. van; DELPHI Collaboration
Determination of $P(c \rightarrow D^{+})$ and $BR(c \rightarrow I^+)$ at LEP 1*
Eur. Phys. J. C **12** (2000) 209-224
- [32] Abreu, P. *et al.*; Blom, H.M.; Boudinov, E.; Kjaer, N.; Kluit, P.; Mulders, M.; Reid, D.; Timmermans, J.; Apeldoorn, G.W. van; Dam, P. van; Eldik, J. van; Vulpen, I. van; DELPHI Collaboration
Search for SUSY with R-parity violating $LL\bar{E}$ couplings at $\sqrt{s} = 9$ GeV
Phys. Lett. **B 487** (2000) 36-52
- [33] Abreu, P. *et al.*; Blom, H.M.; Boudinov, E.; Kjaer, N.; Kluit, P.; Mulders, M.; Reid, D.; Timmermans, J.; Apeldoorn, G.W. van; Dam, P. van; Eldik, J. van; Vulpen, I. van; DELPHI Collaboration
Limits on the masses of supersymmetric particles at $\sqrt{s} = 9$ GeV
Phys. Lett. **B 489** (2000) 38-54
- [34] Abreu, P. *et al.*; Blom, H.M.; Boudinov, E.; Kjaer, N.; Kluit, P.; Mulders, M.; Reid, D.; Timmermans, J.; Apeldoorn, G.W. van; Dam, P. van; Eldik, J. van; Vulpen, I. van; DELPHI Collaboration
Measurements of the Z partial decay width into $c\bar{c}$ and multiplicity of charm quarks per b decay
Eur. Phys. J. C **12** (2000) 225-241
- [35] Abreu, P. *et al.*; Blom, H.M.; Boudinov, E.; Kjaer, N.; Kluit, P.; Mulders, M.; Reid, D.; Timmermans, J.; Apeldoorn, G.W. van; Dam, P. van; Eldik, J. van; Vulpen, I. van; DELPHI Collaboration
Measurement of the B_s^0 lifetime and study of $B_s^0 - \bar{B}_s^0$ oscillations using $D_s^ l$ events*
Eur. Phys. J. C **16** (2000) 555-578
- [36] Abreu, P. *et al.*; Blom, H.M.; Boudinov, E.; Kjaer, N.; Kluit, P.; Mulders, M.; Reid, D.; Timmermans, J.; Apeldoorn, G.W. van; Dam, P. van; Eldik, J. van; Vulpen, I. van; DELPHI Collaboration
Rapidity-rank structure of $p\bar{p}$ pairs in hadronic Z^0 decays
Phys. Lett. **B 490** (2000) 61-70
- [37] Abreu, P. *et al.*; Blom, H.M.; Boudinov, E.; Kluit, P.; Mulders, M.; Reid, D.; Timmermans, J.; Apeldoorn, G.W. van; Dam, P. van; Eldik, J. van; Vulpen, I. van; DELPHI Collaboration
Photon events with missing energy at $\sqrt{s} = 183$ to 189 GeV
Eur. Phys. J. C **17** (2000) 53-65
- [38] Abreu, P. *et al.*; Blom, H.M.; Boudinov, E.; Kluit, P.; Mulders, M.; Reid, D.; Timmermans, J.; Apeldoorn, G.W. van; Dam, P. van; Eldik, J. van; Vulpen, I. van; DELPHI Collaboration
Searches for Neutral Higgs Bosons in e^+e^- Collisions around $\sqrt{s}=189$ GeV
Eur. Phys. J. C **17** (2000) 187-205 addendum 17 (2000) 549-551
- [39] Abreu, P. *et al.*; Blom, H.M.; Boudinov, E.; Kluit, P.; Mulders, M.; Reid, D.; Timmermans, J.; Apeldoorn, G.W. van; Dam, P. van; Eldik, J. van; Vulpen, I. van; DELPHI Collaboration
Cross-sections and leptonic forward-backward asymmetries from the Z^0 running of LEP
Eur. Phys. J. C **16** (2000) 371-405
- [40] Abreu, P. *et al.*; Blom, H.M.; Boudinov, E.; Kluit, P.; Mulders, M.; Reid, D.; Timmermans, J.; Apeldoorn, G.W. van; Dam, P. van; Eldik, J. van; Vulpen, I. van; DELPHI Collaboration
Determination of the $e^+e^- \rightarrow \gamma\gamma(\gamma)$ cross-section at centre-of-mass energies ranging from 189 GeV to 202 GeV
Phys. Lett. **B 491** (2000) 67-80
- [41] Abreu, P. *et al.*; Blom, H.M.; Boudinov, E.; Kluit, P.; Mulders, M.; Reid, D.; Timmermans, J.; Apeldoorn, G.W. van; Dam, P. van; Eldik, J. van; Vulpen, I. van; DELPHI Collaboration
Identified charged particles in quarks and gluon jets
Eur. Phys. J. C **17** (2000) 207-222
- [42] Abreu, P. *et al.*; Blom, H.M.; Boudinov, E.; Kluit, P.; Montenegro, J.; Mulders, M.; Reid, D.; Timmermans, J.; Dam,

- P. van; Eldik, J. van; Vulpen, I. van; DELPHI Collaboration
Search for the goldstino at \sqrt{s} from 189 to 202 GeV
Phys. Lett. **B 494** (2000) 203-214
- [43] Abreu, P. *et al.*; Blom, H.M.; Boudinov, E.; Kjaer, N.; Kluit, P.; Mulders, M.; Reid, D.; Timmermans, J.; Apeldoorn, G.W. van; Dam, P. van; Eldik, J. van; Vulpen, I. van; DELPHI Collaboration
 Λ_b polarization in Z^0 decays at LEP W CERN-EP-99-155
Phys. Lett. **B 474** (2000) 205-222
- [44] Abreu, P. *et al.*; Blom, H.M.; Boudinov, E.; Kjaer, N.; Kluit, P.; Mulders, M.; Reid, D.; Timmermans, J.; Apeldoorn, G.W. van; Dam, P. van; Eldik, J. van; Vulpen, I. van; DELPHI Collaboration
Measurement of the $\overline{B} \rightarrow D^{()}\pi l\overline{\nu}_l$ branching fraction*
Phys. Lett. **B 475** (2000) 407-428
- [45] Abreu, P. *et al.*; Blom, H.M.; Boudinov, E.; Kjaer, N.; Kluit, P.; Mulders, M.; Reid, D.; Timmermans, J.; Apeldoorn, G.W. van; Dam, P. van; Eldik, J. van; Vulpen, I. van; DELPHI Collaboration
Inclusive Σ^- and $\Lambda(1520)$ production in hadronic Z decays
Phys. Lett. **B 475** (2000) 429-447
- [46] Acciari, M. *et al.*; Bobbink, G.J.; Colijn, A.P.; Dierendonck, M. van; Duinker, P.; Ern , F.C.; Gulik, R. van; Jong, P. de; Linde, F.L.; Massaro, G.G.G.; Muijs, A.J.M.; Chekanov, S.V.; Dalen, J.A. van; Kittel, W.; K nig, A.C.; Mangeol, D.; Metzger, W.J.; Petersen, B.; Sanders, M.P.; Schotanus, D.J.; Timmermans, C.; Wilkens, H.; Buijs, A.; Rhee, T. van; L3 collaboration
Measurement of the probability of gluon splitting into charmed quarks in hadronic Z decays
Phys. Lett. **B 476** (2000) 243-255
- [47] Acciari, M. *et al.*; Bobbink, G.J.; Colijn, A.P.; Dierendonck, M. van; Duinker, P.; Ern , F.C.; Gulik, R. van; Jong, P. de; Linde, F.L.; Massaro, G.G.G.; Muijs, A.J.M.; Chekanov, S.V.; Dalen, J.A. van; Kittel, W.; K nig, A.C.; Mangeol, D.; Metzger, W.J.; Petersen, B.; Sanders, M.P.; Schotanus, D.J.; Timmermans, C.; Wilkens, H.; Buijs, A.; Rhee, T. van; L3 collaboration
Measurement of R_b and $B_r(b \rightarrow l\nu X)$ at LEP using double-tag methods
Eur. Phys. J. **C 13** (2000) 47-61
- [48] Acciari, M. *et al.*; Bobbink, G.J.; Colijn, A.P.; Dierendonck, M. van; Duinker, P.; Ern , F.C.; Gulik, R. van; Jong, P. de; Linde, F.L.; Massaro, G.G.G.; Muijs, A.J.M.; Chekanov, S.V.; Dalen, J.A. van; Kittel, W.; K nig, A.C.; Mangeol, D.; Metzger, W.J.; Petersen, B.; Sanders, M.P.; Schotanus, D.J.; Timmermans, C.; Wilkens, H.; Buijs, A.; Rhee, T. van; L3 collaboration
Measurement of the $e^+e^- \rightarrow Z\gamma\gamma$ cross section and determination of quartic gauge boson couplings at LEP
Phys. Lett. **B 478** (2000) 39-49
- [49] Acciari, M. *et al.*; Bobbink, G.J.; Colijn, A.P.; Dierendonck, M. van; Duinker, P.; Ern , F.C.; Gulik, R. van; Jong, P. de; Linde, F.L.; Massaro, G.G.G.; Muijs, A.J.M.; Chekanov, S.V.; Dalen, J.A. van; Kittel, W.; K nig, A.C.; Mangeol, D.; Metzger, W.J.; Petersen, B.; Sanders, M.P.; Schotanus, D.J.; Timmermans, C.; Wilkens, H.; Buijs, A.; Rhee, T. van; L3 collaboration
Measurement of the lifetime of the τ lepton
Phys. Lett. **B 479** (2000) 067-78
- [50] Acciari, M. *et al.*; Bobbink, G.J.; Colijn, A.P.; Dierendonck, M. van; Duinker, P.; Ern , F.C.; Gulik, R. van; Jong, P. de; Linde, F.L.; Massaro, G.G.G.; Muijs, A.J.M.; Chekanov, S.V.; Dalen, J.A. van; Kittel, W.; K nig, A.C.; Mangeol, D.; Metzger, W.J.; Petersen, B.; Sanders, M.P.; Schotanus, D.J.; Timmermans, C.; Wilkens, H.; Buijs, A.; Rhee, T. van; L3 collaboration
Inclusive Σ^+ and Σ^0 production in hadronic Z decays
Phys. Lett. **B 479** (2000) 079-88
- [51] Acciari, M. *et al.*; Bobbink, G.J.; Colijn, A.P.; Dierendonck, M. van; Duinker, P.; Ern , F.C.; Gulik, R. van; Jong, P. de; Linde, F.L.; Massaro, G.G.G.; Muijs, A.J.M.; Chekanov, S.V.; Dalen, J.A. van; Kittel, W.; K nig, A.C.; Mangeol, D.; Metzger, W.J.; Petersen, B.; Sanders, M.P.; Schotanus, D.J.; Timmermans, C.; Wilkens, H.; Buijs, A.; Rhee, T. van; L3 collaboration
Measurement of hadron and lepton-pair production at $\sqrt{s}=130-189$ GeV at LEP
Phys. Lett. **B 479** (2000) 101-117
- [52] Acciari, M. *et al.*; Bobbink, G.J.; Colijn, A.P.; Dierendonck, M. van; Duinker, P.; Ern , F.C.; Gulik, R. van; Jong, P. de; Linde, F.L.; Massaro, G.G.G.; Muijs, A.J.M.; Chekanov, S.V.; Dalen, J.A. van; Kittel, W.; K nig, A.C.; Mangeol, D.; Metzger, W.J.; Petersen, B.; Sanders, M.P.; Schotanus, D.J.; Timmermans, C.; Wilkens, H.; Buijs, A.; Rhee, T. van; L3 collaboration
Measurements of the $b\overline{b}$ production cross section and forward-backward asymmetry at centre-of-mass energies above the Z pole at LEP
Phys. Lett. **B 485** (2000) 71-84
- [53] Acciari, M. *et al.*; Bobbink, G.J.; Colijn, A.P.; Dierendonck, M. van; Duinker, P.; Ern , F.C.; Gulik, R. van; Jong, P. de; Linde, F.L.; Massaro, G.G.G.; Muijs, A.J.M.; Chekanov, S.V.; Dalen, J.A. van; Kittel, W.; K nig, A.C.; Mangeol, D.; Metzger, W.J.; Petersen, B.; Sanders, M.P.; Schotanus, D.J.; Timmermans, C.; Wilkens, H.; Buijs, A.; Rhee, T. van; L3 collaboration
Search for charginos and neutralinos in e^+e^- collisions at $\sqrt{s}=189$ GeV
Phys. Lett. **B 472** (2000) 420-433
- [54] Acciari, M. *et al.*; Bobbink, G.J.; Colijn, A.P.; Dierendonck, M. van; Duinker, P.; Ern , F.C.; Gulik, R. van; Jong, P. de; Linde, F.L.; Massaro, G.G.G.; Muijs, A.J.M.; Chekanov, S.V.; Dalen, J.A. van; Kittel, W.; K nig, A.C.; Mangeol, D.; Metzger, W.J.; Petersen, B.; Sanders, M.P.; Schotanus, D.J.; Timmermans, C.; Wilkens, H.; Buijs, A.; Rhee, T. van; L3 collaboration
Search for an invisibly decaying Higgs boson in e^+e^- collisions at $\sqrt{s}=183-189$ GeV
Phys. Lett. **B 485** (2000) 85-94
- [55] Acciari, M. *et al.*; Bobbink, G.J.; Colijn, A.P.; Dierendonck, M. van; Duinker, P.; Ern , F.C.; Gulik, R. van; Jong, P. de; Linde, F.L.; Massaro, G.G.G.; Muijs, A.J.M.; Chekanov, S.V.; Dalen, J.A. van; Kittel, W.; K nig, A.C.; Mangeol, D.; Metzger, W.J.; Petersen, B.; Sanders, M.P.; Schotanus, D.J.; Timmermans, C.; Wilkens, H.; Buijs, A.; Rhee, T. van; L3 collaboration
Measurement of cross sections and forward backward asymmetries at the Z resonance and determination of electroweak parameters
Eur. Phys. J. **C 16** (2000) 1-40
- [56] Acciari, M. *et al.*; Bobbink, G.J.; Colijn, A.P.; Dierendonck, M. van; Duinker, P.; Ern , F.C.; Gulik, R. van; Jong, P. de; Linde, F.L.; Massaro, G.G.G.; Muijs, A.J.M.; Chekanov, S.V.; Dalen, J.A. van; Kittel, W.; K nig, A.C.; Mangeol,

- D.; Metzger, W.J.; Petersen, B.; Sanders, M.P.; Schotanus, D.J.; Timmermans, C.; Wilkens, H.; Buijs, A.; Rhee, T. van; L3 collaboration
Production of single W bosons at $\sqrt{s} = 189$ GeV and measurement of $WW\gamma$ gauge couplings
 Phys. Lett. **B 487** (2000) 229-240
- [57] Acciari, M. *et al.*; Bobbink, G.J.; Colijn, A.P.; Dierendonck, M. van; Duinker, P.; Erné, F.C.; Gulik, R. van; Jong, P. de; Linde, F.L.; Massaro, G.G.G.; Muijs, A.J.M.; Chekanov, S.V.; Dalen, J.A. van: Kittel, W.; König, A.C.; Mangeol, D.; Metzger, W.J.; Petersen, B.; Sanders, M.P.; Schotanus, D.J.; Timmermans, C.; Wilkens, H.; Buijs, A.; Rhee, T. van; L3 collaboration
Search for anomalous $ZZ\gamma$ and $Z\gamma\gamma$ couplings in the process $e^+e^- \rightarrow Z\gamma$ at LEP
 Phys. Lett. **B 489** (2000) 55-64
- [58] Acciari, M. *et al.*; Bobbink, G.J.; Colijn, A.P.; Dierendonck, M. van; Duinker, P.; Erné, F.C.; Gulik, R. van; Jong, P. de; Linde, F.L.; Massaro, G.G.G.; Muijs, A.J.M.; Chekanov, S.V.; Dalen, J.A. van: Kittel, W.; König, A.C.; Mangeol, D.; Metzger, W.J.; Petersen, B.; Sanders, M.P.; Schotanus, D.J.; Timmermans, C.; Wilkens, H.; Buijs, A.; Rhee, T. van; L3 collaboration
QCD studies in e^+e^- annihilation from 30 GeV to 189 GeV
 Phys. Lett. **B 489** (2000) 65-80
- [59] Acciari, M. *et al.*; Bobbink, G.J.; Colijn, A.P.; Dierendonck, M. van; Duinker, P.; Erné, F.C.; Gulik, R. van; Jong, P. de; Linde, F.L.; Massaro, G.G.G.; Muijs, A.J.M.; Chekanov, S.V.; Dalen, J.A. van: Kittel, W.; König, A.C.; Mangeol, D.; Metzger, W.J.; Petersen, B.; Sanders, M.P.; Schotanus, D.J.; Timmermans, C.; Wilkens, H.; Buijs, A.; Rhee, T. van; L3 collaboration
Search for manifestations of new physics in fermion-pair production at LEP
 Phys. Lett. **B 489** (2000) 81-92
- [60] Acciari, M. *et al.*; Bobbink, G.J.; Colijn, A.P.; Dierendonck, M. van; Duinker, P.; Erné, F.C.; Gulik, R. van; Jong, P. de; Linde, F.L.; Massaro, G.G.G.; Muijs, A.J.M.; Chekanov, S.V.; Dalen, J.A. van: Kittel, W.; König, A.C.; Mangeol, D.; Metzger, W.J.; Petersen, B.; Sanders, M.P.; Schotanus, D.J.; Timmermans, C.; Wilkens, H.; Buijs, A.; Rhee, T. van; L3 collaboration
Determination of γ/Z interference in e^+e^- annihilation at LEP
 Phys. Lett. **B 489** (2000) 93-101
- [61] Acciari, M. *et al.*; Bobbink, G.J.; Colijn, A.P.; Dierendonck, M. van; Duinker, P.; Erné, F.C.; Gulik, R. van; Jong, P. de; Linde, F.L.; Massaro, G.G.G.; Muijs, A.J.M.; Chekanov, S.V.; Dalen, J.A. van: Kittel, W.; König, A.C.; Mangeol, D.; Metzger, W.J.; Petersen, B.; Sanders, M.P.; Schotanus, D.J.; Timmermans, C.; Wilkens, H.; Buijs, A.; Rhee, T. van; L3 collaboration
Search for anomalous couplings in the Higgs sector at LEP
 Phys. Lett. **B 489** (2000) 102-114
- [62] Acciari, M. *et al.*; Bobbink, G.J.; Colijn, A.P.; Dierendonck, M. van; Duinker, P.; Erné, F.C.; Gulik, R. van; Jong, P. de; Linde, F.L.; Massaro, G.G.G.; Muijs, A.J.M.; Chekanov, S.V.; Dalen, J.A. van: Kittel, W.; König, A.C.; Mangeol, D.; Metzger, W.J.; Petersen, B.; Sanders, M.P.; Schotanus, D.J.; Timmermans, C.; Wilkens, H.; Buijs, A.; Rhee, T. van; L3 collaboration
Search for charginos with a small mass difference with the lightest supersymmetric particle at $\sqrt{s} = 189$ GeV
 Phys. Lett. **B 489** (2000) 115-124
- [63] Acciari, M. *et al.*; Bobbink, G.J.; Colijn, A.P.; Dierendonck, M. van; Duinker, P.; Erné, F.C.; Gulik, R. van; Jong, P. de; Linde, F.L.; Massaro, G.G.G.; Muijs, A.J.M.; Chekanov, S.V.; Dalen, J.A. van: Kittel, W.; König, A.C.; Mangeol, D.; Metzger, W.J.; Petersen, B.; Sanders, M.P.; Schotanus, D.J.; Timmermans, C.; Wilkens, H.; Buijs, A.; Rhee, T. van; L3 collaboration
Search for excited leptons at $\sqrt{s} = 189$ GeV
 Phys. Lett. **B 473** (2000) 177-185
- [64] Acciari, M. *et al.*; Bobbink, G.J.; Colijn, A.P.; Dierendonck, M. van; Duinker, P.; Erné, F.C.; Gulik, R. van; Jong, P. de; Linde, F.L.; Massaro, G.G.G.; Muijs, A.J.M.; Chekanov, S.V.; Dalen, J.A. van: Kittel, W.; König, A.C.; Mangeol, D.; Metzger, W.J.; Petersen, B.; Sanders, M.P.; Schotanus, D.J.; Timmermans, C.; Wilkens, H.; Buijs, A.; Rhee, T. van; L3 collaboration
Measurement of the $W^+W^- \gamma$ cross section and direct limits on anomalous quartic gauge couplings at LEP
 Phys. Lett. **B 490** (2000) 187-195
- [65] Acciari, M. *et al.*; Bobbink, G.J.; Colijn, A.P.; Dierendonck, M. van; Duinker, P.; Erné, F.C.; Gulik, R. van; Jong, P. de; Linde, F.L.; Massaro, G.G.G.; Muijs, A.J.M.; Chekanov, S.V.; Dalen, J.A. van: Kittel, W.; König, A.C.; Mangeol, D.; Metzger, W.J.; Petersen, B.; Sanders, M.P.; Schotanus, D.J.; Timmermans, C.; Wilkens, H.; Buijs, A.; Rhee, T. van; L3 collaboration
Search for charginos with a small mass difference to the lightest supersymmetric particle at $\sqrt{s} = 189$ GeV
 Phys. Lett. **B 482** (2000) 31-42
- [66] Acciari, M. *et al.*; Bobbink, G.J.; Colijn, A.P.; Dierendonck, M. van; Duinker, P.; Erné, F.C.; Gulik, R. van; Jong, P. de; Linde, F.L.; Massaro, G.G.G.; Muijs, A.J.M.; Chekanov, S.V.; Dalen, J.A. van: Kittel, W.; König, A.C.; Mangeol, D.; Metzger, W.J.; Petersen, B.; Sanders, M.P.; Schotanus, D.J.; Timmermans, C.; Wilkens, H.; Buijs, A.; Rhee, T. van; L3 collaboration
Measurement of Bose-Einstein correlations in $e^+e^- \rightarrow W^+W^-$ at $\sqrt{s} \simeq 189$ GeV
 Phys. Lett. **B 493** (2000) 233-248
- [67] Acciari, M. *et al.*; Bobbink, G.J.; Colijn, A.P.; Dierendonck, M. van; Duinker, P.; Erné, F.C.; Gulik, R. van; Jong, P. de; Linde, F.L.; Massaro, G.G.G.; Muijs, A.J.M.; Chekanov, S.V.; Dalen, J.A. van: Kittel, W.; König, A.C.; Mangeol, D.; Metzger, W.J.; Petersen, B.; Sanders, M.P.; Schotanus, D.J.; Timmermans, C.; Wilkens, H.; Buijs, A.; Rhee, T. van; L3 collaboration
Direct observation of longitudinally polarised W^\pm bosons
 Phys. Lett. **B 474** (2000) 194-204
- [68] Acciari, M. *et al.*; Bobbink, G.J.; Colijn, A.P.; Dierendonck, M. van; Duinker, P.; Erné, F.C.; Gulik, R. van; Jong, P. de; Linde, F.L.; Massaro, G.G.G.; Muijs, A.J.M.; Chekanov, S.V.; Dalen, J.A. van: Kittel, W.; König, A.C.; Mangeol, D.; Metzger, W.J.; Petersen, B.; Sanders, M.P.; Schotanus, D.J.; Timmermans, C.; Wilkens, H.; Buijs, A.; Rhee, T. van; L3 collaboration
Hard-Photon production and tests of QED at LEP
 Phys. Lett. **B 475** (2000) 198-205
- [69] Acciari, M. *et al.*; Bobbink, G.J.; Colijn, A.P.; Dierendonck, M. van; Duinker, P.; Erné, F.C.; Gulik, R. van; Jong, P. de; Linde, F.L.; Massaro, G.G.G.; Muijs, A.J.M.; Chekanov, S.V.; Dalen, J.A. van: Kittel, W.; König, A.C.; Mangeol, D.; Metzger, W.J.; Petersen, B.; Sanders, M.P.; Schotanus, D.J.; Timmermans, C.; Wilkens, H.; Buijs, A.; Rhee, T. van; L3 collaboration

- van; L3 collaboration
Measurement of the running of the fine-structure constant
Phys. Lett. **B 476** (2000) 40-48
- [70] Acciari, M. *et al.*; Bobbink, G.J.; Colijn, A.P.; Dierendonck, M. van; Duinker, P.; Ern , F.C.; Gulik, R. van; Hu, Y.; Jong, P. de; Linde, F.L.; Massaro, G.G.G.; Muijs, A.J.M.; Dalen, J.A. van; Kittel, W.; K nig, A.C.; Mangeol, D.; Metzger, W.J.; Petersen, B.; Sanders, M.P.; Schotanus, D.J.; Timmermans, C.; Wilkens, H.; Buijs, A.; Rhee, T. van; L3 collaboration
Measurement of the photon structure function at high Q^2 at LEP
Phys. Lett. **B 483** (2000) 373-386
- [71] Acciari, M. *et al.*; Bobbink, G.J.; Colijn, A.P.; Dierendonck, M. van; Duinker, P.; Ern , F.C.; Gulik, R. van; Jong, P. de; Linde, F.L.; Massaro, G.G.G.; Muijs, A.J.M.; Chekanov, S.V.; Dalen, J.A. van; Kittel, W.; K nig, A.C.; Mangeol, D.; Metzger, W.J.; Petersen, B.; Sanders, M.P.; Schotanus, D.J.; Timmermans, C.; Wilkens, H.; Buijs, A.; Rhee, T. van; L3 collaboration
Higgs candidates in e^+e^- interactions at $\sqrt{s} = 206.6$ GeV.
Phys. Lett. **B495**(2000) 18-25.
- [72] Acciari, M. *et al.*; Bobbink, G.J.; Colijn, A.P.; Dierendonck, M. van; Duinker, P.; Ern , F.C.; Gulik, R. van; Jong, P. de; Linde, F.L.; Massaro, G.G.G.; Muijs, A.J.M.; Chekanov, S.V.; Dalen, J.A. van; Kittel, W.; K nig, A.C.; Mangeol, D.; Metzger, W.J.; Petersen, B.; Sanders, M.P.; Schotanus, D.J.; Timmermans, C.; Wilkens, H.; Buijs, A.; Rhee, T. van; L3 collaboration
Search for charged Higgs bosons in e^+e^- collisions at center of mass energies up to 202 GeV.
Phys. Lett. **B496** (2000) 34-42.
- [73] Acciari, M. *et al.*; Bobbink, G.J.; Colijn, A.P.; Dierendonck, M. van; Duinker, P.; Ern , F.C.; Gulik, R. van; Jong, P. de; Linde, F.L.; Massaro, G.G.G.; Muijs, A.J.M.; Chekanov, S.V.; Dalen, J.A. van; Kittel, W.; K nig, A.C.; Mangeol, D.; Metzger, W.J.; Petersen, B.; Sanders, M.P.; Schotanus, D.J.; Timmermans, C.; Wilkens, H.; Buijs, A.; Rhee, T. van; L3 collaboration
Measurement of the W pair production cross section and W decay branching fractions in e^+e^- interactions at $\sqrt{s} = 189$ GeV.
Phys. Lett. **B496** (2000) 19-33.
- [74] Ackerstaff, K. *et al.*; Amarian, M.; Aschenauer, E.C.; Blouw, J.; Bulten, H.J.; Witt Huberts, P.K.A. de; Guidal, M.G.; Henkes, T.; Ihssen, H.; Kolstein, M.; Poolman, H.R.; Brand, J.F.J. van den; Steenhoven, G. van der; Hunen, J.J. van; Visser, J.; HERMES collaboration
Nuclear Effects on $R = \sigma_L/\sigma_T$ in Deep-Inelastic Scattering
Phys. Lett. **B 475** (2000) 475 (2000) 386-394
- [75] Ackerstaff, K. *et al.*; Amarian, M.; Aschenauer, E.C.; Blouw, J.; Bulten, H.J.; Henkes, T.; Ihssen, H.; Kolstein, M.; Poolman, H.R.; Brand, J.F.J. van den; Steenhoven, G. van der
Measurement of angular distributions and $R = \sigma_L/\sigma_T$ in diffractive electroproduction of neutral ρ mesons
Eur. Phys. J. **C 18** (2000) 303-316
- [76] Adam, W. *et al.*; Eijk, B. van; Hartjes, F.; RD42 Collaboration
Micro-strip sensors based on CVD Diamond
Nucl. Instr. Meth. **A 453** (2000) 141-148
- [77] Adam, W. *et al.*; van Eijk, B.; Hartjes, F.
Pulse height distribution and radiation tolerance of CVD diamond detectors
Nucl. Instr. Meth. **A 447** (2000) 244-250
- [78] Adams, D. *et al.*; Cuhadar, T.; Dantzig, R. van; Groot, N. de; Ketel, T.J.; Klostermann, L.; Litmaath, M.; Middelkoop, G. van; Oberski, J.E.J.; Postma, H.; Sichtermann, E.P.; Spin Muon Collaboration
Measurement of the SMC muon beam polarisation using the asymmetry in the elastic scattering off polarised electrons
Nucl. Instr. Meth. **A 443** (2000) 1-19
- [79] Aggarwal, M.M. *et al.*; Buijs, A.; Eijndhoven, N.J.A.M. van; Geurts, F.J.M.; Kamermans, R.; Pijll, van der; WA98 Collaboration
 Δ^{++} production in 158 AGeV $^{208}\text{Pb}+^{208}\text{Pb}$ interactions at the CERN SPS
Phys. Lett. **B 477** (2000) 37-44
- [80] Aggarwal, M.M. *et al.*; Buijs, A.; Eijndhoven, N.J.A.M. van; Geurts, F.J.M.; Kamermans, R.; Pijll, van der; WA98 Collaboration
Central Pb+Pb collisions at 158 AGeV studied by $\pi^-\pi^-$ interferometry
Eur. Phys. J. **C 16** (2000) 445-451
- [81] Aggarwal, M.M. *et al.*; Buijs, A.; Eijndhoven, N.J.A.M. van; Geurts, F.J.M.; Kamermans, R.; Pijll, van der; WA98 Collaboration
Three-pion interferometry results from central Pb+Pb collisions at 158 AGeV
Phys. Rev. Lett. **85** (2000) 2895-2899
- [82] Aggarwal, M.M. *et al.*; Buijs, A.; Eijndhoven, N.J.A.M. van; Geurts, F.J.M.; Kamermans, R.; Pijll, van der; WA98 Collaboration
Observation of direct photons in central 158 AGeV $^{208}\text{Pb}+^{208}\text{Pb}$ collisions
Phys. Rev. Lett. **85** (2000) 3595-3599
- [83] Aggarwal, M.M. *et al.*; Buijs, A.; Eijndhoven, N.J.A.M. van; Geurts, F.J.M.; Kamermans, R.; Pijll, van der; WA98 Collaboration
Collective flow and HBT in Pb+Pb collisions at the CERN-SPS
Nucl. Phys. **A 663-664** (2000) 729-732
- [84] Aggarwal, M.M. *et al.*; Buijs, A.; Eijndhoven, N.J.A.M. van; Geurts, F.J.M.; Kamermans, R.; Pijll, van der; WA98 Collaboration
Search for disoriented chiral condensates in 158 AGeV Pb+Pb collisions
Nucl. Phys. **A 663-664** (2000) 745-748
- [85] Agosteo, S.; Altieri, S.; Belli, G.; Bonifas, A.; Carabelli, V.; Gatignon, L.; Hesse, N.; Maggi, M.; Peigneu, J.P.; Reithler, H.; Silari, M.; Vitulo, P.; Wegner, M.
A facility for the test of large-area muon chambers at high rates
Nucl. Instr. Meth. **bf A 452** (2000) 94-104
- [86] Airapetian, A. *et al.*; Amarian, M.; Aschenauer, E.C.; Blouw, J.; Bulten, H.J.; Witt Huberts, P.K.A. de; Guidal, M.G.; Henkes, T.; Ihssen, H.; Kolstein, M.; Poolman, H.R.; Brand, J.F.J. van den; Steenhoven, G. van der; Hunen, J.J. van; Visser, J.; HERMES collaboration
Measurement of the spin asymmetry in the photoproduction of pairs of high-pT hadrons at HERMES
Phys. Rev. Lett. **84** (2000) 2584-2588
- [87] Airapetian, A. *et al.*; Amarian, M.; Blouw, J.; Bulten, H.J.; Witt Huberts, P.K.A. de; Guidal, M.G.; Henkes, T.; Ihssen,

- H.; Kolstein, M.; Brand, J.F.J. van den; Steenhoven, G. van der; Hunen, J.J. van; Visser, J.; HERMES collaboration *Evidence for a single-spin azimuthal asymmetry in semi-inclusive pion electroproduction* Phys. Rev. Lett. **84** (2000) 4047-4051
- [88] Airapetian, A. *et al.*; Amarian, M.; Aschenauer, E.C.; Bulten, H.J.; Witt Huberts, P.K.A. de; Ferro-Luzzi, M.; Garutti, E.; Heesbeen, D.; Hesselink, W.H.A.; Hoffman-Rothe, P.; Laziev, A.; Brand, J.F.J. van den; Steenhoven, G. van der; Hunen, J.J. van; Visser, J.; HERMES collaboration *The Q^2 dependence of the generalized Gerasimov-Drell-Hearn integral for the proton* Phys. Lett. **B 494** (2000) 1-8
- [89] Airapetian, A. *et al.*; Amarian, M.; Aschenauer, E.C.; Bulten, H.J.; Witt Huberts, P.K.A. de; Ferro-Luzzi, M.; Garutti, E.; Heesbeen, D.; Hesselink, W.H.A.; Hoffman-Rothe, P.; Ihssen, H.; Kolstein, M.; Kolster, H.; Laziev, A.; Simani, C.; Steijger, J.J.M.; Brand, J.F.J. van den; Steenhoven, G. van der; Hunen, J.J. van; Visser, J.; HERMES collaboration *Exclusive lepton production of ρ^0 mesons from hydrogen at intermediate virtual photon energies* Eur. Phys. J. **C 17** (2000) 389-398
- [90] Albada G.D. van *et al.*; Graaf, H. van der; Heijboer, G.; Holten, J.W. van; Kasdorp, W.J.; Laan, J.B. van der; Lapikás, L.; Nooren, G.J.L.; Noteboom, C.W.J.; Oberski, J.E.J.; Peek, H.Z.; Schimmel, A.; Sluijk, T.G.B.W.; Steiman, P.; Venema, J.; Witt Huberts, P.K.A. de *Measurement of mechanical vibrations excited in aluminum resonators by 0.6 GeV electrons* Rev. Sci. Instrum. **71** (2000) 1345-1354
- [91] Aleksa, M.; Deile, M.; Dubbert, J.; Fabjan, C.W.; Gruhn, C.; Hessey, N.P.; Riegler, W.; Sammer, T. *Rate effects in high-resolution drift chambers* Nucl.Instr.Meth. **bf A 446** (2000) 435-443
- [92] Aleksandrov, I. *et al.*; Hart, R. *Performance and scalability of the back-end sub-system in the ATLAS DAQ/EF prototype* IEEE Trans. Nucl. Sci. **47** (2000) 244-249
- [93] Annis, P. *et al.*; Dantzig, R. van; Konijn, J.; Visschers, J. *High-resolution tracking using large capillary bundles filled with liquid scintillator* Nucl. Instr. Meth. **A 449** (2000) 60-80
- [94] Antinori, F. *et al.*; Botje, M.; Haas, A.P. de; Kamermans, R.; Kuijer, P.; Muigg, D.; Schillings, E.; Brink, A. van den; Ven, P. van de; Eijndhoven, N. van; NA57 collaboration *Probing the specific entropy produced in ultra-relativistic heavy-ion collisions with a silicon pixel multiplicity detector: a simulation study* Nucl. Instr. Meth. **A 452** (2000) 323-337
- [95] Arnault, C. *et al.*; Bentvelsen, S.; Atlas collaboration *A generic approach to the detector description in Atlas* CHEP 2000, Computing in high energy and nuclear physics (2000) 269-272
- [96] Baumeister, D. *et al.*; Bakel, N. van; Brand, J.F.J. van den; *Design of a readout chip for LHCb* Proceedings of the Sixth Workshop on Electronics for LHC Experiments) Krakow, Poland, September 11 - 15, 2000.
- [97] Boersma, D.J.; *Neutron electric form factor from $^3\text{He}(\vec{e}, e'n)$* Nucl. Phys. **A 663-664** (2000) 417-420
- [98] Boos, E.; Brient, J.-C.; Reid, D.W.; Schreiber, H.J.; Shanidze, R. *Measuring the Higgs branching fraction to two photons at future linear e^+e^- colliders* DESY preprint 00-162
- [99] Botje, Michiel *Patronen van partonen. Hot paper: Improved parton distributions from global analysis of recent deep inelastic scattering and inclusive jet data / by Lai H.L. et al.: Phys. Rev. D 55 (1997) (3) 1280-1296* Natuur en Techniek **68** (2000) (5) 34-35
- [100] Botje, M.A.J. *A QCD analysis of HERA and fixed target structure function data* Eur. Phys. J. **C 14** (2000) 285-297
- [101] Branco, G.C.; Rebelo, M.N.; Silva-Marcos, J.I. *Large neutrino mixing with the universal strength of the Yukawa couplings* Phys. Rev. **D 62** (2000) 073004
- [102] Breitweg, J. *et al.*; Bokel, C.; Botje, M.; Bruemmer, N.; Engelen, J.; Koffeman, E.; Kooijman, P.; Sighem, A. van; Tiecke, H.; Tuning, W.; Velthuis, J.J.; Verkerke, M.; Vossebeld, J.; Wiggers, L.; Wolf, E. de; ZEUS Collaboration *W production and the search for events with an isolated high-energy lepton and missing transverse momentum at HERA* Phys. Lett. **B 471** (2000) 411-428
- [103] Breitweg, J. *et al.*; Bokel, C.; Botje, M.; Bruemmer, N.; Engelen, J.; Koffeman, E.; Kooijman, P.; Sighem, A. van; Tiecke, H.; Tuning, W.; Verkerke, M.; Vossebeld, J.; Wiggers, L.; Wolf, E. de; ZEUS Collaboration *The Q^2 dependence of dijet cross-sections in γp interactions at HERA* Phys. Lett. **B 479** (2000) 037-52
- [104] Breitweg, J. *et al.*; Bokel, C.; Botje, M.; Bruemmer, N.; Engelen, J.; Koffeman, E.; Kooijman, P.; Sighem, A. van; Tiecke, H.; Tuning, W.; Verkerke, M.; Vossebeld, J.; Wiggers, L.; Wolf, E. de; ZEUS Collaboration *Measurement of inclusive prompt photon photoproduction at HERA* Phys. Lett. **B 472** (2000) 175-188
- [105] Breitweg, J. *et al.*; Bokel, C.; Botje, M.; Bruemmer, N.; Engelen, J.; Grippink, S.; Koffeman, E.; Kooijman, P.; Schagen, S.; Sighem, A. van; Tiecke, H.; Tuning, W.; Velthuis, J.J.; Vossebeld, J.; Wiggers, L.; Wolf, E. de; ZEUS Collaboration *Measurement of azimuthal asymmetries in deep inelastic scattering* Phys. Lett. **B 481** (2000) 199-212
- [106] Breitweg, J. *et al.*; Bokel, C.; Botje, M.; Bruemmer, N.; Engelen, J.; Grippink, S.; Koffeman, E.; Kooijman, P.; Schagen, S.; Sighem, A. van; Tiecke, H.; Tuning, W.; Velthuis, J.J.; Vossebeld, J.; Wiggers, L.; Wolf, E. de; ZEUS Collaboration *Measurement of inclusive D_s photoproduction at HERA* Phys. Lett. **B 481** (2000) 213-227
- [107] Breitweg, J. *et al.*; Bokel, C.; Botje, M.; Bruemmer, N.; Engelen, J.; Grippink, S.; Koffeman, E.; Kooijman, P.; Schagen, S.; Sighem, A. van; Tiecke, H.; Tuning, W.; Velthuis, J.J.; Vossebeld, J.; Wiggers, L.; Wolf, E. de; ZEUS Collaboration *Measurement of diffractive photoproduction of vector*

- mesons at large momentum transfer at HERA*
Eur. Phys. J. C **14** (2000) 213-238
- [108] Breitweg, J. *et al.*; Bokel, C.; Botje, M.; Bruemmer, N.; Engelen, J.; Grijpink, S.; Koffeman, E.; Kooijman, P.; Schagen, S.; Sighem, A. van; Tiecke, H.; Tuning, W.; Velthuis, J.J.; Vossebeld, J.; Wiggers, L.; Wolf, E. de; ZEUS Collaboration
Search for contact interactions in deep inelastic $e^+p \rightarrow e^+X$ scattering at HERA
Eur. Phys. J. C **14** (2000) 239-254
- [109] Breitweg, J. *et al.*; Bokel, C.; Botje, M.; Bruemmer, N.; Engelen, J.; Grijpink, S.; Koffeman, E.; Kooijman, P.; Schagen, S.; Sighem, A. van; Tiecke, H.; Tuning, W.; Velthuis, J.J.; Vossebeld, J.; Wiggers, L.; Wolf, E. de; ZEUS Collaboration
Search for resonances decaying to e^+ -jet in e^+p interactions at HERA
Eur. Phys. J. C **16** (2000) 253-267
- [110] Breitweg, J. *et al.*; Bokel, C.; Botje, M.; Bruemmer, N.; Engelen, J.; Grijpink, S.; Koffeman, E.; Kooijman, P.; Schagen, S.; Sighem, A. van; Tiecke, H.; Tuning, W.; Velthuis, J.J.; Vossebeld, J.; Wiggers, L.; Wolf, E. de; ZEUS Collaboration
Measurement of exclusive omega electroproduction at HERA
Phys. Lett. **B 487** (2000) 273-288
- [111] Breitweg, J. *et al.*; Bokel, C.; Botje, M.; Bruemmer, N.; Engelen, J.; Grijpink, S.; Koffeman, E.; Kooijman, P.; Schagen, S.; Sighem, A. van; Tiecke, H.; Tuning, W.; Velthuis, J.J.; Vossebeld, J.; Wiggers, L.; Wolf, E. de; ZEUS Collaboration
Measurement of the proton structure function F_2 at very low Q^2 at HERA
Phys. Lett. **B 487** (2000) 53-73
- [112] Breitweg, J. *et al.*; Bokel, C.; Botje, M.; Bruemmer, N.; Engelen, J.; Koffeman, E.; Kooijman, P.; Sighem, A. van; Tiecke, H.; Tuning, W.; Verkerke, M.; Vossebeld, J.; Wiggers, L.; Wolf, E. de; ZEUS Collaboration
Measurement of D^{\pm} production and the charm contribution to F_2 in deep inelastic scattering at HERA*
Eur. Phys. J. C **12** (2000) 35-52 erratum 16 (2000) 181-183
- [113] Breitweg, J. *et al.*; Bokel, C.; Botje, M.; Bruemmer, N.; Engelen, J.; Koffeman, E.; Kooijman, P.; Sighem, A. van; Tiecke, H.; Tuning, W.; Verkerke, M.; Vossebeld, J.; Wiggers, L.; Wolf, E. de; ZEUS Collaboration
Measurement of the spin-density matrix elements in exclusive electroproduction of ρ^0 mesons at HERA
Eur. Phys. J. C **12** (2000) 393-410
- [114] Breitweg, J. *et al.*; Bokel, C.; Botje, M.; Bruemmer, N.; Engelen, J.; Koffeman, E.; Kooijman, P.; Sighem, A. van; Tiecke, H.; Tuning, W.; Verkerke, M.; Vossebeld, J.; Wiggers, L.; Wolf, E. de; ZEUS Collaboration
Measurement of high- Q^2 charged-current e^+p deep inelastic scattering cross sections at HERA
Eur. Phys. J. C **12** (2000) 411-428
- [115] Breitweg, J. *et al.*; Bokel, C.; Botje, M.; Bruemmer, N.; Engelen, J.; Koffeman, E.; Kooijman, P.; Sighem, A. van; Tiecke, H.; Tuning, W.; Verkerke, M.; Vossebeld, J.; Wiggers, L.; Wolf, E. de; ZEUS Collaboration
Measurement of the $E_T^2, jet/Q^2$ dependence of forward-jet production at HERA
Phys. Lett. **B 474** (2000) 223-233
- [116] Breitweg, J. *et al.*; Bokel, C.; Botje, M.; Bruemmer, N.; Engelen, J.; Koffeman, E.; Kooijman, P.; Sighem, A. van; Tiecke, H.; Tuning, W.; Verkerke, M.; Vossebeld, J.; Wiggers, L.; Wolf, E. de; ZEUS Collaboration
Angular and current-target correlations in deep inelastic scattering at HERA
Eur. Phys. J. C **12** (2000) 53-68
- [117] Bruemmer, N.; ZEUS collaboration
Searches for SUSY at HERA. Contributed to International Europhysics Conference on High-Energy Physics (EPS-HEP 99), Tampere, Finland, 15-21 Jul. 1999
Proceedings Tampere 1999. 755-
- [118] Buuren, L.D. van
Electron scattering experiments with polarized hydrogen/deuterium internal targets
AIP Conference Proceedings 512, Nuclear Physics at Storage Rings, edited by H.-O. Meyer and P. Schwandt, 2000, p.356.
- [119] Buuren, L.D. van *et al.*; Brand, J.F.J. van den; Bulten, H.J.; Ferro-Luzzi, M.; Simani, M.C.
High density polarized hydrogen/deuterium internal target
Nucl. Phys. **A 663-664** (2000) 1049c-1052c
- [120] Buijs, A.; Eijndhoven, N.J.A.M. van; Geurts, F.J.M.; Kamermans, R.; Pijll, E.C. van der
Direct photon production in 158 AGeV Pb+Pb collisions.
Nucl. Phys. **A 663-664** (2000) 769-777.
- [121] Buijs, A.
The formation of charmonium states in photon photon collisions at LEP.
Nucl. Phys. B, Proc. Suppl. **82** (2000) 300-305, in "Freiburg 1999, Structure and interactions of the photon".
- [122] Dalen, J.A. van
Bose-Einstein correlations in W -pair production at LEP
Nucl. Phys. **B (Proc. Suppl.) 86** (2000) 21-24
- [123] Deile, M. *et al.*; Hessey, N.P.
Dependence of drift tube performance on the anode wire diameter
Nucl.Instr.Meth. **A 449** (2000) 528-536
- [124] Dinapoli, R.; Campbell, M.; Cantatore, E.; Cencelli, V.; Heijne, E.; Jarron, P.; Lamanna, P.; O'Shea, V.; Quiquempoix, V.; San Segundo Bello, D.; Snoeys, W.; Koningsveld, B. van; Wyllie, K.
An analog front-end in standard 0.25mm CMOS for silicon pixel detectors in ALICE and LHCb
Proceedings of the Sixth Workshop on Electronics for LHC Experiments Krakow, Poland, September 11 - 15, 2000, ISBN: 92-9083-172-3, pp. 110-114
- [125] Eynck, T.; Moch, S.
Soft gluon resummation for polarized deep inelastic production of heavy quarks
Phys.Lett. **B 495** (2000) 87
- [126] Erné, F.C.
Measurements of the photon structure function at L3
Nucl. Phys. **B (Proc. Suppl.) 82** (2000) 19-24
- [127] Eskut, E. *et al.*; Dantzig, R. van; Jong, M. de; Konijn, K.; Melzer, O.; Oldeman, R.G.C.; Pesen, E.; Poel, C.A.F.J. van der; Uiterwijk, J.W.E.; Visschers, J.L.; CHORUS Collaboration
New results from a search for $\nu_\mu \rightarrow \nu_\tau$ and $\nu_e \rightarrow \nu_\tau$ oscillation
Phys.Lett. **B 497** (2000) 8-22

- [128] Eynck, T.; Moch, S.
Soft gluon resummation for polarized deep inelastic production of heavy quarks
Phys.Lett. **B 495** (2000) 87
- [129] Ferro-Luzzi, M.
Recent G_E^p results from Amsterdam
Nucl. Phys. **A 666** (2000) 94c-99c
- [130] Frixione, S.; Kramer, M.; Laenen, E.
 D^ production in two-photon collisions*
Nucl. Phys. **B 571** (2000) 169-184
- [131] Frixione, S.; Kramer, M.; Laenen, E.;
Heavy flavour production in two-photon collisions
J. Phys. **G 26** (2000) 723-726
- [132] Fuchs, J.; Huiszoon, L.R.; Schellekens, A.N.; Schweigert, C.; Walcher, J.
Boundaries, crosscaps and simple currents
Phys. Lett. **B 495** (2000) 427
- [133] Greene, Brian R. ; Schalm, Koenraad; Shiu, Gary
Warped compactifications in M and F theory
Nucl. Phys. **B 584** (2000) 480-508
- [134] Groot Nibbelink, S.
Line bundles in supersymmetric coset models
Phys. Lett. **B 473** (2000) 258-263
erratum Phys. Lett. **B 486** (2000) 454
- [135] Groot Nibbelink, S.; Holten, J.W. van
Consistent σ models in N=1 supergravity
Nucl. Phys. **B 588** (2000) 57-89
- [136] Gulik, R. van
GaGaRes: a Monte Carlo generator for resonance production in two-photon physics
Nucl. Phys. **B (Proc. Suppl.) 82** (2000) 311-315
- [137] Heide, J. van der; Laenen, E.; Phaf, L.; Weinzierl, S.
Helicity amplitudes for single top quark production
Phys. Rev. **D 62** (2000) 074025
- [138] Hesselink, W.H.A.; Groep, D.L.; Jans, E.; Starink, R.
Probing short-range correlations in ^3He and ^{16}O using the reaction $(e, e'pp)$
Progress in Particle and Nuclear Physics **44** (2000) 89-98
- [139] Hesselink, W.H.A.; Jans, E.
Heftige botsingen tussen nucleonen in atoomkernen
Nederlands Tijdschrift voor Natuurkunde, 2 juni 2000
- [140] Higinbotham, D.W.; Bauer, Th.; Boersma, D.J.; Brand, J.F.J. van den; Bulten, H.J.; Buuren, L.D. van; Ferro-Luzzi, M.; Geurts, D.; Harvey, M.; Heimberg, P.; Passchier, I.; Poolman, H.R.; Steenbakkers, M.F.M.; Szczerba, D.; Vries, H. de
Recoil detection with a polarized ^3He target
Nucl. Instrum. and Methods in Phys. Research **A 444** (2000) 547-558
- [141] Holten, J.W. van
Killing-Yano tensors, non-standard supersymmetry and an index theorem
Ann. d. Physik **9** (2000), 83
- [142] Holten, J.W. van
Gravitational waves and massless particle fields
Proc. XXXVth Karpacz Winterschool of Theor. Physics Polonica, Poland, 2000
- [143] Horvathy, P.A.; Macfarlane, A.J.; Holten, J.W. van
Monopole supersymmetries and the Biedenharn operator
Phys. Lett. **B 486** (2000) 346-352
- [144] Huiszoon, L.R.; Schellekens, A.N.
Crosscaps, boundaries and T-duality
Nucl. Phys. **B 584** (2000) 705-719
- [145] Huiszoon, L.R.; Schellekens, A.N.; Sousa, N.;
Open descendants of non-diagonal invariants
Nucl. Phys. **B 575** (2000) 401-415
- [146] Jong, M. de
Neutrino physics at the muon collider
Nucl. Instr. Meth. **A 451** (2000) 229-232
- [147] Jong, Sijbrand de (ed.); Koffeman, Els (ed.)
VERTEX99: proceedings 8th International Workshop on Vertex Detectors, Texel, The Netherlands, 20-25 Jun. 1999
Nucl. Instr. Meth. **A 447** (2000) 1-300
- [148] Kaczmarek, Olaf et al.; Laermann, Edwin
Heavy quark potentials in quenched QCD at high temperature
Phys. Rev. **D 62** (2000) 034021
- [149] Khodjamirian, A. et al.; Weinzierl, S.
Predictions on $B \rightarrow \pi l \nu_l$, $D \rightarrow \pi l \nu_l$ and $D \rightarrow K l \nu_l$ from QCD Light-Cone Sum Rules
Phys. Rev. **D 62** (2000) 114002
- [150] Koffeman, E.N.
A silicon micro vertex detector for the ZEUS experiment
Nucl. Instr. Meth. **A 453** (2000) 89-92
- [151] Konijn, Joop
Overgangen in de atmosfeer. Hot paper: Evidence for oscillation of atmospheric neutrinos / by Fukuda, Y. et al.:
Phys. Rev. Lett. **81** (1998) (8) 1562-1567
Natuur en Techniek **68** (2000) (7-8) 46-47
- [152] Kooijman, P.
Deep Inelastic Neutral and Charged Current Scattering at High Q^2
Contributed to International Europhysics Conference on High-Energy Physics (EPS-HEP 99), Tampere, Finland, 15-21 Jul. 1999
- [153] Kuijter, P.
The ALICE silicon strip detector system
Nucl. Instr. Meth. **A 447** (2000) 251-256
- [154] Laenen, E.
NLO calculations for charm production in DIS
J. Phys. **G 26** (2000) 734-736
- [155] Laenen, Eric
Heavy flavours at colliders.
J. Phys. **G 26** (2000) 493-504
- [156] Laenen, Eric; Serman, George; Vogelsang, Werner
Higher-order QCD corrections in prompt photon production
Phys. Rev. Lett. **84** (2000) 4296-4299
- [157] Lapikás, L.; Steenhoven, G. van der;
Transparency of ^{12}C for protons
Phys. Rev. **C 61** (2000) 064325-
- [158] Lapikás, L.; Wesseling, J.; Wiringa, R.B.
Correlations in the ground-state wave function of ^7Li
Nucl. Phys. **A 663-664** (2000) 377c-380c
- [159] Manevich, A.I.; Boudinov, E.
An efficient conjugate directions method without linear minimization
NIM **A 455** (2000) 698-705

- [160] Melzer, O.; CHORUS collaboration
Data handling in the CHORUS emulsion experiment at CERN. Contributed to International Europhysics Conference on High-Energy Physics (EPS-HEP 99), Tampere, Finland, 15-21 Jul. 1999
Proceedings Tampere 1999. 1022-
- [161] Moch, S.; Vermaseren, J.A.M.
The Mellin moments of deep inelastic structure functions at two loops
Nucl. Phys.Proc.Suppl. **86** (2000) 78-81.
- [162] Moch, S.; Vermaseren, J.A.M.
Deep-inelastic structure functions at two loops
Nucl. Phys. **B 573** (2000) 853-907
- [163] Moch, S.; Vermaseren, J.A.M.;
The Mellin moments of deep inelastic structure functions at two loops
Nucl. Phys. **B (Proc. Suppl.) 86** (2000) 78-81
- [164] Moch, S.; Vermaseren, J.A.M.
Deep inelastic structure functions: reconstruction from Mellin moments. - Zeuthen Workshop on Elementary Particle Theory: Loops and Legs in Quantum Field Theory, Koenigstein-Weissig, Germany, 9-14 Apr. 2000
Nucl. Phys. **B (Proc. Suppl.) 89** (2000) 137-142
- [165] Mulders, Piet
Glimp van het Higgs boson?
Ned. T. Nat. **66** (2000) 308-309
- [166] Pascalutsa, V.; Tjon, J.A.
Pion nucleon interaction in a covariant hadron exchange model
Phys. Rev. **C 61** (2000) 054003
- [167] Passchier, I.;
The charge form factor of the neutron from ${}^2\overline{H}(\vec{e}, e' n)p$
Nucl. Phys. **A 663-664** (2000) 421c-424c
- [168] Passchier, I., Poolman, H.R., Brand, J.F.J., van den, Buuren, L.D. van., Bulten, H.J., Ferro-Luzzi, M., Geurts, D.
Longitudinally polarized electrons in a storage ring below 1 GeV
AIP Conference Proceedings 512, Nuclear Physics at Storage Rings, edited by H.-O. Meyer and P. Schwandt (2000) p. 353.
- [169] Plefka, J.; Serone, M.; Waldron, A.
Matrix Theory and Feynman Diagrams
Fortschr. Phys. **48** (2000) 191-194
- [170] Poolman, H.R.; Boersma, D.J.; Harvey, D.W.; Higinbotham, D.W.; Passchier, I.; Six, E.; Amersfoort, P.W. van; Bauer, Th.; Boer Rookhuizen, H.; Brand, J.F.J.; Bulten, H.J.; Buuren, L.D. van; Ferro-Luzzi, M.; Geurts, D.G.; Heimberg, P.; Kroes, F.; Laan, J.B. van der; Luijckx, G.; Militsyn, B.; Noomen, J.; Putte, M.J.J. van den; Szczerba, D.; Steijger, J.J.M.; Vries, H. de
Experiments with longitudinally polarized electrons in a storage ring using a Siberian snake
Phys. Rev. Lett. **84** (2000) 3855
- [171] Poolman, H.R.; Brand, J.F.J. van den; Bulten, H.J.; Doets, M.; Ferro-Luzzi, M.; Geurts, D.G.; Mul, F.A.
A polarized ${}^3\text{He}$ internal target for storage rings
Nucl. Instr. Meth. **A 439** (2000) 91-110
- [172] Prendergast, E.P.; Brink A. van den; Haas A.P. de; Kamer-mans, R. ; Kuijjer, P. G.; Laat, C. T. A. M. de; Oti, E.;
Flow and multifragmentation of ${}^{24}\text{Mg}+{}^{27}\text{Al}$ at intermediate energies
Phys. Rev. **C 61** (2000) 4611-
- [173] Remiddi, E.; Vermaseren, J.A.M.
Harmonic polylogarithms
Int. J. Mod. Phys. **A 15** (2000) 725-754
- [174] Riegler, W.; Aleksa, M.; Deile, M.; Dubbert, J.; Fabjan, C.W.; Gruhn, C.; Hessey, N.P.; Sammer, T.
Resolution limits of drift tubes
Nucl.Instr.Meth. **A 443** (2000) 156-163
- [175] Riegler, W.; Aleksa, M.; Deile, M.; Dubbert, J.; Fabjan, C.W.; Gruhn, C.; Hessey, N.P.; Sammer, T.
Front-end electronics for drift tubes in a high-rate environment
Nucl.Instr.Meth. **A 446** (2000) 555-559
- [176] Ropotar, I. et al.; Buis, E.J.; Eijk, B. van
The LHC1 pixel detector studied in a 120 GeV/c pion test beam
Nucl. Instr. Meth. **A 439** (2000) 536-546
- [177] San Segundo Bello, D; Nauta, B; Visschers J.
Design of pixel-level ADCs for energy-sensitive hybrid pixel detectors
Proceedings of the 11th ProRISC workshop, pp.489 - 493 Veldhoven, the Netherlands, November 30 -December 1, 2000 ed. Jean Pierre Veen, ISBN: 90-73461-24-3 Utrecht, STW, Technology foundation
- [178] Szczerba, D., Buuren, L.D. van, Brand, J.F.J. van den, Bulten, H.J., Ferro-Luzzi, M., Klous, S., Kolster, H., Mul, F.A., Poolman, H.R., Simani, M.C.
A polarized hydrogen/deuterium atomic beam source for internal target experiments
Nucl. Instr. Meth. **A 455** (2000) 769.
- [179] Starink, R.; Batenburg, M.F. van; Groep, D.L.; Heimberg, P.; Hesselink, W.H.A.; Jans, E.; Lapikás, L.; Onderwater, C.J.G.; Steenbakkers, M.F.M.;
Evidence for short-range correlations in ${}^{16}\text{O}$
Phys. Lett. **B 474** (2000) 33-40
- [180] Steenhoven, G. van der
Vector meson production and deep-inelastic scattering on (polarized) ${}^1\text{H}$, ${}^2\text{H}$, ${}^3\text{He}$ and ${}^{14}\text{N}$ targets
Nucl. Phys. **A 663-664** (2000) 320c-323c
- [181] Steijger, J.J.M.
The HERMES silicon project
Nucl. Instr. Meth. **A 447** (2000) 55-60
- [182] Steijger, J.J.M.
The lambda wheels, a silicon vertex detector for HERMES
Nucl. Instr. Meth. **A 453** (2000) 98-102
- [183] Vermaseren, J.A.M.; Moch, S.
Mathematics for structure functions
Nucl. Phys. **B (Proc. Suppl.) 89** (2000) 131-136
- [184] Vossebeld, J.H.
The Partonic structure of the Quasi Real Photon
Contributed to International Europhysics Conference on High-Energy Physics (EPS-HEP 99), Tampere, Finland, 15-21 July 1999
Proceedings Tampere 1999. 471-
- [185] Weinzierl, S.
QCD corrections to $e^+e^- \rightarrow 4jets$
J. Phys. **G 26** (2000) 654-657
- [186] Weinzierl, Stefan
Computational techniques (not only) for single top production.
Zeuthen Workshop on Elementary Particle Theory: Loops

and Legs in Quantum Field Theory, Koenigstein-Weissig, Germany, 9-14 Apr. 2000
Nucl. Phys. **B (Proc. Suppl.) 89** (2000) 256-261

- [187] Weinzierl, S.; Yakovlev, O.;
QCD sum rules on the light cone and $B \rightarrow \pi$ form factors
J. Phys. **G 26** (2000) 737-740
- [188] Witt Huberts, P.K.A. de
Multi-GeV electron accelerators in Europe
Nucl. Phys. **A 663-664** (2000) 1083-1086
- [189] Witt Huberts, P.K.A. de
The spin structure of the nucleon: flavour, sea and glue
Proc. of the 2nd international conf. on 'Perspectives in hadronic physics', ICTP, Trieste, Italy, 10 - 14 May 1999, Eds. S Boffi, C. Ciofi degli Atti, M Giannini, World Scientific, Singapore (2000) 405
- [190] Zaitsev, N.Y.; Wiggers, L.W.
The LHCb vertex triggers
Nucl. Instr. Meth. **A 447** (2000) 235-243

2 PhD Theses

- [1] Groep, David Leo
Correlations and currents in ^3He studied with the $(e,e'pp)$ reaction
Universiteit Utrecht, January 2000
- [2] Rhee, Tasja van
Charmonium formation in two-photon collisions
Universiteit Utrecht, January 2000
- [3] Sighem, Adrianus Izaak van
Charged current deep inelastic scattering at HERA
Universiteit van Amsterdam, February 2000
- [4] Berg, Frenk Dimitri van den
Gas-filled micro-patterned radiation detectors
Technische Universiteit Delft, February 2000
- [5] Hunen, Jeroen Jaap van
Deep-inelastic scattering off ^{14}N
Universiteit Utrecht 6 maart 2000
- [6] Hendriks, Patrick John
ATLAS muon reconstruction from a C++ perspective: a road to the Higgs
Universiteit van Amsterdam, April 2000
- [7] Passchier, Igor
The charge form factor of the neutron from double-polarized electron-deuteron scattering
Vrije Universiteit Amsterdam, June 2000
- [8] Oldeman, Rudolf Gerhard Christaan
Measurement of differential cross-sections and structure functions in neutrino and anti-neutrino scattering on lead
Universiteit van Amsterdam, June 2000
- [9] Boudinov, Edouard
Measurement of the strange quark forward-backward asymmetry around the Z^0 peak
Universiteit van Amsterdam, June 2000
- [10] Volmer, Jochen
The pion charge form factor via pion electroproduction on the proton
Vrije Universiteit Amsterdam, October 2000
- [11] Zaitsev, Nikolai
Study of the LHCb pile-up trigger and the $B_s \rightarrow J/\psi\phi$ decay
Universiteit van Amsterdam, October 2000
- [12] Groot Nibbelink, Stefan
Supersymmetric non-linear unification in particle physics: Kaehler manifolds, bundles for matter representations and anomaly cancellation
Vrije Universiteit Amsterdam, November 2000

3 Invited Talks

- [1] G. Bardelloni
A New Read-out System for an Imaging Pixel Detector
2000 IEEE Nuclear Science Symposium and Medical Imaging Conference, October 15-20 (2000), Lyon, France
- [2] H.P. Blok
Nuclear structure studies with $(e,e'X)$ reactions
Nuclear Physics Group, University of Warschaw, Poland, March 24, 2000
- [3] J.F.J. van den Brand
Lectures on CP Violation and B physics
HEP Student School, Monchau, Germany, September 12-13, 2000
- [4] J.F.J. van den Brand
Spin dependent electron scattering
Workshop on polarized jet targets, Brookhaven National Laboratory, USA, January 25-26, 2000
- [5] L. van Buuren
Measurement of spin correlation parameters in the Delta region for the $1H(e,e')$ reaction
Spin 2000, Osaka, Japan, October 16-21, 2000
- [6] L. van Buuren
Measurement of spin correlation parameters in the Delta region for the $1H(e,e')$ reaction
16th IUPAP International Conference on Few-Body Problems in Physics, Taipei, Taiwan, March 6-10, 2000
- [7] A. Buijs
The Quark Gluon Plasma
NNV fall meeting, Petten, The Netherlands, October 27, 2000
- [8] N.J.A.M. van Eijndhoven
Heavy-ion physics within the ALICE LHC experiment
QFTHEP'2000, Tver, Russia, September 13-20, 2000
- [9] N.J.A.M. van Eijndhoven
Heavy-ion physics in a nutshell
General Physics Colloquium, Nijmegen University, The Netherlands, March 28, 2000
- [10] N.J.A.M. van Eijndhoven
Towards a library for the new millennium
Invited talk for the opening ceremony of the new library, Utrecht University, The Netherlands, May 25, 2000
- [11] N.J.A.M. van Eijndhoven
Selected topics in high-energy physics
Lectures given at the University of Cape Town, South Africa, August 2000
- [12] N.J.A.M. van Eijndhoven
Towards a heavy-ion programme for the new millennium
University of Cape Town, Rondebosch, South Africa, August 2000
- [13] N.J.A.M. van Eijndhoven
Probing the Plasma temperature
University of Cape Town, Rondebosch, South Africa, August 2000
- [14] N.J.A.M. van Eijndhoven
Can we use p_{\perp} spectra to probe thermalisation and collective effects in heavy-ion collisions ?
University of Cape Town, Rondebosch, South Africa, August 2000
- [15] N.J.A.M. van Eijndhoven
Exploring the cosmos
University of Cape Town, Rondebosch, South Africa, August 2000
- [16] N.J.A.M. van Eijndhoven
The quest for a quark-gluon plasma in nucleus-nucleus collisions
University of the Western Cape, Belville, South Africa, August 2000
- [17] J. Engelen
Recent QCD Results from HERA
SLAC Summer Institute, Topical Conference, USA, August 23-25, 2000
- [18] M. Ferro-Luzzi
Spin structure of the deuteron from the reaction $^2H(e, e'p)n$
16th IUPAP International Conference on Few-Body Problems in Physics, Taipei, Taiwan, March 6-10, 2000
- [19] M. Ferro-Luzzi
The AmPS spin physics program in Amsterdam
Gordon Conference, New Hampshire, USA, August, 2000.
- [20] M. Ferro-Luzzi
The polarized source for hydrogen and deuterium at AmPS
Workshop on polarized jet targets, Brookhaven National Laboratory, USA, January 25-26, 2000
- [21] A. Fornaini, D. Calvet, J. Visschers
Soft X-ray sensitivity of a photon-counting hybrid pixel detector with a Silicon sensor matrix
Second International Workshop on Radiation Imaging Detectors (IWoRID 2000), Freiburg, Germany, July 2-6, 2000.
- [22] E. Garutti
Nuclear Effects on R in Deep-Inelastic Scattering
Workshop on Hadron structure 2000, Stara Lesna, Slovakia, October 2-6, 2000
- [23] E. Garutti
Physics at HERMES
The ZEUS weekly seminar, DESY, Hamburg, Germany, December 1, 2000
- [24] Hartjes, F.
Radiation tolerance of CVD diamond detectors for pions and protons
3rd International conference on Radiation Effects on Semiconductor Materials, Detectors and Devices, Florence, Italy, June 2000
- [25] Hesselink, W.H.A.
Violent Collisions between Nucleons in Atomic Nuclei
International Symposium on Strong Correlations in Many Body Systems, Mount Nikko, Tokyo, Japan, 26-30 juni 2000
- [26] J.W. van Holten
Over de grenzen van de natuurkunde
Oratio, Vrije Universiteit Amsterdam, The Netherlands, June 9, 2000
- [27] J.W. van Holten
Consistent supersymmetric sigma-models
Workshop Beyond the Standard Model, Bad Honnef, Germany, February 2, 2000

- [28] J.W. van Holten
Het vroege heelal
University of Twente, Enschede, The Netherlands, March 16, 2000
- [29] J.W. van Holten
Supersymmetry
Rijksuniversiteit Groningen, Groningen, The Netherlands, April 10, 2000
- [30] J.W. van Holten
Anomalies and charge quantization in $d=4$ supersymmetric scalar field theories
SUSY 2000 Conference, CERN, Geneva, Switzerland, July 1, 2000
- [31] J.W. van Holten
Gravitational Waves
Theory Colloquium, CERN, Geneva, Switzerland, November 30, 2000
- [32] J.W. van Holten
Beyond the standard model
Winterschool Theoretical High Energy Physics DRSTP, Nijmegen, The Netherlands, January 24-28, 2000
- [33] J.W. van Holten
Supersymmetric spheres
Theor. Physics Symposium, Univ. Wuppertal, Wuppertal, Germany, December 11, 2000
- [34] B. Hommels
The LHCb Outer Tracker Beauty 2000, Sea of Galilee, Israel, September 2000.
- [35] L. Huiszoon
Open strings and Conformal Field Theory
Workshop "Beyond the standard model", Bad Honnef, Germany, February 21-24, 2000.
- [36] Jans, E.
Investigation of the exclusive $^3\text{He}(e, e'pp)$ Reaction
Fall Meeting of the American Physical Society, Williamsburg, VA, USA, October 4-7, 2000
- [37] P.M. Kluit
B physics at LEP, Status of the CKM Matrix
QUARKS2000, St. Petersburg, Russia, May 2000.
- [38] P.M. Kluit
Rare B decays at LEP
Beauty 2000, Sea of Galilee, Israel, September 2000.
- [39] J.H. Koch
Form factors in pion electroproduction
Workshop on the Pion Form Factor, NIKHEF, Amsterdam, The Netherlands, January 18, 2000
- [40] B. Koene
CP violation and design principles of the LHCb experiment
Colloquium at Tsinghua University, Beijing, People's Republic of China, April 11, 2000
- [41] B. Koene
Tracking detectors for LHCb
Colloquium at Tsinghua University, Beijing, People's Republic of China, April 12, 2000
- [42] E. Laenen
Issues in Heavy Quark Fragmentation
B-physics Workshop, Fermilab, USA, February 25, 2000
- [43] E. Laenen
Summary of Production, Fragmentation, Spectroscopy Working Group
B-physics Workshop, Fermilab, USA, February 26, 2000
- [44] E. Laenen
Lectures on resummation in QCD
Jyvaskyla Summer School, Jyvaskyla, Finland August 2000
- [45] E. Laenen
Recoil and Threshold resummation in prompt photon production
DIS Workshop, Leiden University, Leiden, The Netherlands, July 2000
- [46] E. Laenen
Combined recoil and threshold resummation in hard scattering cross sections
ICHEP 2000, Osaka, Japan, July 2000
- [47] E. Laenen
NLO heavy flavour production in two-photon collisions
Photon 2000, Ambleside, United Kingdom, August 2000
- [48] E. Laenen
NLO QCD calculations for heavy flavour production in two-photon collisions
Photon 2000, Ambleside, United Kingdom, August 2000
- [49] E. Laenen
Combined recoil and threshold resummation in hard scattering cross sections
Lund University, Lund, Sweden, November 2000
- [50] E. Laenen
Quarks, Gluons and Strings
Lund University, Lund, Sweden, November 2000
- [51] E. Laenen
Current issues in prompt photon production
DIS 2000, Liverpool, United Kingdom
- [52] E. Laenen
Combined recoil and threshold resummation in hard scattering cross sections
Nordita, Denmark, November 2000
- [53] L. Lapikás
Probing the nuclear standard model with the $(e, e'p)$ reaction.
Workshop on The Nuclear Standard Model: Ieri, Oggi, Domani, Elba, France, June 2000
- [54] S. Moch
Structure functions: Reconstruction from Mellin moments
Workshop "Loops and Legs in Quantum Field Theory", Bastei, Germany, April 13, 2000
- [55] S. Moch
Soft gluon resummation for polarized deep-inelastic heavy quark production
DIS2000, Leiden, The Netherlands, July 28, 2000
- [56] S. Moch
Towards the deep-inelastic structure functions at three loops
International workshop QCDNET2000, Paris, France, September 14, 2000
- [57] R. Muis
Hardware developments for the ANTARES experiment
SAP Seminar, Utrecht, The Netherlands, October 2, 2000
- [58] G.J.L. Nooren
Technical aspects of the ANTARES project
SAP Seminar, Utrecht, The Netherlands, January 31, 2000
- [59] G.J.L. Nooren
Influence of temperature and pressure on light propagation in fibres
ANTARES Collaboration Meeting, CERN, Geneva, Switzerland, June 7, 2000

- [60] G.J.L. Nooren
The Inner Tracking System in ALICE
International Symposium LHC Detectors and Physics,
Dubna, Russia, 28-30 June 2000
- [61] R.G.C. Oldeman
Measurement of differential neutrino-nucleon cross-sections and structure functions using the CHORUS Lead calorimeter
XXXth International Conference on High Energy Physics (ICHEP2000), Osaka, Japan, July 27 -August 2, 2000
- [62] R.G.C. Oldeman
Deep inelastic scattering with neutrinos at CHORUS
University of Pennsylvania, USA, April 17, 2000,
- [63] D.W. Reid
Neutral Current Review
Tau2000, Victoria, Canada, September 2000.
- [64] David San Segundo Bello
Design of analog-to-digital converters for energy-sensitive hybrid pixel detectors
Second International Workshop on Radiation Imaging Detectors (IWoRID 2000), Freiburg, Germany, July 2-6, 2000.
- [65] David San Segundo Bello
Pixel-Level Analog to Digital Converters for Hybrid Pixel Detectors with energy sensitivity
2000 IEEE Nuclear Science Symposium and Medical Imaging Conference, Lyon, France, October 15-20, 2000
- [66] K. Schalm
Warped compactifications in M and F theory
Massachusetts Institute of Technology, USA, March 2000
- [67] K. Schalm
Warped compactifications in M and F theory
University of Groningen, Groningen, The Netherlands, May 2000
- [68] A.N. Schellekens
Meromorphic $c=24$ conformal field theories
Workshop on Algebraic Combinatorics, Monster and Vertex Operator Algebras, Santa Cruz (CA), USA, July 24- 28, 2000.
- [69] A.N. Schellekens
Open Strings, Simple currents and fixed points
ESI-Workshop "Duality, Strings and M-Theory" Erwin Schrodinger Institut, Vienna, Austria, April 16, 2000.
- [70] A.N. Schellekens
Open Strings, Simple currents and fixed points
University Freiburg, Freiburg, Germany, January 19, 2000.
- [71] A.N. Schellekens
Boundaries, crosscaps and simple currents
ITP, Universidad Autonoma, Madrid, Spain, November 2000.
- [72] E. Schillings
Strangeness 2000: A Summary
SAP Seminar, Utrecht, The Netherlands, November 16, 2000
- [73] G. van der Steenhoven
Recoil Detection at HERMES
Workshop on ELFE Detectors, CERN, Geneva, Switzerland, January 21, 2000
- [74] G. van der Steenhoven
The FAST Detector Concept
Workshop on ELFE Detectors, CERN, Geneva, Switzerland, January 21, 2000
- [75] G. van der Steenhoven
Quarks en gluonen
Technische Universiteit Eindhoven, Eindhoven, February 8, 2000
- [76] G. van der Steenhoven
Nuclear Effects on $R = \sigma_L/\sigma_T$ in Deep-Inelastic Scattering
Workshop on "Deep-Inelastic Scattering 2000", Liverpool, United Kingdom, April 25-30, 2000
- [77] G. van der Steenhoven
The HERMES physics program
DESY Workshop on "Skewed Parton Distributions and Lepton-Nucleon Scattering", Hamburg, Germany, September 11-12, 2000:
- [78] J. van Tilburg
Vertexing Performance of the HERA-B detector
SAP Seminar, Utrecht, The Netherlands, October 16, 2000
- [79] J. Vermaseren
Physics and Computer Algebra
Univ. Madrid, Madrid, Spain, February 2000
- [80] J. Vermaseren
Mathematics for Structure Functions
Workshop "Loops and Legs in Quantum Field Theory", Bastei, Germany, April 13, 2000
- [81] J. Vermaseren
Towards three loop QCD structure functions
Univ. Granada, Granada, Spain, June 2000
- [82] J. Vermaseren
Attempts to evaluate the three loop anomalous dimensions in deep inelastic scattering
DIS Workshop, Leiden, The Netherlands, July 2000
- [83] J. Vermaseren (with D. Fliegner)
A Parallel version of FORM
ACAT2000, Fermilab, USA, October 2000
- [84] J. Vermaseren
Review of the parallel session of symbolic problem solving
ACAT2000, Fermilab, USA, October 2000
- [85] J. Vermaseren
Symbolic Problem Solving in Perturbative Field Theory
University of Wuppertal, Wuppertal, Germany, October 2000
- [86] J. Vermaseren
Physics and Computer Algebra
University of Madrid, Madrid, Spain, December 12, 2000
- [87] J. Vermaseren
Perturbative QCD in the future
University of Madrid, Madrid, Spain, December 13, 2000
- [88] G. de Vries
Direct photons as a probe of quark-gluon plasma
Institute for Theoretical Physics, Utrecht University, The Netherlands, July 6, 2000
- [89] I. van Vulpen
2-fermion & 4-fermion production at LEP2
XXXV-th Rencontres de Moriond QCD (2000), Les Arcs, France, March 11-18, 2000
- [90] S. Weinzierl
Single top production at hadron colliders
DESY, Hamburg, Germany, July 12, 2000
- [91] S. Weinzierl
Dimensional regularization, γ_5 and K-theory
6th ECFA/DESY Workshop, Padova, Italy, May 2000

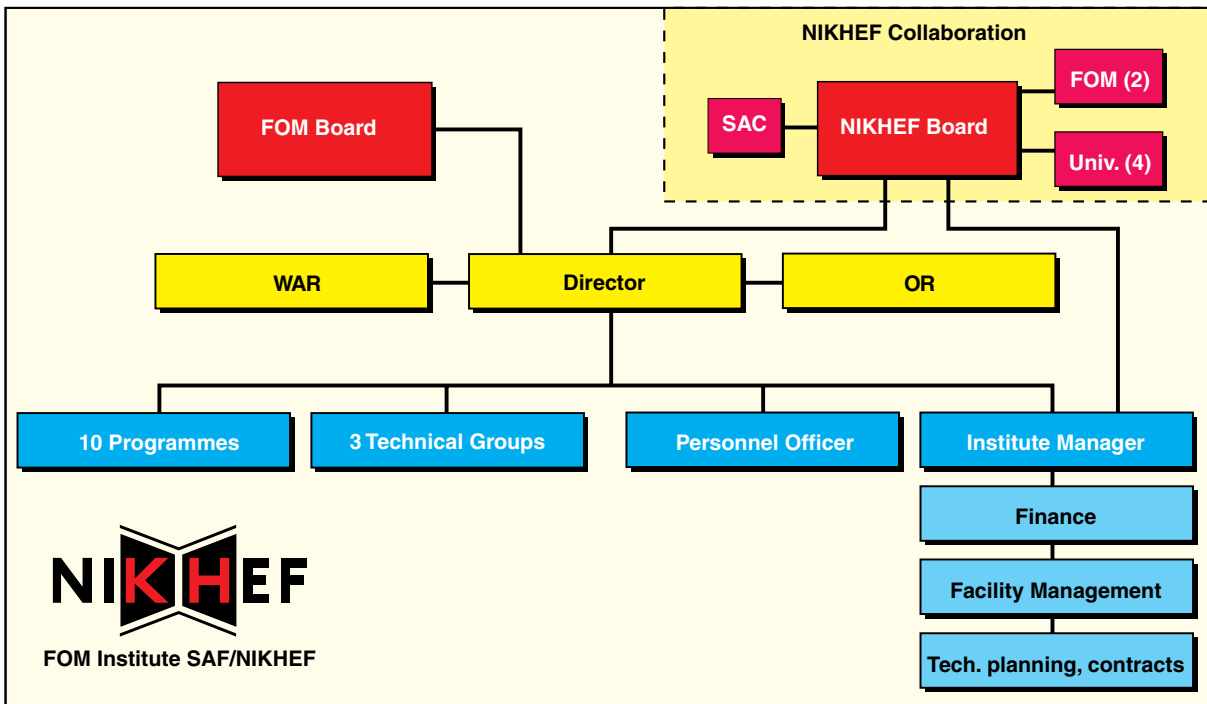
- [92] S. Weinzierl
Dimensional regularization and K-theory
LPTHE Jussieu, Paris, France, April 27, 2000

4 Seminars at NIKHEF

- [1] January 24, 2000, Amsterdam
David Groep (NIKHEF)
Correlations and Currents in ^3He Studies with the (e,e,pp) Reaction
- [2] February 4, 2000, Amsterdam
K. Rummukainen (Niels Bohr Institute, Copenhagen)
New developments in the lattice electroweak phase transition calculations
- [3] February 11, 2000, Amsterdam
S. Forte (Roma)
Structure functions and parton distributions: recent progress and new ideas
- [4] February 17, 2000, Amsterdam
G. Sigl (Meudon Observatory)
High Energy Cosmic Neutrinos as Probes of Astrophysics and Physics beyond the Standard Model
- [5] February 18, 2000, Amsterdam
G. D'Agostini (ROMA)
Bayesian inference
- [6] March 7, 2000, Amsterdam
K. Rith (Erlangen)
The HERMES physics program until the year 2006
- [7] March 10, 2000, Amsterdam
W. Snoeijis (CERN-MIC)
Pixel tracking detectors for High-Energy Physics experiments, IC-design and Radiation effects
- [8] March 24, 2000, Amsterdam
R. Jakob (Wuppertal)
Generalized parton distributions: a new tool in the investigation of hadron structure
- [9] March 31, 2000, Amsterdam
J. Rachen (Utrecht)
Neutrino's from Cosmic Accelerators
- [10] April 14, 2000, Amsterdam
B. Hertzberger (UvA)
ICES/KIS: The virtual laboratory
- [11] May 12, 2000, Amsterdam
D. Zeppenfeld (UW Madison)
Measuring Higgs boson properties: prospects for the LHC
- [12] May 12, 2000, Amsterdam
M. Ouchrif (Bologna)
Recent Macro Data on Magnetic Monopoles Searches and its implication for the SLIM experiment
- [13] May 19, 2000, Amsterdam
J. Smit (UvA/UU)
Baryogenesis and quantum field dynamics
- [14] May 24, 2000, Amsterdam
R. Jones (CERN), L. Mapelli (CERN), R. Hart (NIKHEF)
ATLAS Trigger/DAQ Back-end Software
- [15] May 26, 2000, Amsterdam
N. Magnussen (Barcelona)
Ground-Based Gamma-Ray Astronomy: Present and Future
- [16] June 9, 2000, Amsterdam
U. Baur (SUNY-Buffalo)
Probing weak boson couplings in collider experiments
- [17] June 21, 2000, Amsterdam
C.J.G. Onderwater (University of Illinois)
The $g-2$ experiment at Brookhaven
- [18] June 23, 2000, Amsterdam
R. Brandenberger (Brown University)
Inflationary Cosmology: Progress and Problems
- [19] June 30, 2000, Amsterdam
M. Pohl (CERN/Nijmegen)
The FAST experiment at PSI
- [20] July 7, 2000, Amsterdam
P. Kooijman (NIKHEF)
Summary of DIS2000 Structure Function Working Group
- [21] July 14, 2000, Amsterdam
K. Hicks (University of Ohio)
Hadronization lengths determined at FNAL
- [22] September 15, 2000, Amsterdam
E. Laenen et al
ICHEP 2000 - Summary talks
- [23] September 22, 2000, Amsterdam
J.J. Engelen (NIKHEF/UvA)
Status of the LHC experimental programme
- [24] September 27, 2000, Amsterdam
A. Turcot
Higgs Search at D0
- [25] October 6, 2000, Amsterdam
R. Timmermans (KVI)
Physics beyond the Standard Model with trapped isotopes
- [26] October 13, 2000, Amsterdam
K. Rajagopal (MIT)
The Phases of QCD in Heavy Ion Collisions and Compact Stars
- [27] October 20, 2000, Amsterdam
S. Menary (Toronto)
The BTeV experiment
- [28] November 3, 2000, Amsterdam
W.D. Nowak (DESY-Zeuthen)
Electron Scattering at TESLA with Polarized and Unpolarized Nucleon Targets
- [29] November 10, 2000, Amsterdam
R. van Dantzig (NIKHEF)
Summary of NOW2000 workshop
- [30] November 17, 2000, Amsterdam
R. Stock
First observation of the QCD parton-hadron phase transition
- [31] November 24, 2000, Amsterdam
A. Mueller
The parton model and a Boltzmann equation for the early stages of a relativistic heavy ion collision
- [32] December 1, 2000, Amsterdam
M. Botje (NIKHEF)
Parton Distributions from Deep Inelastic Scattering
- [33] December 21, 2000, Amsterdam
W. Verkerke
First CP Physics results from Babar

5 NIKHEF Annual Scientific Meeting, December 14-15, 2000, Amsterdam

- [1] J. Timmermans
Higgs physics at LEP
- [2] J. van Dalen
Cross-Talk Phenomena in WW Events
- [3] M. Needham
Nikhef on LHCb: Status Report
- [4] N. van Bakel
Vertexing at LHCb
- [5] M. Mevius
Status and Prospects of Hera-B
- [6] P. Kooijman
Recent results from ZEUS
- [7] J. Velthuis
The ZEUS vertex chamber
- [8] E. Pesen
Results and outlook from the CHORUS experiment
- [9] H. van der Graaf
The GRAPPA project
- [10] J. Vermaseren
3-Loop Structure Functions
- [11] K. Schalm
String theory and experiment
- [12] E. de Wolf
The ANTARES project
- [13] A. Heijboer
ANTARES' view on the universe
- [14] J. Visschers
MediPix, X-ray imaging with Pixel detectors
- [15] M. Vreeswijk
NIKHEF contributions in ATLAS and the making of BOL-0
- [16] W. Lavrijsen
ComBined Reconstruction in Atlas
- [17] O. Peters
D0 status and Muon Spectrometer
- [18] K. Bos
GRID and the local Farm
- [19] J. Steijger
The Hermes silicon project
- [20] J. Visser
Nuclear Effects in DIS
- [21] L. van Buuren
Quadrupols of the proton
- [22] A. Buijs
Status of ALICE
- [23] P. van der Ven
Transverse mass spectra of Λ and $\bar{\Lambda}$ in Pb-Pb collisions at 158 A GeV/c
- [24] M. van Leeuwen
Strangeness production in NA49
- [25] M. Pohl
Colliders for Future Physics



The organisational chart.

F Resources and Personnel

1 Resources

In 2000 NIKHEF received a budget for exploitation (including salaries) of some MHfl 37.4 (Fig. 1.1). The budget figures of the NIKHEF partners were: FOM-institute (SAF/NIKHEF): MHfl 25.5, universities MHfl 9.3 of which FOM supplied MHfl 3.1 through the Reserach Division Subatomic Physics (SAF). Third parties contributed MHfl 2.6 to the NIKHEF income.

The largest program, ATLAS, consumed about a quarter of the exploitation budget. Theory is for the first time recognizable in budget terms as a separate program. Capital investments in 2000 were directed at the three LHC experiments to which NIKHEF contributes, while the computing, networking and technical infrastructure were strengthened by a capital injection of MHfl 2.4.

Income 2000: 37,4 Mfl

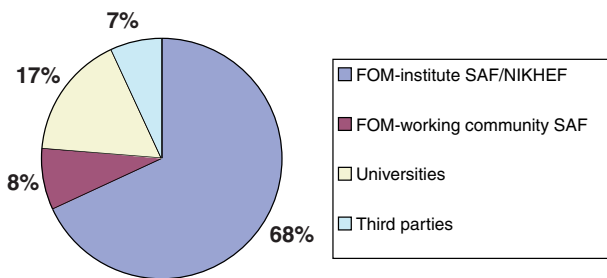


Figure 1.1: NIKHEF funding.

Capital investments 2000: 7 Mfl

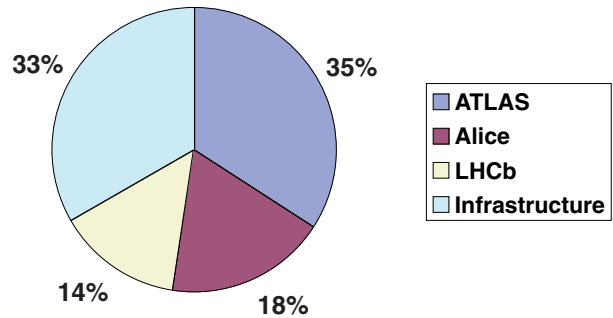


Figure 1.3: Capital investments.

Expenses 2000: 37,4 Mfl

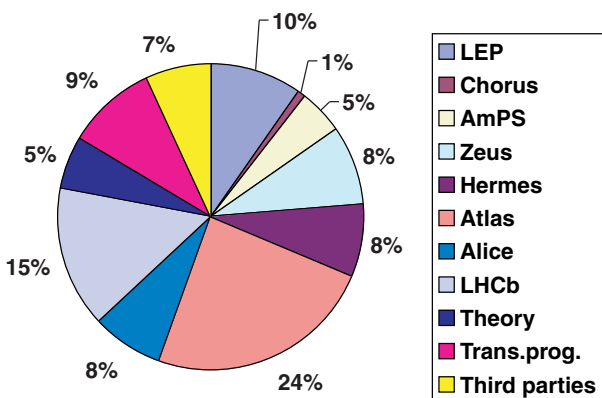


Figure 1.2: Exploitation budget.

NIKHEF Personnel

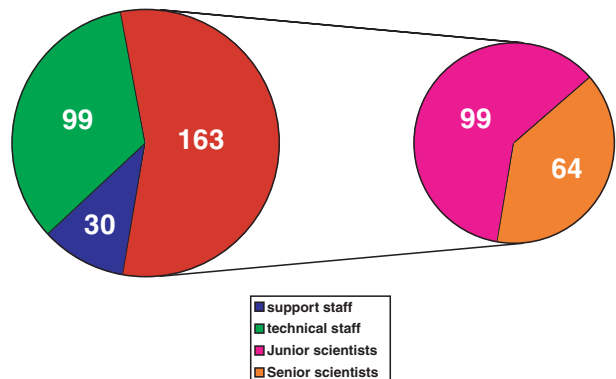


Figure 1.4: Personnel as of December 31, 2000. Subdivision of personnel: the scientists are divided into senior and junior scientists (right plot).

2 Membership of Councils and Committees during 2000

NIKHEF Board

F.T.M.Nieuwstadt (FOM, Chairman)
K.H. Chang (FOM)
J.J.M. Franse (UvA)
S. Groenewegen (VU)
C.W.P.M. Blom (KUN)
J.G.F. Veldhuis (UU)
H.G. van Vuren (secretary, FOM)

Scientific Advisory Committee NIKHEF

P. Söding (DESY, Chairman)
B. Frois (CEA Saclay)
G. Goggi (CERN)
D. von Harrach (Univ. Mainz)
G. Ross (Univ. Oxford)
J. Stachel (Univ. Helderberg)

NIKHEF Works Council

L.W. Wiggers (Chairman)
R.G.K. Hart (1st secretary)
J.J. Hogenbirk (2nd secretary)
H. Boer Rookhuizen
J.H.G. Dokter
W.D. Hulsbergen
F.B. Kroes

FOM Board

J.J. Engelen

Fund for Scientific Research, Flanders, Belgium

G. van Middelkoop

SPC-CERN

J.J. Engelen
K.J.F. Gaemers

LHCC-CERN

J.J. Engelen (Chairman)

SPSC-CERN

B. Koene

Extended Scientific Council, DESY

K.J.F. Gaemers

ECFA

J.J. Engelen, K.J.F. Gaemers, R. Kamermans, E.W. Kittel,
G. van Middelkoop (also in Restricted ECFA)

NuPECC

G. van Middelkoop

HEP Board EPS

J.J. Engelen

Research Board CERN

J.J. Engelen

Extended Scientific Council DESY

J.J. Engelen

EPAC

G. Luijckx

Beleidsadvies college KVI

G. Luijckx

Scientific Committee

Frascati Laboratory

G. van Middelkoop

Scientific Advisory Committee,

Physique Nucleaire, Orsay

P.K.A. de Witt Huberts

Scientific Advisory Committee,

DFG 'Hadronen Physik'

J.H. Koch

P.K.A. de Witt Huberts

Program Advisory Committee,

ELSA (Bonn) / MAMI (Mainz)

H.P. Blok

Program Advisory Committee,

Jefferson Laboratory

H.P. Blok

Other committees

ASP Board W. Hoogland

ASTRON W. Hoogland

EPCS W. Heubers

ESRF G. Luijckx

HTASK K. Bos

ICANN R. Blokzijl

IRI J.H. Koch

IUPAP, C11 committee W. Hoogland

Kuratorium HEPHY, Vienna E.W. Kittel

NOMINET R. Blokzijl

OECD Global Science Forum Consultative Group G. van Middelkoop

RIPE R. Blokzijl

SURF W. Hoogland

WCW Board A.J. van Rijn

3 Personnel as of December 31, 2000

FOM, and the universities UVA, VU, KUN and UU are partners in NIKHEF (See colofon). UL and UT denote the universities of Leiden and Twente. TE stands for temporary employee, GST for guest. Other abbreviations refer to the experiments, projects and departments.

1. Experimental Physicists

Agasi, Drs. E.E.	GST	DELPHI	FOM	HERMES
Akker, Drs. M. van den	KUN	L3	UVA	ANTARES
Apeldoorn, Dr. G.W. van	UVA	B Phys	GST	Other Projects
Bakel, Drs. N.A. van	FOM	B Phys	VU	HERMES.
Baldew, Drs. S.V.	UVA	L3	FOM	ATLAS
Balm, Drs. P.W.	FOM	ATLAS	FOM-VU	B Phys
Barneo González, Drs. P.J.	FOM	AmPS Phys	FOM	B Phys
Batenburg, Drs. M.F. van	GST	AmPS Phys	UVA	B Phys
Bauer, Dr. T.S.	FOM-UU	B Phys	FOM-KUN	L3
Bentvelsen, Dr. S.C.M.	FOM	ATLAS	FOM	B Phys
Blekman, Drs. Mw. F.	FOM	ATLAS	FOM	AmPS Phys
Blok, Dr. H.P.	VU	AmPS Phys	FOM	ANTARES
Blom, Drs. H.M.	FOM	DELPHI	FOM	ATLAS
Bobbink, Dr. G.J.	FOM	L3	KUN	ATLAS
Boer, Dr. F.W.N. de	GST	ALGEMEEN	FOM-UU	ALICE
Boersma, Drs. D.J.	GST	AmPS Phys	FOM-VU	B Phys
Bokel, Drs. C.H.	GST	ZEUS	KUN	L3
Bos, Dr. K.	FOM	ATLAS	FOM-KUN	ATLAS
Botje, Dr. M.A.J.	FOM	ALICE	FOM-VU	B Phys
Bouhali, Dr. O.	FOM	HERMES	FOM	ATLAS
Brand, Prof.Dr. J.F.J. van den	VU	AmPS Phys	FOM	B Phys
Bruinsma, Drs. M.	FOM	B Phys	FOM	ATLAS
Bruinsma, Ir. P.J.T.	GST	ANTARES	FOM-KUN	ATLAS
Buis, Drs. E.J.	GST	ATLAS	FOM-VU	HERMES
Buijs, Prof.Dr. A.	UU	ALICE	FOM	ALICE
Bulten, Dr. H.J.	FOM-VU	HERMES	UVA	ATLAS
Buuren, Drs. L.D. van	FOM	AmPS Phys	FOM	ATLAS
Calvet, Dr. D.	GST	ATLAS	FOM	ALICE
Cârloganu, Dr. Mw. F.C.	FOM	ANTARES	UVA	ATLAS
Crijns, Dipl.Phys.F.J.G.H.	FOM-KUN	ATLAS	FOM	ATLAS
Dalen, Drs. J. van	FOM-KUN	L3	FOM	ATLAS
Dam, Dr. P.H.A. van	UVA	DELPHI	FOM	ALICE
Dantzig, Dr. R. van	GST	CHORUS	FOM	B Phys
Daum, Prof.Dr. C.	GST	ATLAS	KUN	L3
Derrick, Prof.Dr. M.	GST	ZEUS	FOM-UU	B Phys
Diddens, Prof.Dr. A.N.	GST	DELPHI	FOM-BR	HERMES
Dierckxsens, Drs. M.E.T.	FOM	L3	VU	DIR
Dierendonck, Drs. D.N. van	GST	L3	GST	L3
Duensing, Drs. Mw. S.	KUN	ATLAS	FOM-UU	ALICE
Duinker, Prof.Dr. P.	FOM	L3	GST	L3
Eijk, Prof.Dr. B. van	FOM	ATLAS	GST	DELPHI
Eijk, Ir. R.M. van der	FOM	B Phys	FOM	ATLAS+
Eldik, Drs. J.E. van	GST	DELPHI	FOM	B Phys
Engelen, Prof.Dr. J.J.	UVA	ZEUS	FOM	Other Projects
Erné, Prof.Dr.Ir F.C.	GST	L3	FOM-UU	ALICE
Ferreira Montenegro, Drs. Mw. J.	FOM	DELPHI	FOM	B Phys
Filthaut, Dr. F.	KUN	L3	FOM	ATLAS
Fornaini, Drs. A.	FOM	ATLAS	FOM	CHORUS
Garutti, Drs. Mw. E.	FOM	HERMES	UVA	ATLAS
Gouz, Dr. I	GST	B Phys	KUN	L3
Graaf, Dr.Ir. H. van der	FOM	ATLAS		
Grijpink, Drs. S.J.L.A.	FOM	ZEUS		
Groep, Drs. D.L.	FOM	Other Projects		
Gulik, Drs. R.C.W.	UL	L3		
Hartjes, Dr. F.G.	FOM	ATLAS		
Heesbeen, Drs. D.	FOM			
Heijboer, Drs. A.J.	UVA			
Heijne, Dr. H.M.	GST			
Hesselink, Dr. W.H.A.	VU			
Hessey, Dr. N.P.	FOM			
Hierck, Drs. R.H.	FOM-VU			
Hommels, Ir. L.B.A.	FOM			
Hoogland, Prof.Dr. W.	UVA			
Hu, Drs. Y.	FOM-KUN			
Hulsbergen, Drs. W.D.	FOM			
Jans, Dr. E.	FOM			
Jong, Dr. M. de	FOM			
Jong, Dr. P.J.	FOM			
Jong, Prof.Dr. S.J.	KUN			
Kamermans, Prof.Dr. R.	FOM-UU			
Ketel, Dr. T.J.	FOM-VU			
Kittel, Prof.Dr. E.W.	KUN			
Klok, Drs. P.F.	FOM-KUN			
Klous, Drs. S.	FOM-VU			
Kluit, Dr. P.M.	FOM			
Koene, Dr. B.K.S.	FOM			
Koffeman, Dr.Ir. Mw. E.N.	FOM			
König, Dr. A.C.	KUN			
Konijn, Dr.Ir. J.	GST			
Kooijman, Prof.Dr. P.M.	UVA			
Kuijer, Dr. P.G.	FOM			
Laan, Dr. J.B. van der	FOM			
Lapikás, Dr. L.	FOM			
Lavrijsen, Drs. W.T.L.P.	FOM-KUN			
Laziev, Drs. A.E.	FOM-VU			
Leeuwen, Drs. M. van	FOM			
Linde, Prof.Dr. F.L.	UVA			
Luijckx, Ir. G.	FOM			
Lutterot, Drs. M.	FOM			
Maas, Dr. R.	FOM			
Maddox, Drs. E.	UVA			
Mangeol, Drs. D.	FOM			
Massaro, Dr. G.G.G.	FOM			
Melzer, Dipl.Phys. O.	FOM			
Merk, Dr. M.H.M.	FOM			
Metzger, Dr. W.J.	KUN			
Mevius, Drs. Mw. M.	FOM-UU			
Mexner, Drs. Mw. I.V.	FOM-BR			
Middelkoop, Prof.Dr. G. van	VU			
Mil, Drs. A. van	GST			
Muigg, Dr.Mw. D.	FOM-UU			
Muijs, Drs. Mw. A.J.M.	GST			
Mulders, Ir. M.P.	GST			
Naumann, Drs. A.	FOM			
Needham, Dr. M.D.	FOM			
Noomen, Ir. J.G.	FOM			
Nooren, Dr.Ir. G.J.L.	FOM-UU			
Ouchrif, Dr. M.	FOM			
Peeters, Ir. S.J.M.	FOM			
Pesen, Dr. E.	FOM			
Peters, Drs. O.	UVA			
Petersen, Drs. B.	KUN			

Phaf, Drs. L.K.	FOM	ATLAS	Mulders, Prof.Dr. P.J.G.	VU
Pijll Drs. E.C. van der	FOM-UU	WA93/98	Nyawelo, B.Sc. T.S.	FOM
Reid, Dr. D.W.	FOM	DELPHI	Schalm, Dr. K.E.	FOM
Reischl, Drs. A.J.	FOM	HERMES	Schellekens, Prof.Dr. A.N.J.J.	FOM
Roux, Drs. B.	FOM-KUN	L3	Veltman, Prof.Dr. M.J.G.	GST
San Segundo Bello, Drs. D.	FOM-HCM	Other Projects	Vermaseren, Dr. J.A.M.	FOM
Sanders, Drs. M.	KUN	L3	Wit, Prof.Dr. B.Q.P.J. de	UU
Schagen, Drs. S.E.S.	FOM	ZEUS	Zhou, Dr. M.	FOM
Schillings, Drs. E.	FOM-UU	ALICE		
Scholte, Ir. R.C.	UT	ATLAS		
Schotanus, Dr. D. J.	KUN	L3		
Sichtermann, Drs. E.P.	GST	SMC		
Simani Drs. Mw. M.C.	FOM-VU	HERMES		
Steenbakkens, Drs. M.F.M.	GST	AmPS Phys		
Steenhoven, Prof.Dr. G. van der	FOM	HERMES		
Steijger, Dr. J.J.M.	FOM	HERMES		
Tassi, Dr. E.	FOM	ZEUS		
Tiecke, Dr. H.G.J.M.	FOM	ZEUS		
Tilburg, Drs. J.A.N.	FOM	B Phys		
Timmermans, Dr. J.J.M.	FOM	DELPHI		
Toet, Dr. D.Z.	GST	Other Projects		
Tuning, Drs. N.	UVA	ZEUS		
Tvaskis, Drs. V.	VU	HERMES		
Uiterwijk, Ir. J.W.E.	GST	CHORUS		
Velthuis, Ir. J.J.	FOM	ZEUS		
Ven, Drs. P.A.G. van de	FOM-UU	WA93/98		
Vermeulen, Dr.Ir. J.C.	UVA	ATLAS		
Visschers, Dr. J.L.	FOM	ATLAS		
Visser, Drs. E.	GST	ATLAS		
Visser, Drs. J.	FOM	HERMES		
Vos, Drs. M.A.	UT	ATLAS		
Vreeswijk, Dr. M.	FOM	ATLAS		
Vries, Drs. G. de	UU	ANTARES		
Vries, Dr. H. de	FOM	AmPS Phys		
Vulpen, Drs. I.B. van	FOM	DELPHI		
Wiggers, Dr. L.W.	FOM	ZEUS		
Wijngaarden, Drs. D.A.	KUN	ATLAS		
Wilkens, Drs. H.	FOM-KUN	L3		
Witt Huberts, Prof.Dr. P.K.A.	FOM	HERMES		
Wolf, Dr. Mw. E. de	UVA	ZEUS		
Woudstra, Ir. M.J.	GST	ATLAS		
Zihlmann, Dr. B.	FOM-VU	AmPS Phys		
2. Theoretical Physicist				
Bachetta, Drs. A.	FOM-VUA			
Eynck, Dipl.Phys. T.O.	FOM			
Gaemers, Prof.Dr. K.J.F.	UVA			
Gato-Rivera, Dr. Mw. B.	GST			
Heide, Drs. J. van der	FOM			
Henneman, Drs. A.	VU			
Holten, Prof.Dr. J.W. van	FOM			
Huiszoon, Drs. L.R.	FOM			
Iersel, Drs. M. van	FOM-UVA			
Kleiss, Prof.Dr. R.H.P.	KUN			
Koch, Prof.Dr. J.H.	FOM			
Laenen, Dr. E.	FOM			
Marques de Sousa, Drs. N.M.	GST			
Metz, Dr. A.	FOM-VU			
3. Computer Technology Group (CT)				
Akker, T.G.M. van den	FOM			
Blokzijl, Dr. R.	FOM			
Boterenbrood, Ir. H.	FOM			
Damen, Ing. A.C.M.	FOM			
Geerts, M.L.	FOM			
Harapan, Drs. D.	FOM			
Hart, Ing. R.G.K.	FOM			
Heubers, Ing. W.P.J.	FOM			
Huyser, K.	FOM			
Kuipers, Drs. P.	FOM			
Leeuwen, Drs. W.M. van	FOM			
Oudolf, J.D.	TE			
Schimmel, Ing. A.	FOM			
Tierie, Mw. J.J.E.	FOM			
Wijk, R.F. van	FOM			
4. Electronics Technology Group (ET)				
Berkien, A.W.M.	FOM			
Beuzekom, Ing. M.G.van	FOM			
Boer, J. de	FOM			
Boerkamp, A.L.J.	FOM			
Born, E.A. van den	FOM			
Es, J.T. van	GST			
Evers, G.J.	FOM			
Gotink, G.W.	FOM			
Groen, P.J.M. de	FOM			
Groenstege, Ing. H.L.	FOM			
Gromov, Drs. V.	FOM			
Haas, Ing. A.P. de	FOM			
Harmsen, C.J.	FOM			
Heine, Ing. E.	FOM			
Heutenik, B.	FOM			
Hogenbirk, Ing. J.J.	FOM			
Jansen, L.W.A.	FOM			
Jansweijer, Ing. P.P.M.	FOM			
Kieft, Ing. G.N.M.	FOM			
Kluit, Ing. R.	FOM			
Kok, Ing. E.	FOM			
Koopstra, J.	UVA			
Kroes, Ir. F.B.	FOM			
Kruijjer, A.H.	FOM			
Kuijt, Ing. J.J.	FOM			
Mos, Ing. S.	FOM			
Peek, Ing. H.Z.	FOM			
Reen, A.T.H. van	FOM			
Rewiersma, Ing. P.A.M.	FOM			
Schipper, Ing. J.D.	FOM			
Sluijk, Ing. T.G.B.W.	FOM			

Stolte, J.	FOM
Timmer, P.F.	FOM
Trigt, J.H. van	FOM
Verkooijen, Ing. J.C.	FOM
Vink, Ing. W.E.W.	FOM
Wieten, P.	FOM
Zwart, Ing. A.N.M.	FOM
Zwart, F. de	FOM

5. Mechanical Technology Group (MT)

Arink, R.P.J.	FOM
Band, H.A.	FOM
Beumer, H.	FOM
Boer, R.P. de	FOM
Boer Rookhuizen, H.	FOM
Boomgaard-Hilferink, Mw. J.G.	FOM
Boucher, A.	FOM
Bron, M.	FOM
Brouwer, G.R.	FOM
Buis, R.	FOM
Buskens, J.P.M.	UVA
Buskop, Ir. J.J.F.	FOM
Ceelie, L.	UVA
Doets, M.	FOM
Homma, J.	FOM
Hover, Ing. E.P.	FOM
Jacobs, J.	FOM
Jaspers, M.J.F.	UVA
Kaan, Ir. A.P.	FOM
Kok, J.W.	FOM
Korporaal, A.	FOM
Kraan, Ing. M.J.	FOM
Kruiper, H.A.	TE
Kuilman, W.C.	FOM
Langedijk, J.S.	FOM
Lassing, P.	FOM
Lefévere, Y.	FOM
Leguyt, R.	FOM
Mul, F.A.	FOM-VU
Munneke, Ing. B.	FOM
Overbeek, M.G. van	FOM
Petten, O.R. van	FOM
Rietmeijer, A.A.	FOM
Roeland, E.	FOM
Römers, L.W.E.G.	FOM
Rövekamp, J.C.D.F.	UVA
Schuijlenburg, Ing. H.W.A.	FOM
Snippe, Ir. Q.H.C.	FOM
Thobe, P.H.	FOM
Veen, J. van	FOM
Verlaat, Ing. B.A.	FOM
Werneke, Ing. P.J.M.	FOM
Zegers, Ing. A.J.M.	FOM

6. AmPS Management Project (AMP)

La Rooij, Mw. T.J.	TE
Spelt, Ing. J.B.	FOM

7. Management and Administration (M&A)

Bakker, C.N.M.	FOM
Berg, A. van den	FOM
Brammerloo, A.V.	TE
Buitenhuis, W.E.J.	FOM
Bulten, F.	FOM
Doest, Mw. C.J.	TE
Dokter, J.H.G.	FOM
Dulmen, Mw. A.C.M. van	FOM
Echtelt, Ing. H.J.B. van	FOM
Egdom, T. van	FOM
Geerincx, Ir. J.	FOM
Gerritsen-Visser, Mw. J.	FOM
Greven-van Beusekom, Mw. E.C.L.	FOM
Heuvel, Mw. G.A. van den	FOM
Kerkhoff, Mw. E.H.M. van	FOM
Kesgin-Boonstra, Drs. Mw. M.J.	FOM
Laan, Mw. F.M.	FOM
Langelaar, Dr. J.	UVA
Langenhorst, A.	FOM
Lemaire-Vonk, Mw. M.C.	FOM
Louwrier, Dr. P.W.F.	FOM
Mors, A.G.S.	FOM
Pancar, M.	FOM
Ploeg, F.	FOM
Post, Mw. E.C.	FOM
Post, Dr. J.C.	GST
Rijksen, C.	FOM
Rijn, Drs. A.J. van	FOM
Visser, J.	FOM
Vries, W. de	FOM

8. Apprentices in 2000

Abouelkhir, M.	MT
Belkasmí, M.	ET
Boezaart, T.J.	ET
Bruchem, D.G. van	MT
Dalhuizen, J.M.	ATLAS
Davidse, F.	Theory
Davidse, M.	Theory
Donders, R.S.	ANTARES
Dongen, B.J. van	MT
Ejere, D.	HERMES
Enthoven, J.	MT
Francke, J.	MT
Goede, D.J.	MT
Grashuis, M.A.	ET
Groot, B.P.	CT
Haan, M.	MT
Haddaoui, R. E.	ET
Hal, M.C. van	MT
Heide, J. van der	Theory
Hoogstraten, V.G. van	MT
Hristova, I.R.	CHORUS
Huítíng, R.	MT
John, D.	MT
Krijger, E.	MT
Köper, D.H.	ZEUS

Leeuwen, S.A. van	MT	Steman, W.A.	AMP
Maat, B. van der	MT	Stoffelen, A.C.	AMP
Maddox, E.	ZEUS	Tuyn, Dr. J.W.N.	M&A
Mirani, R.	ANTARES	Volmer, Dipl.Phys. J.	AmPS Phys
Muis, R.	ANTARES	Wassenaar, Drs. E. † 10/4/00	CT
Mus, P.	MT	Weinzierl, Dr. S.D.	Theory
Nijenhuis, N.	ANTARES	Zaitsev, Dr. N.U.	B Phys
Pinto, Y.	ZEUS		
Pronk, M.	CT		
Rens, B.A.P. van	ATLAS		
Rétif, C.F.J.M.	MT		
Schong, D.	ET		
Sloosema, R.L.	ATLAS		
Spoor, V.	ATLAS		
Vliet, E. van	MT		
Vogelvang, M.	ATLAS		
Windt, D.N. de	ET		
Wit, R.	MT		
Wong, W.Y.	ET		
Zand, J.A. van 't	CT		

9. They left us

Amersfoort, Dr.Ir. P.W. van	B Phys
Boontje, Ing. R.	CT
Boudinov, Dr. E.	DELPHI
Colijn, Dr. A.P.	ZEUS
Eites, P.	MT
Ferro Luzzi, Dr. M.M.E.	B Phys
Goede, D.J.	MT
Groot Nibbelink, Dr. S.	Theory
Grootheest, J.E. van	CT
Haan, M.	MT
Hendriks, Dr. P.J.	ATLAS
Hunen, Dr. J.J. van	HERMES
IJzermans, P.A.	MT
Kapusta, Dr. P.	B Phys
Kolkman, J.	M&A
Kolster, Dr. H.	HERMES
Kruszynska-Straszewicz, Drs. Mw. M.N.	CT
Kuijjer, L.H.	AMP
Kwakkel, Ir. E.	M&A
Laermann, Dr. E.	Theory
Leeftink, J.S.	M&A
Moch, Dr. S.O.	Theory
Mueller, Prof.Dr. A.	Theory
Mur, Drs. Mw. L.	M&A
Nirsoe, R.S.	M&A
Oberski, Dr. J.E.J.	Other Projects
Oldeman, Dr. R.G.C.	CHORUS
Payre, Dr. P.	ANTARES
Pettis, R.E.	M&A
Poolman, Dr. H.R.	AmPS Phys
Postma, Ing. O.	MT
Rhee, Drs. Mw. T. van	L3
Schäfer-van der Weijden, Mw. W.	M&A
Schoemaker-Weltevreden, Mw. S.	M&A
Schwebke, H.	AMP
Spruit, Drs. A.	AMP